UNIVERSIDADE FEDERAL DE PERNAMBUCO
CENTRO DE TECNOLOGIA E GEOCIÊNCIAS
DEPARTAMENTO DE GEOLOGIA
PROGRAMA DE PÓS-GRADUAÇÃO EM GEOCIÊNCIAS

VALDIELLY LARISSE SILVA

ANÁLISE ESTRUTURAL E TERMOBAROMETRIA DE ROCHAS METASSEDIMENTARES DA REGIÃO DE FEIRA NOVA, SUBPROVÍNCIA CENTRAL - PROVÍNCIA BORBOREMA

Recife
2020

VALDIELLY LARISSE SILVA

ANÁLISE ESTRUTURAL E TERMOBAROMETRIA DE ROCHAS METASSEDIMENTARES DA REGIÃO DE FEIRA NOVA, SUBPROVÍNCIA CENTRAL - PROVÍNCIA BORBOREMA

Dissertação apresentada ao Programa de Pós-Graduação em Geociências da Universidade Federal de Pernambuco, como requisito parcial para a obtenção do título de Mestra em Geociências.

Área de concentração: Geoquímica, Geofísica e Evolução Crustal

Orientador: Prof. Dr. Sérgio Pacheco Neves.

Coorientador: Prof. Dr. Andres Bustamante Londoño.

Recife

2020

Catalogação na fonte
Bibliotecário Gabriel Luz, CRB-4 / 2222

S586a Silva, Valdielly Larisse
Análise estrutural e termobarometria de rochas metassedimentares da região de Feira Nova, subprovíncia central - Província Borborema / Valdielly Larisse Silva – Recife, 2020.
92 f.: figs.

Orientador: Prof. Dr. Sérgio Pacheco Neves.
Coorientador: Prof. Dr. Andres Bustamante Londoño.
Dissertação (Mestrado) – Universidade Federal de Pernambuco. CTG. Programa de Pós-Graduação em Geociências, 2020.
Inclui referências.

1. Geociências. 2. Região de Feira Nova. 3. Termobarometria. 4. Tectônica transpressiva. 5. Zona de cisalhamento Paudalho. I. Neves, Sérgio Pacheco (Orientador). II. Londoño, Andres Bustamante (Coorientador). III. Título.

UFPE

551 CDD (22. ed.) BCTG / 2021 - 181

VALDIELLY LARISSE SILVA

ANÁLISE ESTRUTURAL E TERMOBAROMETRIA DE ROCHAS METASSEDIMENTARES DA REGIÃO DE FEIRA NOVA, SUBPROVÍNCIA CENTRAL - PROVÍNCIA BORBOREMA

Dissertação apresentada ao Programa de Pós-Graduação em Geociências da Universidade Federal de Pernambuco, como requisito parcial para a obtenção do título de Mestra em Geociências.

Aprovada em: 27/11/2019

BANCA EXAMINADORA

Prof. Dr. Sérgio Pacheco Neves (Orientador)
Universidade Federal de Pernambuco

Prof. Dr. José Maurício Rangel da Silva (Examinador Externo)
Universidade Federal de Pernambuco

Prof. Dr. Caetano Juliani (Examinador Externo)
Universidade de São Paulo

Dedicado a Maria Lúcia e Maria Alita (in memoriam)

AGRADECIMENTOS

Agradecimentos são devidos à minha primeira família, por seu apoio e compreensão incessantes, mesmo distantes. Maria Lúcia, Valdeci, Vandiel, Beta e demais familiares, obrigada por todo o carinho e expectativas (e à mainha e painho, incluo o apoio financeiro nesses meses sem bolsa).

À minha segunda família, agradeço o apoio e compreensão incessantes proximais. A Wilson Andrade, obrigada pelo companheirismo de vida e pela ajuda técnica neste trabalho. A Maria Alita (in memoriam), agradeço pelos anos de convivência e exemplo de força feminina. A Eliene Andrade, agradeço todo o carinho e cuidado. A Clóvis, Adrienny e seu Fernando, agradeço o apoio e confiança. A Sonia Agostinho, companheira de carona, de sala, de almoço e de atrapalhadas, obrigada por tudo.

Aos amigos Nayara, Rafinha, João P., Raphael, Castellan, João A., Amorim, Laís Q., Solluan, Raquel, Hugo, Aldir, Riedel, Phelps, Priscila, Olga, Mário, Vicente, Luís, Laís, Glenda, Igor, Cinthya, Isis, Lília e demais colegas, agradeço todo o apoio, seja compartilhando conhecimento ou com palavras motivadoras. A João e Rafinha, agradeço também pela ajuda na preparação de amostras e pelos “Tá precisando de alguma coisa, avisa” (estendo a Nayara e Hugo).

A Carol, agradeço por me ajudar nessa jornada de autoconhecimento, e ao Mulheres da Ciência, pelas histórias inspiradoras.

Ao Laboratório de Isótopos Estáveis (LABISE), por meio dos professores Sial e Valderez, agradeço por disponibilizar o microscópio e contador para a análise modal.

Ao Laboratório de Dispositivos e Nanoestruturas (LDN), por meio do professor Edval, agradeço pelas análises de MEV na procura de monazitas.

A Daniel e ao professor George, obrigada pelo apoio com as análises de microssonda. Ao professor Lucas, agradeço pela hospedagem e boa companhia em Rio Claro (e pela melhor pizza que eu já comi).

Aos professores Ticiano e Elson, e a Robert e Alice, obrigada pela ajuda na separação de minerais e análises geocronológicas. Em especial, ao Robert, por praticamente interromper seus afazeres por uma semana (e por ir comigo, de moto, da Unicamp a Viracopos buscar amostras). Acredito que os dados vão enriquecer muito este trabalho.

Ao professor Hartmut, agradeço por disponibilizar o microscópio e material para o polimento das seções e por sua ajuda na identificação de minerais opacos.

Ao Laboratório de Geologia Sedimentar e Ambiental (LAGESE), por meio de William, Thales e do professor Virgínio, agradeço por disponibilizar o microscópio para as fotomicrografias.

Ao Conselho Nacional de Desenvolvimento Científico e Tecnológico (CNPq) e à Votorantim Metais, agradeço pelo apoio financeiro.

Finalmente, o meu muito obrigada aos meus orientadores e co-autores, professor Sérgio e professor Andres, e ao co-autor Salviano. Este trabalho não teria saído sem a ajuda de vocês.

RESUMO

Dados geofísicos, estruturais, termobarométricos e mapas de raio-X foram combinados para melhor compreensão sobre a evolução tectonometamórfica da região de Feira Nova, porção leste da Província Borborema. A região é dominada por biotita xistos e granada-biotita xistos e paragnaisses com sillimanita do Complexo Surubim, localmente migmatizados, e é limitada por ortognaisses do embasamento representados pelos complexos Vertentes e Salgadinho e pelo Complexo Metagabro-Anortosítico de Passira. Na porção sul da área, afloram os ortognaisses Açudinho e Terra Nova, considerados pré-transcorrentes, e uma porção do Complexo Vertentes, ambos desenhados por um par sinforme-antiforme macroscópico. Todas essas unidades foram afetadas por foliação de baixo ângulo (S_2) com transporte para NW, associada a zonas de cisalhamento contracionais. Uma foliação prévia desenha dobras intra-S_2. S_2 é transposta por foliação de alto ângulo (S_3) associada a zonas de cisalhamento transcorrentes sinistrais. Relacionadas à S_3, ocorrem dobras fechadas inclinadas e o par sinforme-antiforme. Encurvamento dos traços axiais dessas dobras sugere redobramento, constituindo padrão de interferência do tipo 3. Localmente, bandas de cisalhamento contracionais resultantes da tectônica transpressiva cortam S_3. Os dados sugerem uma deformação progressiva com transição entre um regime contracional e um regime transpressivo. Mapas de raios-X obtidos para o Complexo Surubim mostram alto conteúdo de Ca e Mg em núcleos de granada e de Ti em biotita, os quais sugerem condições de alta temperatura. Essas composições foram atribuídas ao pico do metamorfismo Brasiliano e sincrônicas ao desenvolvimento da foliação regional S_2. A diminuição desses conteúdos em direção às bordas desses minerais sugere esfriamento e descompressão. Os termômetros granada-biotita e o barômetro granada-Al_2SiO_5-quartzo-plagioclásio (GASP) forneceram alta temperatura (~650-760°C) e média pressão (~0,6-0,9 GPa) para o pico metamórfico, e mínimas de ~590-520°C e 0,4-0,3 GPa para o retrometamorfismo. Os dados sugerem que as rochas atingiram profundidades entre ~23 e 34 km durante o regime compressivo e foram exumadas a ~11-19 km durante o regime transpressivo. A ausência de tramas extensionais favorece exumação por erosão em vez de colapso extensional. Baseado na ocorrência de cianita na região, é inferida uma trajetória pressão-temperatura-tempo (P-T-t) do tipo horária, relacionada a espessamento em um ambiente predominantemente intracontinental, seguido por exumação sob baixas taxas de erosão e esfriamento.

Palavras-chave: Região de Feira Nova. Termobarometria. Tectônica transpressiva. Zona de cisalhamento Paudalho.

ABSTRACT

Geophysical and structural data, thermobarometric estimation and X-ray maps were combined to better understand the tectono-metamorphic evolution of the Feira Nova region, eastern Borborema Province. The region is dominated by sillimanite bearing biotite schist and garnet-biotite schist and paragneisses, locally migmatized, and is bounded by basement orthogneisses of the Vertentes and Salgadinho complexes, and by the Passira Metagabro-Anorthositic Complex. Southern of the study area, the Açudinho and Terra Nova orthogneisses crop out, considered pre-transcurrent, and a portion of the Vertentes Complex, both delineated by a macroscopic synformal-antiformal pair. All these units were affected by a gently dipping foliation (S_2) related to top-to-the-northwest transport and contracional shear zones. A previous foliation delineates intra-S_2 folds. S_2 is locally transposed by steep foliation (S_3) related to transcurrent sinistral shear zones. Folds related to S_3 comprise tight inclined folds and the synformal-antiformal pair. Bending of these folds axial traces suggests refolding, which produced a type 3 interference fold pattern. Locally, contractional shear bands resulting from the transpressive tectonics crosscut S_3. The data suggest a progressive deformation with transition between contraction and a transpression. X-ray maps obtained for the Surubim Complex show high Ca and Mg contents for garnet core compositions and of Ti for biotite, which suggest high grade conditions. These compositions were attributed to Brasiliano peak metamorphism and considered synchronous to development of the regional S_2 foliation. The rimward depletion of these contents suggest cooling and decompression. The garnet-biotite thermometer and the garnet-Al_2SiO_5-quartz-plagioclase barometer yielded high temperature (~650-760°C) and moderate pressure (~0.6-0.9 GPa) for peak conditions and up to ~590-520°C e 0.4-0.3 GPa for the retrometamorphism. The data suggest that the rocks reached ~23-34 km depths during the compressive regime and were exhumed to ~11-19 km during transpressive regime. Lack of extensional fabrics favors erosional unroofing rather than extensional collapse. Based on the occurrence of kyanite in the region, we infer a clockwise pressure-temperature-time path (P-T-t), related to thickening mostly in an intracontinental setting, followed by exhumation under low erosional and cooling rates.

Keywords: Feira Nova region. Thermobarometry. Transpressional tectonics. Paudalho shear zone.

SUMÁRIO

1 INTRODUÇÃO

A determinação do tipo de orogênese e dos diferentes ambientes tectônicos em um sistema orogênico é feita, a princípio, com base em associações petrotectônicas, mas no caso de orógenos antigos, submetidos à erosão intensa, e/ou áreas de alto grau metamórfico, tais associações de rochas podem não ser preservadas, sendo necessário métodos mais sofisticados que permitam a quantificação dos processos envolvidos na sua geração. Nos últimos anos, a reconstrução de trajetórias P-T-t (Pressão-Temperatura-tempo) em orógenos antigos por meio de estudos geocronológicos e termobarométricos muito têm contribuído para a nossa compreensão acerca da evolução de orógenos. Na literatura, porém, poucos trabalhos são dedicados à avaliação quantitativa do metamorfismo Brasiliano e proposição de trajetórias P-T-t para a Província Borborema. Com o objetivo de contribuir com o conhecimento sobre a evolução tectônica da província no Neoproterozoico, o presente trabalho compreende uma análise estrutural e de metamorfismo da região de Feira Nova, Domínio Rio Capibaribe.

1.1 ÁREA DE ESTUDO E VIAS DE ACESSO

A área de estudo está localizada na porção leste do estado de Pernambuco (figura 1), abrangendo os municípios de Feira Nova, Lagoa do Carro e Lagoa do Itaenga, situados próximo aos municípios de Carpina e Limoeiro. O trajeto de Recife a Limoeiro é feito utilizando as rodovias BR-232, BR-408, e a PE-053, em um percurso de 87 km. De Limoeiro, pode-se acessar a área de estudo através da rodovia PE-50, em um percurso de 6 km.

Figura 1 - Localização da área de estudo

Fonte: a autora, 2019.

2 RESULTADOS

Os resultados obtidos no presente trabalho são apresentados na forma de dois artigos científicos. O primeiro é intitulado "*Transition from contractional to transpressive tectonics: evidence from the Feira Nova region, Rio Capibaribe Domain, Borborema Province, NE Brazil"*, aceito para publicação na revista Brazilian Journal of Geology (figura 2), e utiliza dados geofísicos e estruturais interpretados como indicativos de uma deformação progressiva na área de estudo, com transição entre um regime compressivo e um regime transpressivo. O segundo artigo é intitulado *"Metamorphic evolution of metasedimentary rocks of the Feira Nova region: Tectonic implications for the Brasiliano Orogeny in eastern Borborema Province, Northeast Brazil",* publicado na revista Journal of South American Earth Sciences (figura 3), e utiliza dados petrográficos, termobarométricos e mapas de raio-X do Complexo Surubim para estimar a evolução metamórfica dessas rochas através de uma trajetória pressão-temperatura-tempo (P-T-t).

Figura 2 - E-mail de aceite para publicação do Artigo I

Brazilian Journal of Geology - Decision on Manuscript ID BJGEO-2020-0049.R2 Caixa de entrada ×

Claudio Riccomini <onbehalfof@manuscriptcentral.... qua., 7 de out. 12:10 (há 2 dias)
para mim, valdielly-larisse, secretaria

inglês › português Traduzir mensagem Desativar para: inglês ×

07-Oct-2020

Dear Ms. Silva:

It is a pleasure to accept your manuscript entitled "TRANSITION FROM CONTRACTIONAL TO TRANSPRESSIVE TECTONICS: EVIDENCE FROM THE FEIRA NOVA REGION, RIO CAPIBARIBE DOMAIN, BORBOREMA PROVINCE, NE BRAZIL" in its current form for publication in the Brazilian Journal of Geology. The comments of the reviewer(s) who reviewed your manuscript are included at the foot of this letter.

Thank you for your fine contribution. On behalf of the Editors of the Brazilian Journal of Geology, we look forward to your continued contributions to the Journal.

Sincerely,
Dr. Claudio Riccomini
Editor-in-Chief, Brazilian Journal of Geology

Fonte: a autora, 2019.

Figura 3 - Publicação do Artigo II

Journal of South American Earth Sciences 100 (2020) 102590

Contents lists available at ScienceDirect

Journal of South American Earth Sciences

journal homepage: www.elsevier.com/locate/jsames

Metamorphic evolution of metasedimentary rocks of the Feira Nova region: Tectonic implications for the Brasiliano Orogeny in eastern Borborema Province, Northeast Brazil

Valdielly L. Silva*, Salviano Pereira, Andres Bustamante, Sérgio P. Neves

Departamento de Geologia, Universidade Federal de Pernambuco, 50740-530, Recife, Brazil

https://doi.org/10.1016/j.jsames.2020.102590
Received 4 November 2019; Received in revised form 17 March 2020; Accepted 28 March 2020
Available online 05 April 2020

Fonte: a autora, 2019.

2.1 ARTIGO I - TRANSITION FROM CONTRACTIONAL TO TRANSPRESSIVE TECTONICS: EVIDENCE FROM THE FEIRA NOVA REGION, RIO CAPIBARIBE DOMAIN, BORBOREMA PROVINCE, NE BRAZIL

TRANSITION FROM CONTRACTIONAL TO TRANSPRESSIVE TECTONICS: EVIDENCE FROM THE FEIRA NOVA REGION, RIO CAPIBARIBE DOMAIN, BORBOREMA PROVINCE, NE BRAZIL

Valdielly Larisse Silva[1]

Sérgio Pacheco Neves[2]

[1]Programa de Pós-graduação em Geociências, Universidade Federal de Pernambuco - Recife (PE), Brazil. E-mail: vallarisse@gmail.com

[2]Departamento de Geologia, Universidade Federal de Pernambuco - Recife (PE), Brazil. E-mail: sergio.neves@ufpe.br

https://doi.org/10.1590/2317-4889202120200049

ABSTRACT

Differences in tectonic style and kinematics in orogenic belts can result from either multiphase or progressive deformation. In eastern Borborema Province, a regional shallow dipping foliation is multiply folded and crosscut by transcurrent shear zones. Here, we investigate if these fabrics resulted from diachronous deformational events or from a single-phase progressive deformation. The study area, the Feira Nova region, mostly comprises metasedimentary rocks from the Surubim Complex, and is bounded by the NE-trending sinistral Gloria do Goitá (GGSZ) and the sinistral contractional Paudalho (PSZ) shear zones, which separate it from Paleoproterozoic basement rocks. Structures can be grouped into a contractional and a transpressional stage, both related to the Brasiliano Orogeny. The contraction-related structures are represented by a gently dipping foliation (S_2) related to a top-to-the-NW tectonic transport. The contact between the metasedimentary and basement rocks is parallel to S_2, indicating the fabrics in both lithotypes are of Brasiliano age, with strain localization having produced the PSZ. NW-verging macroscopic folds are consistent with this regime. The following transpression generated steep mylonitic foliation (S_3) mainly along the GGSZ, and caused refolding. The data here presented are consistent with a progressive deformation history comprising a gradual transition from contraction to transpression.

Keywords: Feira Nova Fold Region, Transpressional Tectonics, Magnetometry, Paudalho Shear Zone, Glória do Goitá Shear Zone

1. INTRODUCTION

In protracted tectonic events, the transposition of structures formed during progressive deformation is common (e.g. Gray and Mitra, 1999; Baird and Shrady, 2011). Strain partitioning into pure and simple shear components in orogenic belts may result in domains with flat-lying fabrics alternating with domains with steep fabrics in transpressive or

transtensive regimes (e.g. Tikoff & Greene, 1997; Goscombe et al., 2008). Curvatures or geometric irregularities in transcurrent faults and shear zones may also produce local components of extension or shortening, depending on the kinematics of these structures. Alternatively, transcurrent shear zones may develop later in the orogenic evolution, representing a separate deformation phase from that responsible for the development of a regional flat-lying foliation. In the Borborema Province (Figure 1a), formed during the Brasiliano Orogeny (650-550 Ma), a flat-lying foliation related to thrusting precedes development of a transcurrent shear zone system (e.g. Guimarães et al., 2004; Neves et al., 2006a; Viegas et al., 2014; Araújo et al., 2014). In the Central Subprovince (Figure 1b), the latter reflects the accommodation and partitioning of regional strain into E-W-striking dextral and NE-SW striking sinistral conjugate pairs (Vauchez et al., 1995). Folds, which may occur in several phases and produce interference patterns (e.g. Dantas et al., 2003; Neves et al., 2017; 2018), are usually ascribed to transpression during the development of the Borborema shear zone system (e.g. Archanjo et al., 2002; 2013; Santos et al., 2004; Lima et al., 2017). Whether there is partial overlap of the contractional and transpressional regimes or if they resulted from separate deformation phases is a major issue in the tectonic evolution of the region (Neves et al., 2005), and constitutes the aim of the present study.

Here we describe the structural evolution of the Feira Nova region, located in the Rio Capibaribe Domain (Figure 1c). This is a key area to discuss the above issues because previous studies in its southern portion (Lima et al., 2015a, 2015b) documented the existence of contractional and transcurrent shear zones and folds. Lima et al. (2015a) suggested the existence of four deformation phases. D_1 would comprise an episode older than 1.7 Ga, represented by metamafic dikes crosscutting a supposed early gneissic banding. The following deformation phases (D_2 and D_3) were attributed to the Brasiliano Orogeny, of Neoproterozoic age. D_2 would have generated a flat-lying foliation affecting basement orthogneisses and supracrustal rocks

and the Paudalho Reverse Shear Zone, with NW tectonic transport. D_3 would be of transcurrent nature comprising subvertical mylonitic foliation, represented by the NNE-SSW-striking sinistral Gloria do Goitá Shear Zone and by a synformal-antiformal pair with axial traces parallel to this zone. D_4 would comprise late tectonic breccias related to younger tectonics. Through additional structural data and geophysical images, we simplify this complex polycyclic model and reinterpret the meaning of Neoproterozoic orthogneisses with intraplate signature present in the region. We characterize the deformation and folding phases of the region and suggest a new working hypothesis in which foliations and folds were produced during a single progressive event that transitioned from a contractional to a transpressive regime.

2. GEOLOGICAL SETTING

2.1 Rio Capibaribe Domain

The Rio Capibaribe Domain is located in the eastern portion of the Central Subprovince of the Borborema Province (Almeida et al., 1981) (Figure 1b). To the south, the domain is limited by the dextral East Pernambuco Shear Zone, which separates it from the Pernambuco-Alagoas Domain. To the west, it is bounded by the sinistral Congo Shear Zone, which separates it from the Alto Moxotó Domain. A large portion of the Paleoproterozoic basement of the Rio Capibaribe Domain comprises orthogneissic-migmatitic rocks from the Vertentes and Salgadinho complexes (2.18-2.04 Ga) (Neves et al, 2005, 2015). Statherian and Calymmian units (1.7-1.5 Ga) comprise the Serra de Taquaritinga Orthogneisses (Sá et al., 2002) and the Passira Metagabbro-Anorthositic Complex (Accioly, 2000). Supracrustal sequences are dominated by paragneiss and micaschist, with subordinate quartzite, marble, and metavolcanic rocks of the Neoproterozoic Surubim Complex (Neves et al., 2006, 2008). Syn-orogenic

plutonism is represented by the Caruaru-Arcoverde granitic batholith (Neves and Mariano, 1999) and the Timbaúba and Bom Jardim plutons (Guimarães, 1989, 1992).

Neves *et al*. (2005; 2006) documented ESE-trending stretching lineations related to the flat-lying foliation with kinematic indicators pointing to top-to-the-NW transport. According to Neves *et al.* (2005), the main foliation present in the basement and supracrustal rocks of the Rio Capibaribe Domain was affected by three generations of meso- and macroscopic folds: F_3 - south-verging inclined to recumbent, sometimes with axial plane foliation; F_4 - gentle to open NE-SW upright- coeval with transcurrent shear zones; F_5 - NW-SE upright gentle, which bent the axial planes of the previous folds. These latter generations were considered to result from a component of NE-SW shortening coeval to F_4, or the result of late deformation. Intra- and synfolial folds were interpreted as earlier folding episodes (F_1, F_2). Phases of similar geometry were described in the Alto Moxotó Domain (Neves et al., 2017; 2018), but with inverted axial planes between F_4 and F_5, and lack of macroscopic expression for F_3.

2.2 Feira Nova Region

The study area comprises the region defined as Feira Nova Fold Belt by Accioly *et al*. (2003) and Lima *et al*. (2015a, b), which is located in the eastern Rio Capibaribe Domain (Figure 1b). It is limited by the Glória do Goitá and Paudalho shear zones, which separate the so-called Carpina and São Lourenço gneissic-migmatitic blocks, respectively. Outcrops are scarce in the region and frequently moderate to highly weathered. Western basement rocks include the Vertentes and Salgadinho complexes (Neves et al., 2015) and the Passira Metagabbro-Anorthositic Complex (Accioly et al., 2003), while the supracrustal rocks are dominated by locally migmatized pelitic to semi-pelitic paragneiss and schist, and to a lesser extent, quartzite. Some authors (e.g. Lima et al., 2015a, b) attribute these rocks (or part of their occurrence area) to the Vertentes Complex using the original definition of this unit: sequences of mafic to intermediary metavolcanic rocks and pelitic paragneisses (Santos and Medeiros,

1999). Due to the absence of metavolcanic rocks, we consider the metasedimentary rocks to belong to the Surubim Complex (Melo and Siqueira, 1971; Neves et al., 2006b).

The most remarkable structure of the region is an overturned synformal-antiformal pair, located in the southern portion of the study area and highlighted by folding of the Açudinho and Terra Nova orthogneisses (Lima et al., 2015a, b). The Açudinho Orthogneiss comprises garnet and muscovite-bearing peraluminous leuco-orthogneisses, and the Terra Nova Orthogneiss is a riebeckite-, aegirine-augite- and magnetite-bearing orthogneiss, both of which were interpreted as folded tabular intrusions (Lima et al., 2015a, b). The Terra Nova Orthogneiss is peralkaline to slightly peraluminous and with a geochemical signature suggesting a post-collisional to an intraplate setting (Lima et al., 2015b). These authors obtained a U-Pb zircon age of 617 ± 8.8 Ma from a syenitic sample, which they interpreted as suggesting crystallization of the protolith during a transtensional event.

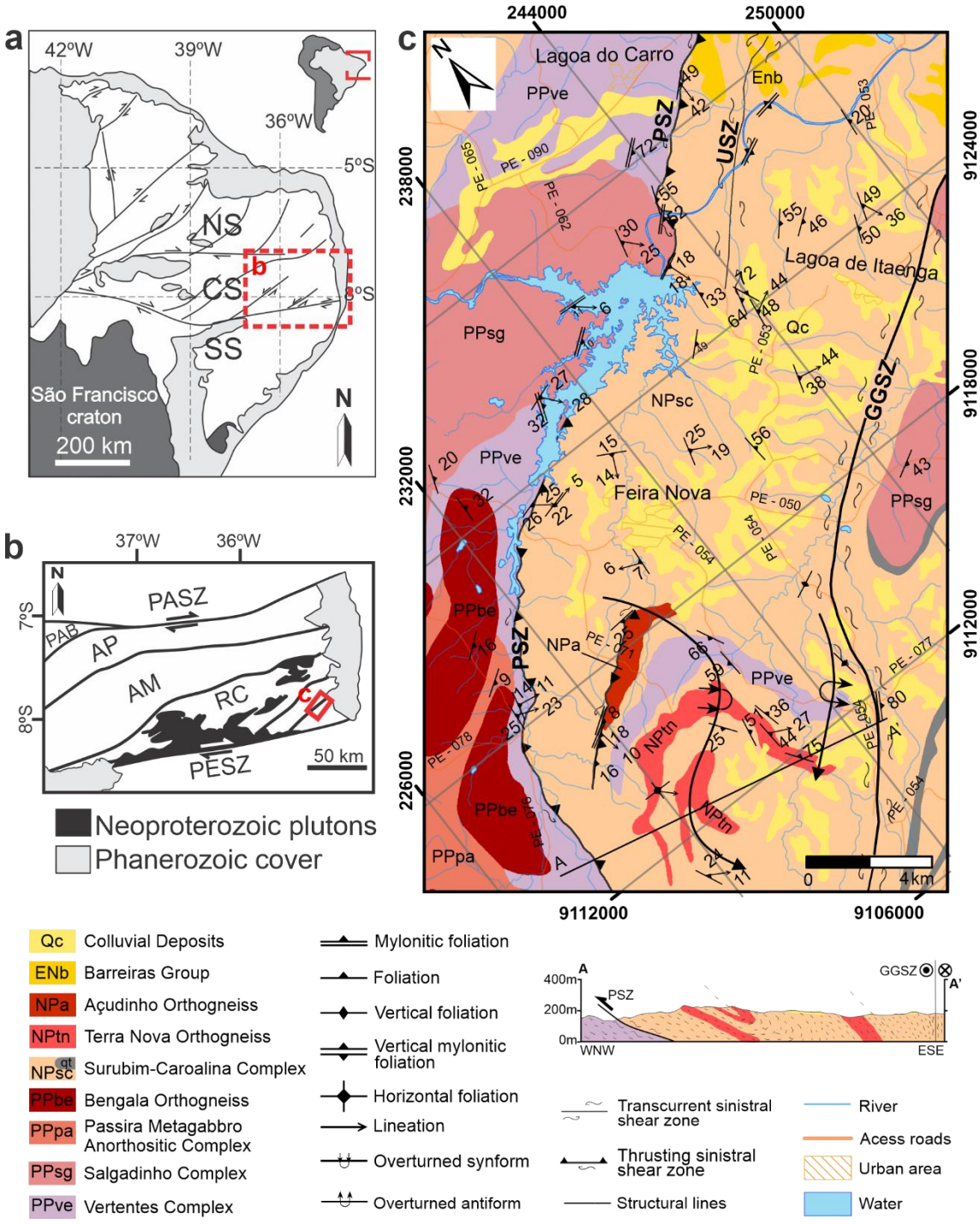

Figure 1: Geological map of the Feira Nova region and its location in the Rio Capibaribe Domain and Central Subprovince of the Borborema Province. NS: Northern Subprovince; CS: Central Subprovince; SS: Southern Subprovince; AP: Alto Pajeú Domain; AM: Alto Moxotó Domain; RC: Rio Capibaribe Domain; PASZ: Patos Shear Zone; PESZ: Pernambuco Shear Zone (modified from Silva et al., 2020).

3. MATERIAL AND METHODS

Aeromagnetic data used in this work are from the *Projeto Aerogeofísico Borda Leste do Planalto da Borborema* (code 1079), made by Lasa Engenharia e Prospecções through a partnership between Serviço Geológico do Brasil - CPRM and Ministério de Minas e Energia. The acquisition was made in 2008 and has N-S flight lines, 100 m of nominal high and 500 m of spacing. Control lines are E-W and have 5 km of spacing. The obtained data were processed by CPRM and by Votorantim Metais Ltda-MMG, including the application of the Reduction to Pole and Vertical Derivative filters to the Total Magnetic Field Anomaly image (Figure 2).

Some anomalies are too gentle to be noticed in an anomaly map, which requires their amplification by filtering. The Vertical Derivative Anomaly Filter (DZ) (Milligan and Gunn, 1997) aims at amplifying, in the vertical direction, the boundaries of anomaly sources and boundaries related to faults and other shallow features, being largely used in geological mapping to identify structural features. The Reduction to Pole filter (Baranov and Naudy, 1964), in its turn, approximately relocates the anomalies over their sources, converting bipolar asymmetrical anomalies into monopolar symmetrical ones, which are usually simpler and easier to interpret. The application of this filter commonly produces instabilities at low latitude regions, but the results for the study area are satisfactory.

In terms of structural geology, we integrate field observations and mapping features from the existing literature and newly collected data (foliation, lineation, and folding axes), as well as additional macro-, meso- and microstructural observations.

4. RESULTS

4.1 Aeromagnetometry

Five magnetic domains were individualized using the Reduction to Pole Map (Figure 2b) and correlated to field and literature data:

- Domain A generally exhibits high magnetic intensity and is separated from Domain B by a well-defined magnetic lineament related to the Paudalho Shear Zone. It comprises basement orthogneisses (Vertentes and Salgadinho complexes). Although aeromagnetometry did not allow us to distinguish between them, magnetic susceptibility measures using a KT-10 kappameter showed higher values for Salgadinho Complex. The extreme south of this domain, where intensity values are relatively low, corresponds to the Passira Gabbro-Anorthositic Complex and Bengala Orthogneiss.
- Domain B has a less rough texture than Domain A, with low values of magnetic intensity; it corresponds to the Surubim-Caroalina Complex.
- Domains C and D are domains of rough texture, with high values of magnetic intensity and anomalies with sigmoidal geometry. Domain C comprises the Surubim Complex, with rocks locally affected by an unnamed sinistral shear zone. Domain D comprises basement orthogneisses and is related to the Glória do Goitá Shear Zone.
- Domain E also shows rough magnetic texture and high values of magnetic intensity. It comprises the Açudinho and Terra Nova orthogneisses and the Vertentes Complex. It also outlines a synformal-antiformal pair which presents NE-SW axial traces gently bent.

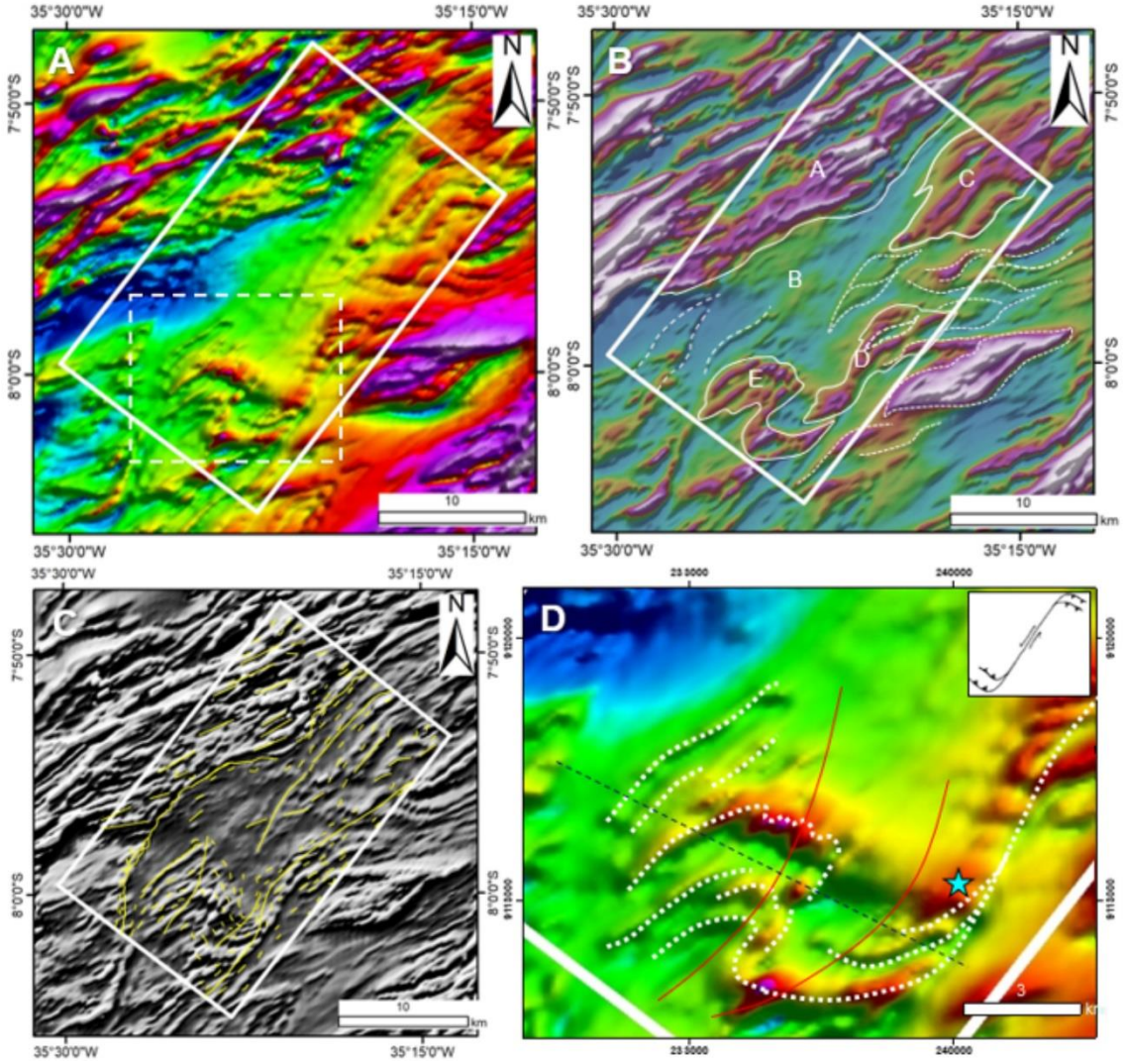

Figure 2: Magnetometric Maps: (a) Total Magnetic Field Anomaly Map; (b) Reduction to Pole Map with magnetic domains and inferred sigmoidal magnetic anomalies; c) Vertical Derivative Map with inferred magnetic lineaments; d) Total Magnetic Field Anomaly Map in the south of the study area showing the inferred fold axial traces and its relationship with the Glória do Goitá Shear Zone. The star indicates an outcrop where reverse shear bands of top-to-the-SW transport were found. The sketch shows the possible thrusting related to transcurrent shear zones with such geometry and kinematics.

Magnetic lineaments traced from the Vertical Derivative Map (Figure 2c) suggest NE-SW-striking features, sometimes sigmoidal, that can be related to field structures. Most of these features are also seen in other magnetometric maps. The Total Magnetic Field Anomaly and Reduction to Pole maps show NE-SW sigmoidal anomalies suggesting sinistral movement

(Figures 2a,b) which are mainly coincident with the shear zones. The folding of Domain E is better observed in the Total Magnetic Field Map, where it is more continuous and shows an apparent inflection of its axial traces. The continuity between domains D and E suggests that these folds and the Glória do Goitá Shear Zone are genetically associated, as pointed out by Lima et al. (2015a), and define a horse-tail ending for the latter (Figure 2d).

4.2 Structural Geology

4.2.1 THRUST TECTONICS

Contour plots of poles to foliation in the study area indicate the prevalence of a flat-lying to SE-moderately-dipping foliation (principal foliation/S_p) in the Brasiliano-age Açudinho and Terra Nova orthogneisses, metasedimentary rocks, and basement orthogneisses, being more systematic in the latter (Figure 3a-c). In basement rocks, a local previous metamorphic foliation delineates intrafolial folds, which allows naming S_p as S_2 (Figure 3d). This previous foliation is also observed petrographically in micaschist and paragneiss, being defined by rare kink biotite porphyroblasts and biotite inclusions in garnet that are orthogonal or oblique to S_2 (Silva et al., 2020). Stretching mineral lineations have dominantly low plunge and medium to high rake and are marked by quartz, feldspar, sillimanite, amphibole, and pressure shadows around garnet (figure 3f). The lineations are less scattered in basement rocks, where they are southeast-plunging, and, locally, south-plunging (Figure 3b).

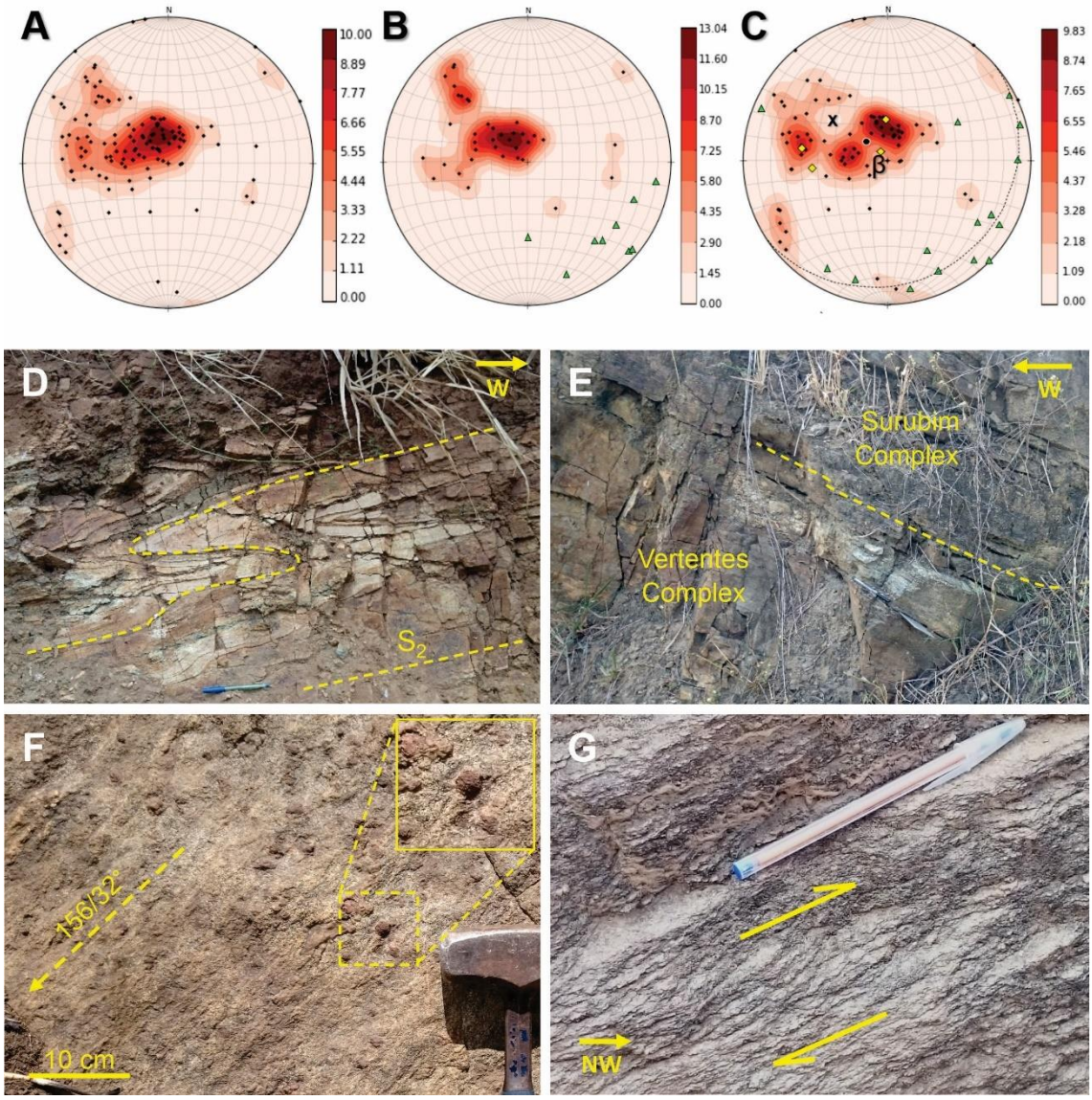

Figure 3: (a) Lower hemisphere, equal area projection of poles to foliation (S_2, S_3) in the study area (n = 126); (b) Contour plots of poles to foliation (S_2, S_3) in basement rocks (n = 38; circles) and lineation plots (n = 9; triangles); (c) Contour plots of poles to foliation (S_2, S_3) in metasedimentary rocks (n = 81) and lineation plots (n = 14; triangles); "x" indicates the approximate pole to a small circle defined by the contour plots of poles to foliation; the β axis was calculated from the great circle defined by lineations. Yellow plots correspond to poles to foliation from Açudinho and Terra Nova orthogneisses; (d) Older foliation defining a tight to isoclinal intrafolial fold (profile view) with an axial plane parallel to S_2 (Vertentes Complex); (e) Contact between Vertentes and Surubim complexes along with the Paudalho Shear Zone (profile view); (f) Surubim Complex paragneiss with stretching lineation (azimuth, plunge) in plain view marked by pressure shadows in garnet (right upper corner); (g) Surubim Complex

paragneiss with shear bands (132°/16°(dip direction, dip) indicating a top-to-the-northwest sense of shear.

Strain localization during S_2 development is represented by the Paudalho Shear Zone (PSZ), which is marked by mylonites and protomylonites. The contact between the basement and metasedimentary rocks observed across the PSZ shows that the banding of the basement orthogneiss and the mylonitic foliation of the metasedimentary rocks (S_2) are parallel to each other and to the contact (Figure 3e). The PSZ also has a sinistral component, which is detailed in section 4.2.2. Kinematic indicators in metasedimentary rocks and along with the aforementioned contact indicate a top-to-the-northwest sense of shear, pointing out a contractional regime (figure 3g). Basement rocks present strong planar fabric and kinematic indicators were not found. Mylonitic foliation related to S_2 is also observed in the west limb of the major synform, along with the Brasiliano orthogneisses and metasedimentary rocks, suggesting that its development started during the thrusting.

In all mapped units, microstructures related to the regional foliation include quartz grains showing dynamic recrystallization by grain boundary migration (Figure 4a), including chessboard extinction (Figure 4b), overlapped by subgrain rotation and bulging recrystallization (Figure 4c, d.) Undulose extinction and deformation bands are ubiquitous. Feldspar show subgrain formation (locally), flame perthite, myrmekite intergrowth in the edges of the grains, undulose extinction, deformation twins, and kink bands.

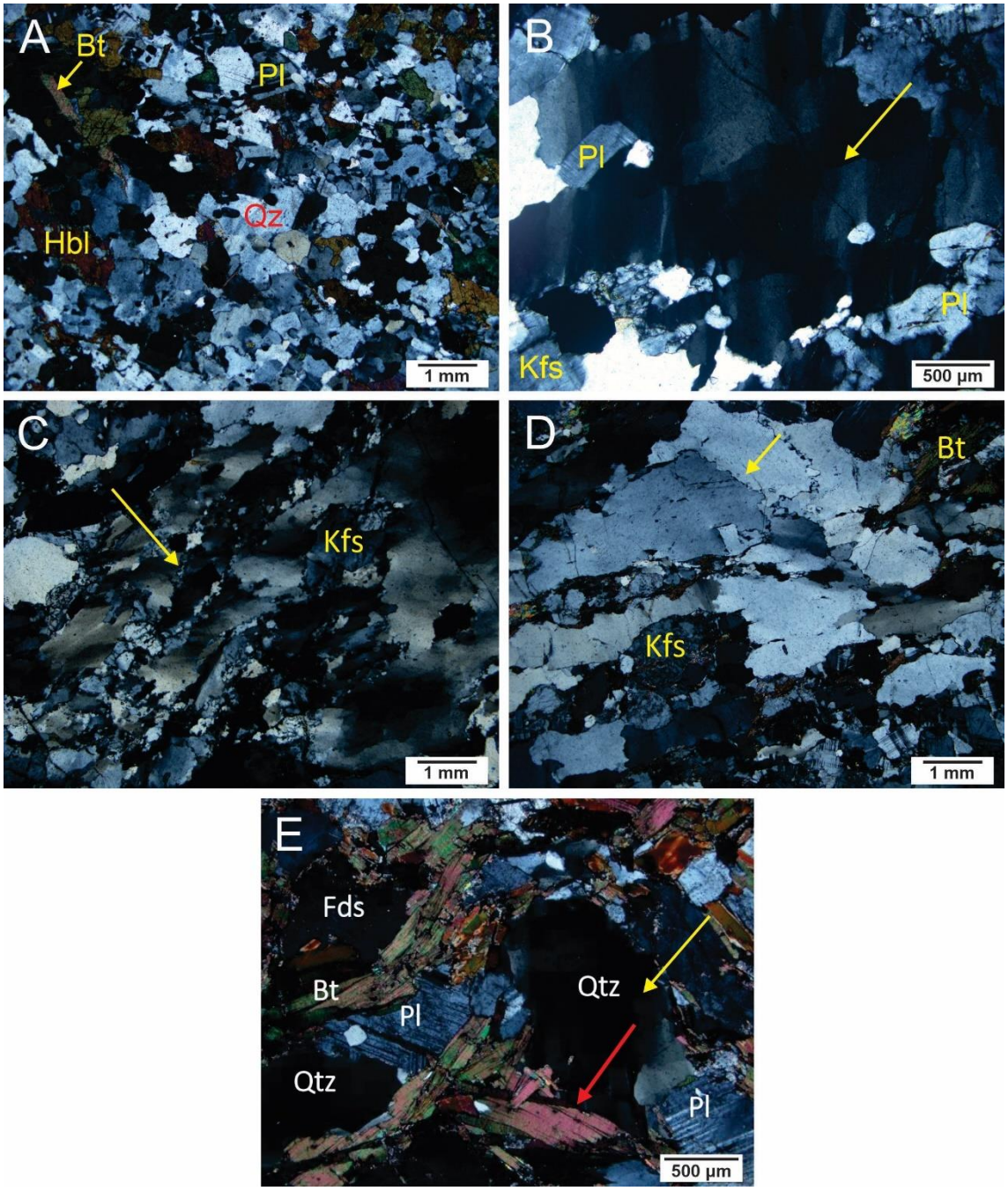

Figure 4: Deformation mechanisms in the study area. (a), (b), (c), and (d) are related to the flat-lying foliation; (a) Quartz chessboard extinction (arrow) in the Terra Nova Orthogneiss. (b) Grain boundary migration in the Salgadinho Complex. (c) Bulging recrystallization (arrow) in the Terra Nova orthogneiss; (d) Bulging recrystallization (arrow) overlapping grain boundary migration in the Açudinho Orthogneiss; (e) Mica fish (red arrow) and quartz chessboard extinction (yellow arrow) in protomylonite from the Gloria do Goitá Shear Zone. Qtz = quartz; Bt = biotite; Kfs = K-feldspar; Fds = feldspar; Pl = plagioclase; Hbl = hornblende.

4.2.2 STRIKE-SLIP TECTONICS

Steep mylonitic foliation characterizes the Glória do Goitá Shear Zone (GGSZ) (Figure 5a) and an unnamed smaller shear zone in the north of the study area (Figure 5b). Sinistral sense of shear in both of them is indicated by S-C fabrics and shear bands in mylonites (Figure 5c) together with regional sigmoidal magnetic anomalies (Figure 2).

Previous works (Accioly, 2000; Lima et al., 2015a,b) defined the PSZ only as a thrust shear zone, though, a sinistral component was also documented in this study. At the northern portion of the structure, a moderate to steep foliation predominates (30-70°) (Figure 1). Additionally, subhorizontal low rake lineations occur locally across the PSZ. These observations allow classifying the PSZ as a thrust (or thrust sinistral) shear zone at the south portion, and as a sinistral thrust at the north portion of the study area.

Brittle-ductile shear zones and pseudotachylyte veins occur in the northern portion of the PSZ and in unnamed shear zones (Figure 5d), indicating late reactivation of these structures. This is further supported by cataclastic microstructures and mesoscopic cataclastic zones.

Microstructural data for the GGSZ are scarce, due to intense weathering of most outcrops or to smooth paving slabs in others, making too hard to sample by hammering. A protomylonite sample from the GGSZ shows features such as feldspar porphyroclasts wrapped by mica, stretching of some quartz grains, and mica fish. Grain boundary migration mechanisms predominate in quartz grains, including chessboard extinction (figure 4e), and are overlapped by bulging recrystallization and cataclasis. Feldspar crystals show local bulging and common deformation twins, and biotite shows strong undulose extinction and local kink bands.

4.2.3 FOLDS

The macroscopic synformal-antiformal pair, which comprises a NW-verging tight fold (synform) and an upright tight fold (antiform), both SW-plunging, is the most remarkable

structural feature in the study area (Fig. 2c). The bending of their NE-SW axial traces (Figure 1c), especially of the synform, indicates refolding by a subsequent folding phase (Lima et al., 2015a; this work), featuring a type 3 interference pattern (Ramsay, 1967). Mesoscopic tight inclined folds, locally with gently curved axial planes (Figure 5e), and open upright folds (Figure 5f) probably are related to these two folding phases.

In the eastern limb of the macroscopic antiform, decimeter-scale reverse shear bands with a top-to-the-SW sense of shear occur locally, cutting across S_3 (Figure 5g). These bands are in accordance with the horsetail termination suggested for the GGSZ.

5. DISCUSSION

We interpret foliations and folds in the Feira Nova region to have formed during two ductile deformation stages that together represent a progressive tectonic evolution rather than a polycyclic one. The parallelism between the gneissic banding in basement orthogneisses, the schistosity in metasedimentary rocks, and of their contact across the PSZ (Figure 3c) support that these fabrics (S_2) were produced during the same tectonic event. Contour plots of pole to foliation also show comparable attitudes for the two lithotypes and for Neoproterozoic orthogneisses (Açudinho and Terra Nova) (Figure 3a,c), supporting that these structures nucleated during the Brasiliano Orogeny. Lima et al. (2015a), on the other hand, suggests that the gneissic banding belongs to a distinct former deformation phase (older than 1.7 Ga), based on metamafic dikes that cut across the banding and were correlated with the 1.7 Ga-old Passira Complex (Accioly, 2000).

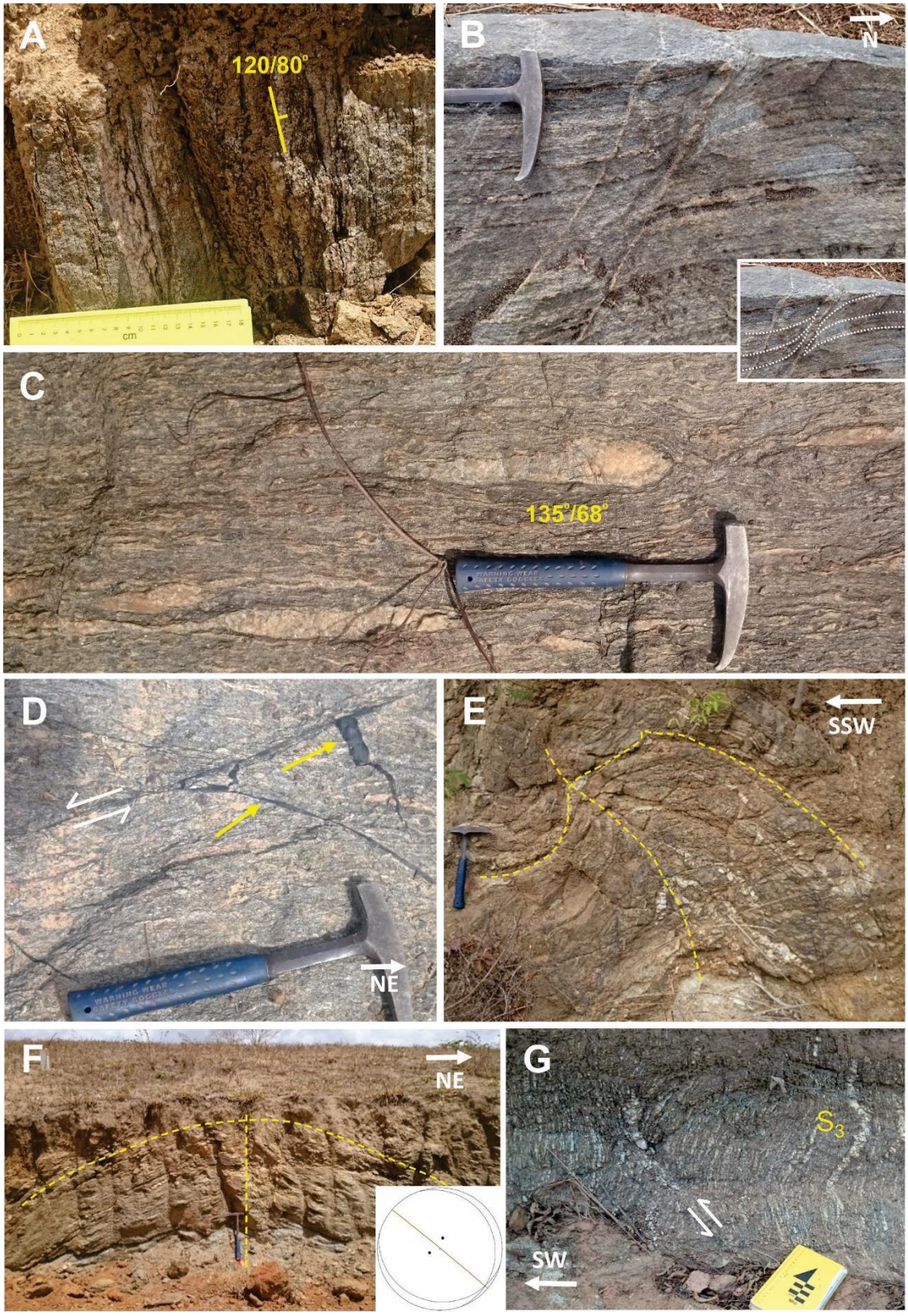

Figure 5: Structures related to the transpressional regime. (a) Subvertical foliation in mylonitic paragneiss from Surubim Complex related to the Glória do Goitá Shear Zone; (b) sinistral shear band related to the Paudalho Shear Zone (Salgadinho Complex; plain view); (c) plain view of stretched quartz

veins in mylonitic paragneiss (Surubim Complex) related to the northern shear zone (Silva et al., 2020); (d) Pseudotachylytes (arrow) in mylonitic paragneiss (Surubim Complex; plain view); (e) Inclined tight fold with a gently curved axial plane (Vertentes Complex; profile view); (f) Open upright fold with the projection of limbs indicating a subhorizontal NW axis (Surubim Complex); (g) Reverse shear bands with top-to-the-SW transport cutting across steep foliation (S_3) (Surubim Complex; profile view).

For these authors, the flat-lying fabric would have been acquired later, sometime between 1.7 and 0.6 Ga. In this work, structures prior to S_2 are limited to a local isoclinally folded foliation present in basement rocks (Figure 3b) and seen petrographically in both basement and Neoproterozoic supracrustal units (Silva et al., 2020). Therefore, this foliation also belongs to the contractional regime and the mentioned dikes may be actually younger than what Accioly (2000) proposed, being related to the late stages of the Brasiliano Orogeny.

As well as the regional fabric, both Terra Nova and Açudinho orthogneisses show a flat-lying to gently dipping foliation (although affected by folding) (Figure 1c), which indicates that these units are older or coeval to the contractional regime, and thus, pre-transcurrent at least. Also, the age of Terra Nova Orthogneiss (617±8,8 Ma) (Lima et al., 2015b) is within the regional time span attributed to pre-transcurrent plutons (630-590 Ma) (e.g. Guimarães et al., 2004; Neves et al., 2006a, 2020; Van Schmus *et al*., 2011; Araújo et al., 2014). Lima et al. (2015a) interpreted the Terra Nova Orthogneiss as a marker of a contractional phase with a top-to-the-NW sense of shear. Lima et al. (2015b), on the other hand, interpreted the Terra Nova Orthogneiss as indicating a syn-orogenic transtensional event based on its relationship with the GGSZ and geochemical signature suggestive of an extensional setting. However, the geochemistry may be reflecting the nature of the source and not the tectonic setting of intrusion. This inference about the influence of the source is consistent with the nearby occurrence of the Passira metagabbro-anorthositic Complex (Accioly, 2000), indicating that sources with intraplate characteristics may be present at depth. Along with the absence of structural data

suggesting syn-orogenic extension (or transtension), it is therefore more likely that the Terra Nova Orthogneiss intruded Surubim Complex as sheets along its foliation in the contractional regime (as previously suggested by Lima et al., 2015a), and was later affected by transcurrent/transpressive deformation.

The microstructures related to both flat-lying and steep foliation (Figure 4) suggest that temperature conditions were high during thrusting, remained high during strike-slip deformation (e.g. chessboard extinction in quartz), and then migrated to lower ones (e.g. bulging recrystallization in quartz). Using conventional garnet-biotite geothermometer, garnet-Al_2SiO_5-quartz-plagioclase (GASP) geobarometer, and X-ray maps, Silva et al. (2020) estimated metamorphic peak conditions of 650-760 °C and ~0.6–0.9 GPa for the Surubim Complex in the study area, coeval with the development of flat-lying foliation and local anatexis. Garnet rims indicated 590-520 °C and 0.4-0.3 GPa, which was interpreted as exhumation with low erosional and cooling rates. In the study area, a mean age of 592±2 Ma yielded by monazite grains from the Surubim Complex (Teixeira et al., in preparation) is consistent with regional early- to syn-transcurrent ages, also suggesting the persistence of high-temperature conditions.

Nucleation of the antiformal-synformal pair probably represents the transition from a contractional to a transpressive regime. Shearing of pre-existing folds, regardless of their initial orientation, tend to rotate them towards parallelism with the shear direction (e.g. Escher and Waterson, 1974; Carreras et al., 2005; Carreras and Druguet, 2019). The accordance between the vergence of these folds and the regional transport (northwest) suggests they nucleated during the contractional regime. This inference is also supported by the occurrence of a small reverse shear zone in the western limb of the synform (Figure 1c), which was possibly formed by limb disruption. Subsequent rotation and steepening of the folds axial planes can be attributed to transpression coeval with the development of the GGSZ.

The orientation of the fold axes that caused the refolding observed at map scale can be inferred through the analysis of contour plots of poles to foliation and lineations (Figure 3c). In the first case, they define a small circle centered at 307º/51º (trend, plunge). In the second, lineations define a great circle, probably resulting from the dispersion of originally SE-plunging lineations (e.g. Duebendorfer, 2003), with a NW-plunging pole (312º/75º). Refolding may be explained by a local SW-NE shortening component developed to accommodate ductile strain at the GGSZ termination, once shear-related folds tend to nucleate at a high angle to the shear direction (Carreras et al., 2005). So, the formation of the late folds would not have required changing the orientation of regional stress axes (e.g. Neves et al., 2018) and most likely constitutes part of the same progressive deformation. Indeed, type 3 interference patterns have been described as a product of progressive or even coeval deformation (e.g. Forbes et al., 2004; Baird & Shrady, 2011; Fossen et al., 2013; Carreras and Druguet, 2019) and explained by limbs that steepened enough to shorten and buckle transversally (Fossen et al., 2013) or by curving of axial surfaces due to instabilities in them (Carreras and Druguet, 2019).

In synthesis, the results of this study indicate that the structural evolution of the Feira Nova region resulted from a progressive sequence of events (Fig. 6): (1) Thrusting produced a regional flat-lying foliation associated with non-coaxial shear with top-to-the-northwest tectonic transport. Strain localization along the contact of the Surubim Complex with basement rocks gave rise to the PSZ. (2) Probably due to rheological contrasts resulting from intercalation of orthogneisses with metasedimentary rocks, folds were developed at the advanced stages of this contractional phase, producing northwest-verging macroscopic folds. (3) Crustal thickening resulting from shortening may have induced escape tectonics and development of the GGSZ. The transition from thrusting to transpression is supported by the local steepening of the PSZ and of the axial plane of the macroscopic antiformal fold. (4) The growing of the GGSZ induced development of NW-trending folds and reverse shear bands at its terminations.

The proposed evolution is in line with propositions that multiple deformation fabrics can be explained by progressive deformation rather than by several temporarily separated events (i.e., polycyclic deformation) (e.g. Holdsworth, 1990; Connors and Lister, 1995; Forster and Lister, 2008; Fossen et al., 2019; Fossen, 2019; Bhattacharya et al., 2019).

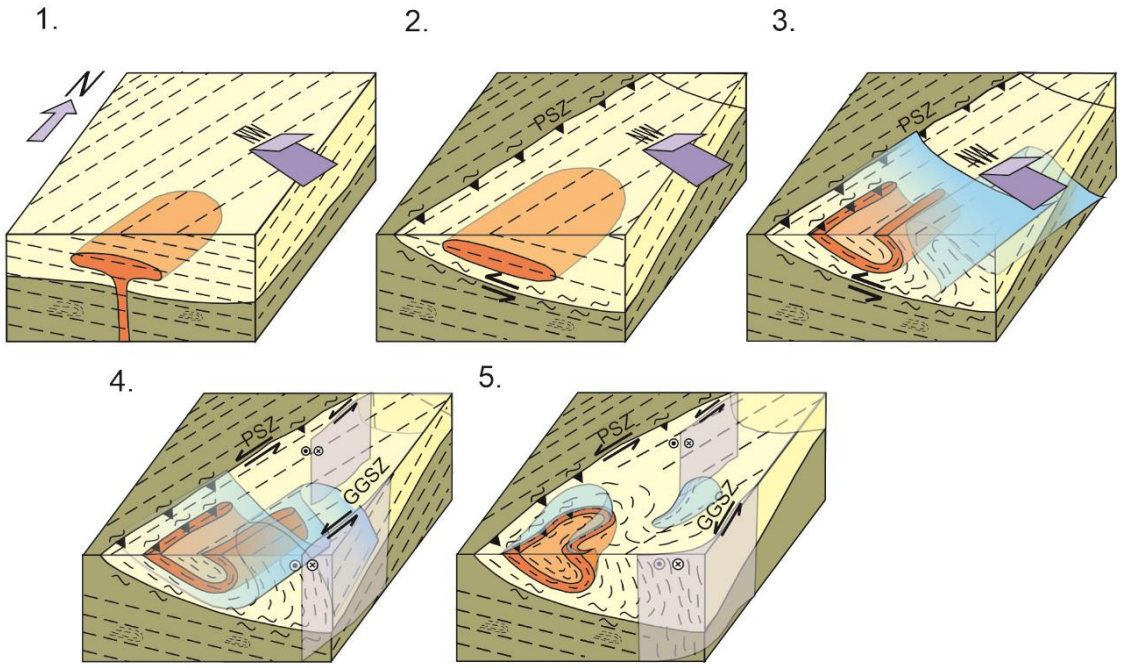

Figure 6. Simplified schematic block diagrams depicting the structural evolution of the study area. 1. Distributed non-coaxial shear with top-to-the-NW tectonic transport and intrusion of the Terra Nova orthogneiss during the development of a flat-lying foliation; 2. nucleation of the PSZ along with the contact between the basement and supracrustal rocks; 3. development of folds induced by the top-to-the-NW tectonics; 4. transition to transpressive tectonics with nucleation of GGSZ and local steepening of PSZ and antiform limbs; 5. Refolding related to local SW-NE shortening developed to accommodate ductile strain at the shear zone termination.

An alternative interpretation compatible with the observed structures in the study area would involve contemporaneous development of the PSZ and GCSZ. In this case, strain partitioning would have resulted in dip-slip-dominated transpression in the west and strike-slip-dominated transpression in the east. We consider this possibility unlikely given the regional context. Indeed, U-Pb dating of regional deformation and metamorphism and of pre-

transcurrent plutons has consistently yielded ages older than 600 Ma whereas syntranscurrent plutons are usually younger than 590 Ma (Guimarães et al., 2004; Neves et al., 2006a, 2006b, 2008, 2020; Archanjo et al., 2008; Van Schmus et al., 2011). So, it is more likely that the GGSZ post-dates development of the PSZ.

6. CONCLUSIONS

Structural and geophysical data suggest two ductile deformation stages for the Feira Nova region, both related to the Brasiliano Orogeny. The first is a contractional stage that produced flat-lying foliation (S_2) with a top-to-the-NW sense of shear and localization of deformation represented by the reverse component of Paudalho Shear Zone (PSZ). S_2 transposed a previous local foliation, also belonging to this regime, and which locally define isoclinal folds. NW-verging folds were nucleated later during this deformation event and steepened during the subsequent transpression. Transpression produced a steep mylonitic foliation associated with sinistral transcurrent shear zones, including Glória do Goitá Shear Zone (GGSZ) and a sinistral component of PSZ. As the GGSZ developed, local shortening was yielded on its SW termination leading to nucleation of NW-trending open folds that refolded the earlier formed folds and produced a type 3 interference pattern. The data are consistent with transition from a contractional to a transpressive regime, related to progressive rather than polycyclic deformation.

ACKNOWLEDGMENTS

We thank former Votorantim Metais for funding this work and Wilson R. A. Freitas for technical support. For their constructive comments, we thank José M. Rangel da Silva, Lauro C. M. L Santos, the reviewers Alain Vauchez and Sebastián Oriolo, and the editor Haakon Fossen. V.L.S. also thanks CNPq for the scholarship.

REFERENCES

Accioly, A.C.A., McReath, I., Santos, E.J., Guimarães, I.P., Vannuci, R., Bottazzi, R., 2000. The Passira meta-anorthositic complex and its tectonic implication, Borborema Province, Brazil. In: Proceedings of the 31st International Geological Congress, International Union of Geological Sciences, Rio de Janeiro.

Accioly, A.C.A., McReath, I., Santos, E.J., Guimarães, I.P., Santos, A.C., 2003. The Ages of Crystallization and Metamorphism of the Passira Anorthosite Complex Borborema Province, Northeastern Brazil. In: IV South American Symposium on Isotope Geology, Salvador, 487-490.

Almeida, F.F.M., Hasui, Y., Brito Neves, B.B., Fuck, R. 1981. Brazilian Structural Provinces: An introduction. *Earth Science Reviews*, **17**:1-29.

Araujo, C.E.G., Weinberg, R.F., Cordani, U.G., 2014. Extruding the Borborema Province (NE-Brazil): a two-stage Neoproterozoic collision process. Terra Nova, 26(2):157-168. https://doi.org/10.1038/ncomms6198

Archanjo, C.J., Trindade, R.I., Bouchez, J.L., Ernesto, M., 2002. Granite fabrics and regional-scale strain partitioning in the Seridó belt (Borborema Province, NE Brazil). Tectonics, 21(1):1-14.

Archanjo, C.J., Hollanda, M.H.B.M., Rodrigues, S.W.O., Brito Neves, B.B., Armstrong, R., 2008. Fabrics of pre- and syntectonic granite plutons and chronology of shear zones in the Eastern Borborema Province, NE Brazil. Journal of Structural Geology 30, 310-326.

Archanjo, C.J., Viegas, L.G.F., Hollanda, M.H.B.M., Souza, L.C., Liu, D., 2013. Timing of the HT/LP transpression in the Neoproterozoic Seridó Belt (Borborema Province, Brazil):

Constraints from U-Pb (SHRIMP) geochronology and implications for the connections between NE Brazil and West Africa. Gondwana Research, 23(2):701-714. https://doi.org/10.1016/j.gr.2012.05.005

Baird, G.B., Shrady, C.H., 2011. Timing and kinematics of deformation in the northwest Adirondack Lowlands, New York State: Implications for terrane relationships in the southern Grenville Province. Geosphere, 7(6):1303-1323.

Baranov, V., Naudy, H., 1964. Numerical Calculation of the Formula of Reduction to the Magnetic Pole. Geophysics, 29:67-79. https://doi.org/10.1130/GES00689.1

Bhattacharya, A., Rekha, S., Sequeira, N., Chatterjee, A., 2019. Transition from shallow to steep foliation in the Early Neoproterozoic Gangpur accretionary orogen (Eastern India): Mechanics, significance of mid-crustal deformation, and case for subduction polarity reversal? Lithos, 348-349:105196. https://doi.org/ 10.1016/ j.lithos.2019.105196

Carreras, J., Druguet, E., Griera, A., 2005. Shear zone-related folds. Journal of Structural Geology, 27: 1229-1251. https://doi.org/10.1016/j.jsg.2004.08.004

Carreras, J., Druguet, E., 2019. Complex fold patterns developed by progressive deformation. Journal of Structural Geology, 125:195-201. https://doi.org/10.1016/ j.jsg.2018.07.015

Connors, K.C., Lister, G.S., 1995. Polyphase deformation in the western Mount Isa Inlier, Australia: episodic or continuous deformation? Journal of Structural Geology, 17(3):305-328.

Dantas, E.L., Silva, A.M., Almeida, T., Moraes, R.A.V., 2003. Old geophysical data applied to modern geological mapping problems: a case-study in the Seridó Belt, NE Brazil. Revista Brasileira de Geociências, 33(2): 65-72.

Duebendorfer, E.M., 2003. The interpretation of stretching lineations in multiply deformed terranes: an example from the Hualapai Mountains, Arizona, USA. Journal of Structural Geology, 25(9):1393-1400.

Escher, A., Waterson, J., 1974. Stretching fabrics, folds and crustal shortening. Tectonophysics, 22:223-231.

Forbes, C.J., Betts, P.G., Lister, G.S., 2004. Synchronous development of Type 2 and Type 3-fold interference patterns: evidence for recumbent sheath folds in the Allendale Area, Broken Hill, NSW, Australia. Journal of Structural Geology, 26(1):113-126. https://doi.org/10.1016/S0191-8141(03)00074-9

Fossen, H., Teyssier, C., Whitney, D.L., 2013. Transtensional folding. Journal of Structural Geology, 56:89-112. http://dx.doi.org/10.1016/j.jsg.2013.09.004

Fossen, H., 2019. Writing papers with an emphasis on structural geology and tectonics: advices and warnings. Brazilian Journal of Geology, 49(4):1-6. https://doi.org/10.1590/2317-4889201920190109

Fossen, H., Cavalcante, G.C., Pinheiro, R.V.L., Archanjo, C.J., 2019. Deformation – progressive or multiphase? Journal of Structural Geology, 125:82-99. https://doi.org/10.1016/j.jsg.2018.05.006

Forster, M.A., Lister, G.S, 2008. Tectonic sequence diagrams and the structural evolution of schists and gneisses in multiply deformed terranes. Journal of Geological Society, 165:923-939. https://doi.org/10.1144/0016-76492007-016

Goscombe, B.D., Gray, D.R., 2008. Structure and strain variation at mid-crustal levels in a transpressional orogen: A review of Kaoko Belt structure and the character of West

Gondwana amalgamation and dispersal. Gondwana Research, 13(1):45-85. https://doi.org/10.1016/j.gr.2007.07.002

Gray, M.B., Mitra, G., 1999. Ramifications of four-dimensional progressive deformation in contractional mountain belts. Journal of Structural Geology, 21(8), 1151–1160. https://doi.org/10.1016/S0191-8141(99)00059-0

Guimarães, I.P., 1989. The petrological evolution and tectonic associations of the Bom Jardim Complex, Pernambuco State, NE Brazil. Tese de doutorado, University of London, London 423p.

Guimarães, I.P., Silva Filho, A.F., 1992. Evolução petrológica e geoquímica do complexo Bom Jardim, Pernambuco. Revista Brasileira, 2(22): 29-42.

Guimarães, I.P., da Silva Filho, A.F., Almeida, C.N., Van Schmus, W.R., Araújo, J.M.M., Melo, S.C., Melo, E.B., 2004. Brasiliano (Pan-African) granitic magmatism in the Pajeú-Paraíba belt, Northeast Brazil: an isotopic and geochronological approach. Precambrian Research, 135:23-53. https://doi.org/10.1016/j.precamres.2004.07. 004

Holdsworth, R.E., 1990. Progressive deformation structures associated with ductile thrusts in the Moine Nappe, Sutherland, N. Scotland. Journal of Structural Geology, 12(4):443-452.

Lima, H.M., Santos, E.J., Santos, L.C.M.L., 2015a. Compartimentação estrutural da faixa Feira Nova e blocos adjacentes: Implicações para a evolução do terreno Rio Capibaribe da Província Borborema, NE do Brasil. Revista Brasileira de Mineração e Meio Ambiente, 5(2):32-38.

Lima, H.M., Ferreira, V.P., Santos, E.J., Pimentel. M.M., Santos, L.C.M.L., 2015b. Origem, significado petrogenético e idade dos ortognaisses Terra Nova: registro de magmatismo

alcalino transtensional Neoproterozoico no domínio da zona transversal da Província Borborema. Geochimica Brasiliensis, 29:70-86.

Lima, H.M., Pimentel, M.M., Santos, L.C.M.L., Mendes, V.A., 2017. Análise tectônica da porção Nordeste da Faixa Sergipana, Província Borborema: Dupla vergência em resposta a colisão oblíqua entre o cráton do São Francisco e o Terreno Pernambuco-Alagoas. Geonomos, 25(2):20-30. https://doi.org/10.18285/ geonomos. v25i2.1078

Melo, A.A., Siqueira, L.P., 1971. Novas considerações sobre a geologia do pré-cambriano de Pernambuco Oriental. Revista da Associação dos Geólogo de Pernambuco, 1(2):32-41.

Milligan, P.R., Gunn P.J., 1997. Enhancement and presentation of airborne geophysical data. AGSO Journal of Australian Geology and Geophysics, 17(2):62-75.

Neves, S.P., Mariano, G., 1999. Assessing the tectonic significance of a large-scale transcurrent shear zone system: the Pernambuco lineament, northeastern Brazil. Journal of Structural Geology, 21(10):1369-1383.

Neves, S.P., Silva, J.M.R., Mariano, G., 2005. Oblique lineations in orthogneisses and supracrustal rocks: vertical partitioning of strain in a hot crust (eastern Borborema Province, NE Brazil). Journal of Structural Geology, 27(8):1513-1527. https://doi.org/10.1016/j.jsg.2005.02.002

Neves S.P., Mariano G., Correia P.B., Silva J.M.R., 2006a. 70 m.y. of synorogenic plutonism in eastern Borborema Province (NE Brazil): temporal and kinematic constraints on the Brasiliano Orogeny. Geodinamica Acta, 19:213-236.

Neves, S.P., Bruguier, O., Vauchez, A., Bosch, D., Silva, J.M.R., Mariano, G., 2006b. Timing of crustal formation, deposition of supracrustal sequences and Transamazonian and

Brasiliano metamorphism in eastern Borborema Province (NE Brazil): Implications for western Gondwana assembly. *Precambrian Research,* 149**:**197-216. https://doi.org/10.1016/j.precamres.2006.06.005

Neves, S.P., Bruguier, O., Bosch, D., Silva, J.M.R., Mariano, G., 2008. U–Pb ages of plutonic and metaplutonic rocks in southern Borborema Province (NE Brazil): Timing of Brasiliano deformation and magmatism. Journal of South American Earth Science, 25(3):285-297. https://doi.org/10.1016/j.jsames.2007.06.003

Neves, S.P., Lages, G.A., Brasilino, R.G., Miranda, A.W.A., 2015. Paleoproterozoic accretionary and collisional processes and the build-up of the Borborema Province (NE Brazil): geochronological and geochemical evidence from the Central Domain. Journal of South American Earth Science, 58:165-187. http://dx.doi.org/ 10.1016/j.jsames.2014.06.009

Neves, S.P., Silva, J.M.R., Bruguier, O., 2017. Geometry, kinematics and geochronology of the Sertânia Complex (central Borborema Province, NE Brazil): Assessing the role of accretionary versus intraplate processes during West Gondwana assembly. Precambrian Research, 298:552-571. http://dx.doi.org/ 10.1016/j.precamres.2017. 07.006

Neves, S.P., Santos, T.A.S., Medeiros, P.C., Amorim, L.Q., Casimiro, D.C.G., 2018. Interference fold patterns in regional unidirectional stress fields; a result of local kinematic interactions. Journal of Structural Geology,115:304-310. https://doi.org/10.1016/j.jsg.2018.04.012

Neves, S.P., Teixeira, C.M.L., Bruguier, O., 2020. Long-lived localized magmatism in central-eastern part of the Pernambuco-Alagoas Domain, Borborema Province (NE Brazil):

Implications for tectonic setting, heat sources, and lithospheric reworking. Precambrian Research, 337, 1055592. https://doi.org/ 10.1016/j.precamres. 2019.105559

Ramsay, J. G., 1967, Folding and Fracturing of Rocks. New York: McGraw-Hill, 568p.

Sá, J.M., Bertrand, J.M., Leterrier, J., Macedo, M.H.F., 2002. Geochemistry and geochronology of pre-Brasiliano rocks from the Transversal Zone, Borborema Province, Northeast Brazil. Journal of South American Earth Sciences 14:851–866.

Santos, E.J., Medeiros, V.C., 1999. Constraints from granitic plutonism on proterozoic crustal growth of the Transverse Zone, Borborema Province, NE-Brazil. Revista Brasileira de Geociências 29:73-84.

Santos, E.J., Nutman, A.P., Brito Neves, B.B., 2004. Idades SHRIMP U-Pb do Complexo Sertânia: implicações sobre a evolução tectônica da Zona Transversal, Província Borborema. Geologia USP - Série Científica, 4(1):1-12.

Silva, V.L, Pereira, S., Bustamante, A., Neves, S.P., 2020. Metamorphic evolution of metasedimentary rocks of the Feira Nova region: Tectonic implications for the Brasiliano orogeny in eastern Borborema Province Northeast Brazil. Journal of South American Earth Sciences, 100, 102590. https://doi.org/10.1016/j.jsames. 2020.102590

Tikoff, B., Greene, D., 1997. Stretching lineations in transpressional shear zones: an example from the Sierra Nevada Batholith, California. Journal of Structural Geology 19:29–39.

Van Schmus, W. R.; Kozuch, M., Brito Neves, B. B., 2011. Precambrian history of the Zona Transversal of the Borborema Province, NE Brazil: Insights from Sm/Nd and U/Pb geochronology. *Journal of South American Earth Sciences*, **31:**227-252. https://doi.org/10.1016/j.jsames.2011.02.010

Vauchez A., Neves S.P., Caby R., Corsini M., Egydio-Silva M., Arthaud M.H., Amaro V., 1995. The Borborema shear zone system, NE Brazil. Journal of South American Earth Sciences, 8:247-266.

Viegas L.G.F., Archanjo C.J., Hollanda M.H.B.M., Vauchez A. 2014. Microfabrics and zircon U-Pb (SHRIMP) chronology of mylonites from the Patos shear zone (Borborema Province, NE Brazil). Precambrian Research, 243:1-17. https://doi.org/10.1016/j.precamres.2013.12.020

2.2 ARTIGO II - METAMORPHIC EVOLUTION OF METASEDIMENTARY ROCKS OF THE FEIRA NOVA REGION: TECTONIC IMPLICATIONS FOR THE BRASILIANO OROGENY IN EASTERN BORBOREMA PROVINCE, NORTHEAST BRAZIL

Metamorphic evolution of metasedimentary rocks of the Feira Nova region: Tectonic implications for the Brasiliano Orogeny in eastern Borborema Province, Northeast Brazil

Valdielly L. Silva*, Salviano Pereira, Andres Bustamante, Sérgio P. Neves
Departamento de Geologia, Universidade Federal de Pernambuco, 50740-530, Recife, Brazil

https://doi.org/10.1016/j.jsames.2020.102590

Abstract

Thermobarometric estimations and X-ray maps were combined to evaluate the metamorphic evolution of metasedimentary rocks (Surubim Complex) in the Feira Nova region, eastern Borborema Province (NE Brazil). Sillimanite-bearing biotite schists, garnet-biotite schists and gneisses were studied. X-ray maps show different growing phases and retrograde zoning patterns for biotite and garnet. High Ca and Mg contents in garnet cores along with high Ti in biotite are interpreted as equilibrium compositions at peak metamorphism. Lower contents of Ca and Mg at garnet rims and of Ti in biotite rims suggest cooling and decompression. Garnet-biotite geothermometer and garnet-Al2SiO5-quartz-plagioclase (GASP) geobarometer constrain high temperature (~650–760 °C) and medium pressure (~0.6–0.9 GPa; burial to ~23–34 km) conditions for the metamorphic peak, which was synchronous to development of a flat-lying foliation and local anatexis. Garnet rims indicate exhumation to ~19-11 km (~0.4–0.3 GPa) at ~590-520 °C,

probably during a transpressional regime. The data points to low exhumation and cooling rates. The lack of extensional fabrics in the region right after the Brasiliano Orogeny supports erosional unroofing rather than extensional collapse. Based on kyanite occurrences nearby, we infer a clockwise P-T path related to thickening in a predominant intracontinental setting, followed by exhumation with low erosional and cooling rates.

1. Introduction

Thermobarometric estimates of successive mineral assemblages - demonstrated by pressure-temperature-time (P-T-t) paths - are useful for describing tectonic settings and orogenic processes. In some cases, obliteration of previous metamorphic assemblages at peak metamorphism only allow definition of partial P-T-t paths, provided by retrograde assemblages and mineral zoning (e.g. Spear and Selverstone, 1983; Hodges and Royden, 1984; Florence and Spear, 1995). These paths can yield important information on the late tectonic history of orogens. They depend mostly on occurrence or not of late-to post-orogenic extension, rates of erosion, magmatism, and radioactive heating (e.g. England and Richardson, 1977; England and Thompson, 1984; Ruppel and Hodges, 1994). The slopes of these paths may define isobaric or near-isobaric cooling (e.g. Halpin et al., 2007; Liu et al., 2016), isothermal decompression (e.g. Ernst, 1988; Sommer et al., 2008), or a combination of these processes.

The Borborema Province (Almeida et al., 1981) is known to have been formed as a result of convergence of old crustal blocks (Amazonian, West-African and São Francisco-Congo cratons) during the Neoproterozoic Brasiliano-Pan African event (e.g. Van Schmus et al., 2008). In this context, local high-P/low-T assemblages have been interpreted either as resulting from long-lived subduction of large oceans (e.g. Caby et al., 2009; Brito Neves et al., 2016) or as short-lived subduction of proto-oceans (e.g. Neves and Mariano, 2003; Neves, 2018).

Few works have provided a quantitative evaluation of the Brasiliano metamorphism in the Borborema Province. Most of them give information on peak metamorphic conditions (e.g. Leite et al., 2000; Neves et al., 2000, 2012; Amaral et al., 2012), while others place constraints on the cooling history of the province (e.g. Corsini et al., 1998; Neves et al., 2000, 2012; Dhuime et al., 2003; Hollanda et al., 2010). Only a few provide P-T-t paths (Castro, 2004; Santos et al., 2009, 2018a) that can give information on orogenic processes (from burial, attainment of peak metamorphism and uplift and erosion), which have been long used to distinguish tectonic settings (e.g. England and Thompson, 1984; Wakabayashi, 2004).

In eastern Borborema Province, preliminary thermobarometric estimates for metamorphism of metasedimentary rocks are limited to only one work (Neves et al., 2012). In order to fill this general lack of information, in this work, we present detailed petrographic and mineral chemistry data (thermobarometry and X-ray maps) to provide a quantitative estimate of the P-T trajectory of the Feira Nova region in eastern Borborema Province (Fig. 1) during peak and post-peak metamorphic conditions. Together with literature data, we discuss on the tectonothermal evolution of the region and place constraints on regional tectonics.

2. Geological setting

2.1. Regional geology

The Borborema Province (Almeida et al., 1981) is usually subdivided into several domains and three major subprovinces: Northern, Central and Southern (Fig. 1a), which are separated by the E-W striking Patos and Pernambuco Shear Zone systems (e.g. Brito Neves et al., 2000; Van Schmus et al., 2011). The Central Subprovince is dominated by a gneissic and migmatitic basement of Paleoproterozoic age and by Neoproterozoic supracrustal associations and granitic to syenitic plutons, all affected by or related to the Brasiliano Orogeny (e.g., Van Schmus et al., 2011). Deformation featured by this event includes widespread flat-lying foliation related to thrusting (650-600 Ma) and major transcurrent shear zones (590-560 Ma) (e.g., Guimarães et al., 2004; Neves et al., 2006, 2020; Araújo et al., 2014). A system of NE-SW striking shear zones divides the Central Subprovince into four main domains, from east to west: Rio Capibaribe, Alto-Moxotó, Alto-Pajeú and Piancó-Alto Brígida (e.g., Van Schmus et al., 2011). Some researchers also point to the São Pedro and São José de Caiana segments in the westernmost portion (eg. Brito Neves et al., 2016; Basto et al., 2019).

Most of the metasedimentary rocks of the Alto-Moxotó and the Rio Capibaribe domains have been classified into the Sertânia and Surubim complexes, respectively (e.g., Santos et al., 2004; Neves et al., 2006, 2009, 2017). Both comprise garnet-biotite gneiss, muscovite-biotite gneiss, micaschist, quartzite, marble and minor metamafic and calc-silicate rocks. Sillimanite-bearing gneisses and schists are common, and along with migmatization, attest to the high-grade metamorphism (Neves et al., 2017). The depositional age of the Surubim complex from the Rio Capibaribe Domain is well defined in the Cryogenian (< 670 Ma) (Neves et al., 2006, 2009; Brito Neves et al., 2013; Da Silva Filho et al., 2014; Teixeira, 2015), while its age of metamorphism is attributed to the Ediacaran (~630-620 Ma) by the dating of leucosome of a

migmatite and zircon overgrowths (Neves et al., 2006; Brito Neves et al., 2013). Neves et al. (2006, 2009; 2017) and Neves and Alcantara (2010) point out to resemblances of lithotypes, metamorphic grade, depositional ages and geochemical signatures of the Surubim Complex and Sertânia Complex from the Alto Moxotó Domain, indicating that they were deposited on a once contiguous tract of continental crust.

2.2. Study area

In the eastern portion of the Rio Capibaribe Domain, metasedimentary rocks related to the Surubim Complex occur in a sigmoidal belt limited by the NE-SW-striking Gloria do Goitá (GGSZ) and Paudalho (PSZ) shear zones, respectively (Fig. 1c), which has been named Feira Nova Fold Belt (Accioly, 2000) (Fig. 1b). Basement rocks of this region comprise the Vertentes, Salgadinho and Passira complexes. The ca. 2.1 Ga Vertentes Complex (Neves et al., 2006, 2015; Brito Neves et al., 2013) comprises locally migmatized and regularly banded garnet bearing hornblende-biotite orthogneisses of quartz-dioritic to monzodioritic composition. The ca. 2.05 Ga Salgadinho Complex (Neves et al., 2015) comprises migmatized and magnetite-bearing hornblende biotite orthogneisses of granodioritic to syenogranitic composition, with local magma mixing with quartz-diorite. The ca. 1.7 Ga Passira Complex is formed by massive meta anorthosites associated with metagabbros (Accioly, 2000; Accioly et al., 2003).

The Feira Nova region is dominated by locally migmatized paragneiss, pelitic to semi pelitic schist, and subordinated quartzite. These rocks are intercalated with sheets of the peraluminous Açudinho Orthogneiss and the peralkaline Terra Nova Orthogneiss (Lima et al., 2015). The Açudinho Orthogneiss comprises finely banded two-mica orthogneisses of syenogranitic composition, containing magnetite and garnet. The Terra Nova orthogneiss has alkali-feldspar syenitic to alkali feldspar granitic composition, containing aegirine-augite, arfvedsonite, riebeckite and magnetite, and has been dated at 617 ± 8.8 Ma (Lima et al., 2015). Basement rocks of the Vertentes Complex also crop out in the central portion of the study area.

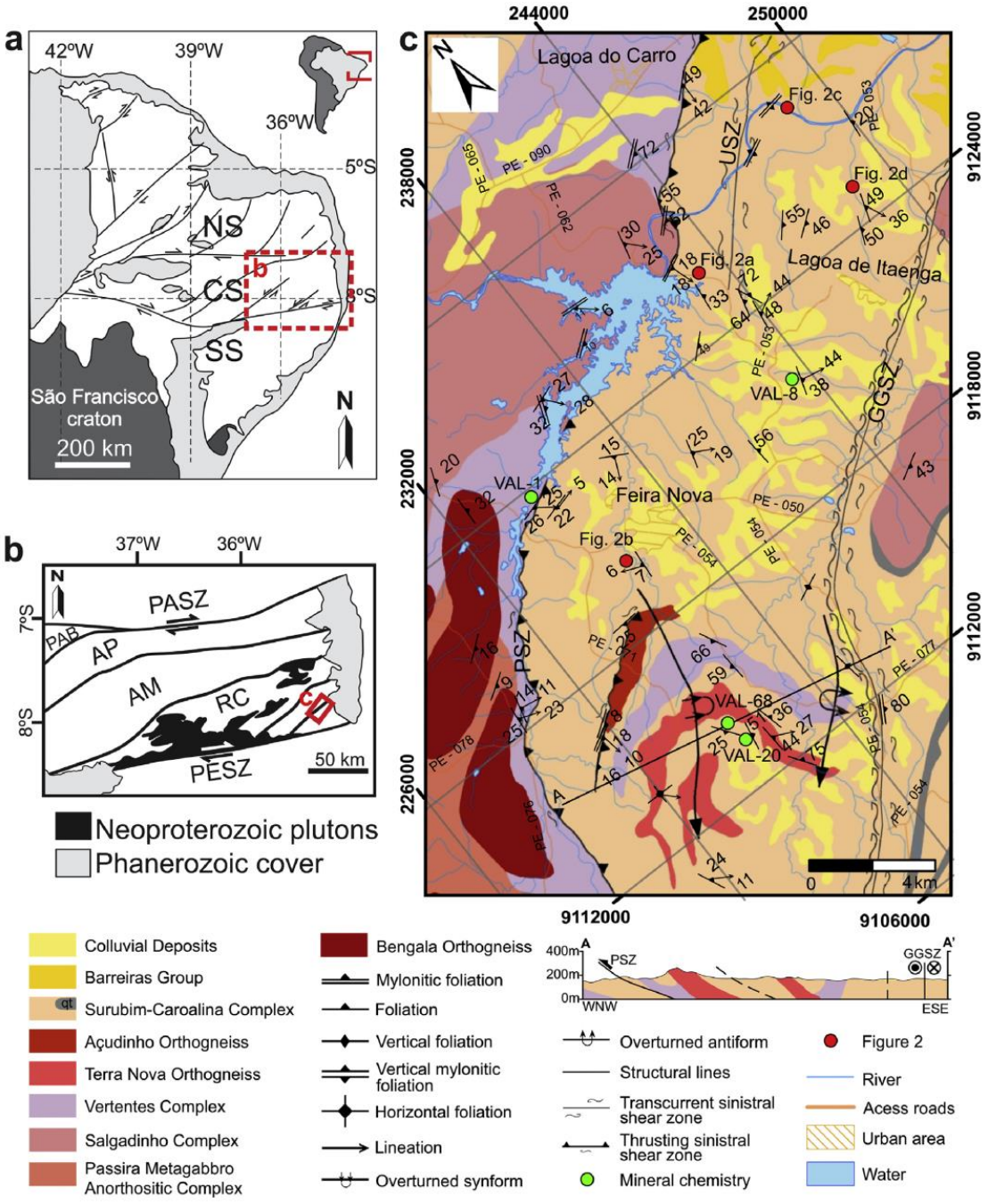

Fig. 1. Sketches showing the subdivision of the Borborema Province in Northern (NS), Central (CS) and Southern (SS) subprovinces (a), and of the Central subprovince in the Rio Capibaribe (RC), Alto Moxotó (AM), Alto Pajeú (AP) and Piancó-Alto Brígida (PAB) domains (b). PASZ = Patos Shear Zone; PESZ = Pernambuco Shear Zone. (c) Geological map of the study area (modified from Santos et al., 2018b; Lima et al., 2015). Location shown in (b). PSZ = Paudalho Shear Zone; GGSZ = Glória do Goitá Shear Zone; USZ = unnamed shear zone.

3. Field relationships

The studied rocks comprise locally migmatized biotite schist and garnet-biotite schist and gneiss of the Surubim Complex (Fig. 2a). They are usually medium-grained tourmaline- and sillimanite-bearing rocks, with the last one occurring as fibrous, and more rarely, as prismatic crystals. Sillimanite is also more common in the central and south portions of the area, around the Açudinho and Terra Nova orthogneisses. Garnet crystals are usually millimeter-sized (Fig. 2b) but may reach up to 3.5 cm in diameter, where they define porphyroblastic texture or are elongate due to mimetic growth (Fig. 2c). Quartz and quartz-feldspathic veins of millimetric to decimetric size are common, sometimes defining intrafolial folds. Migmatitic paragneisses and schists (Fig. 2d) occur mainly around Lagoa do Itaenga city (Fig. 1c), in outcrops where sillimanite and tourmaline are incipient. They are usually stromatic, with a sometimes boudinaged medium-to coarse grained leucosome composed of quartz and feldspar, and a biotite-rich melanosome. Leucosome also occurs as quartz-feldspathic pressure shadows around garnet crystals.

The main foliation in the study area is NE-trending, flat-lying, affected by macroscopic inclined folds in the south, and crosscut by strike-slip shear zones (Fig. 1c). The contact between the Surubim and the Vertentes complexes is tectonic, marked by the sinistral thrusting PSZ, with both units occurring as mylonites and protomylonites. Strike-slip shear zones comprise the sinistral GGSZ, along which the rocks are mylonitized and/or crosscut by shear bands, and a smaller and unnamed shear zone (USZ) occurring in the north-central portion. The structural data suggest the region was affected by a progressive deformation, with transition between a compressional and a transpressional regime, marked by an initial phase of NW-directed thrusting and strain localization along the PSZ, followed by folding of the main foliation and development of transcurrent shear zones (Silva et al., in preparation).

4. Petrography

Biotite schist, garnet-biotite schist and gneiss were studied, with modal compositions comprising quartz (20–44%), biotite (23–39%), plagioclase (21–38%), microcline (≤7%), and garnet (≤8%). These last two also occur as accessory minerals, along with sillimanite, tourmaline, muscovite, apatite, zircon, monazite, graphite, magnetite, ilmenite, and rutile. The sum of these latter may reach up to 7%. Quartz and feldspar are usually segregated from mica into microbands, defining the main foliation (S_2). When not elongated/subidioblastic, quartz

and feldspar dominance over mica defines a lepidogranoblastic texture, and garnet grains are occasionally porphyroblastic. Mylonites present an S-C fabric locally overprinted by cataclastic bands.

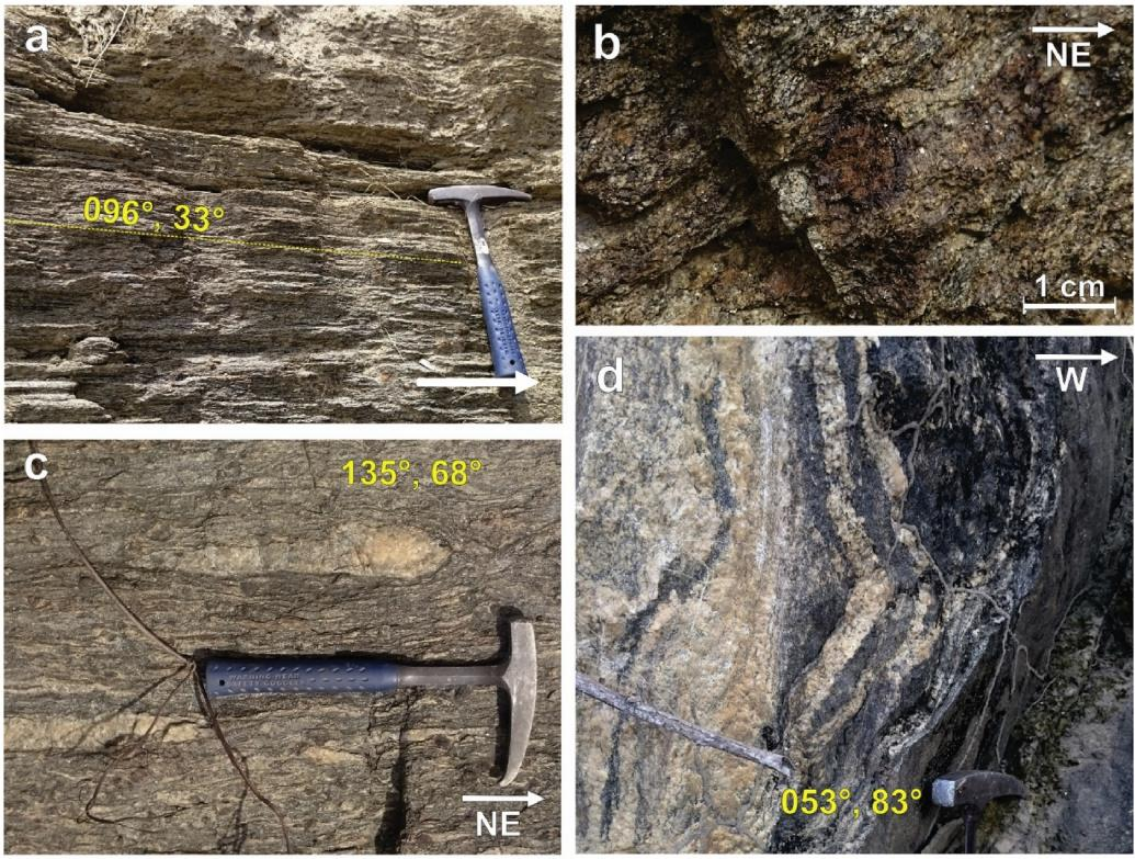

Fig. 2. Field aspects of the Surubim-Caroalina Complex. (a) Flat-lying foliation in garnet-biotite schist. (b) Garnet porphyroblast with corona composed of biotite, quartz, and feldspar in schist. (c) Stretched quartz veins in mylonitic gneiss. d) Migmatite with stromatic structure and a biotite-rich melanosome.

Quartz usually occurs as fine to medium-grained grains and, occasionally, as coarse xenoblastic grains (< 6 mm). In mylonites, lens shaped crystals and aggregates along with plagioclase are common, sometimes forming large sigmoids (< 2 cm). Undulose extinction and/or deformation bands occur in quartz grains from all samples. Most of them show dynamic recrystallization by grain boundary migration, including chessboard extinction (Fig. 3a), overlapped by subgrain rotation and, sometimes, bulging recrystallization.

Plagioclase occurs as fine-to medium-grained (< 4 mm) subidioblastic to xenoblastic crystals, sometimes with anti-perthitic texture. Deformation twins, kink bands and undulose extinction are common. Inclusions of quartz, mainly globular, and biotite are occasional, with some rare poikiloblastic crystals. In some mylonites, plagioclase also occurs with a core-and-

mantle texture. Neoformed K-feldspar occurs in gneisses and schists associated with or near migmatites, the latter consisting of microcline-rich (< 60%) leucosome. K feldspar comprises xenoblastic, fine-to medium-grained (< 2 mm) and sometimes perthitic microcline (Fig. 3b). Myrmekite intergrowth is common on the edges of the grains. Bulging and subgrain formation are local. Sericitization and argilization are common processes in both feldspars.

Biotite usually occurs as fine-to medium subidioblastic lamellae (< 3 mm). Inclusions comprise apatite, opaque minerals, zircon, and monazite. The main foliation (S_2) is defined by biotite along with quartz, feldspar, sillimanite, and graphite. Biotite occurs with or without undulose extinction - and more rarely, folded, or kinked. It commonly wraps around garnet, tourmaline, quartz, and feldspar, which thus represent early-S_2 crystals. Straight biotite inclusions in plagioclase and garnet, and commonly kinked biotite lamellae are orthogonal/oblique to S_2 or define microfolds inside it. It thus suggests an earlier foliation (S_1) (Fig. 3c). Graphite generally occurs as straight or folded lamellae adjacent to biotite or included within it. In mylonites, the S_3 foliation is defined by biotite lamellae that show strong undulose extinction and commonly occur as mica fish or kinked, suggesting that they resulted from reorientation of the S_2 foliation. Nucleation of new biotite grains occurs locally, crosscutting biotite lamellae that define S_2 (Fig. 3d). Later crystallized biotite occurs as clusters that form radial or decussate microstructures (Fig. 3e), and possibly fine biotite lamellae intergrown with plagioclase (Fig. 3d). Occasionally, biotite retrogrades to chlorite, and more rarely, presents white mica rims. This latter mostly occurs as short lamellae or interstitial masses associated with sericitized feldspar, and in less extent, as lamellae intergrown with biotite along S_2.

Sillimanite is almost always fibrolite (Fig. 3f), mostly defining S_2 and occurring adjacent to or inside biotite lamellae. Occasionally, fibrolite partially replaces garnet crystals or forms masses of what seems to be pseudomorphs after this mineral. In some mylonites, sillimanite occurs either straight and along with S_3, or as bent prisms (syn-S_2). Occasionally, fibrolite retrogrades to white mica.

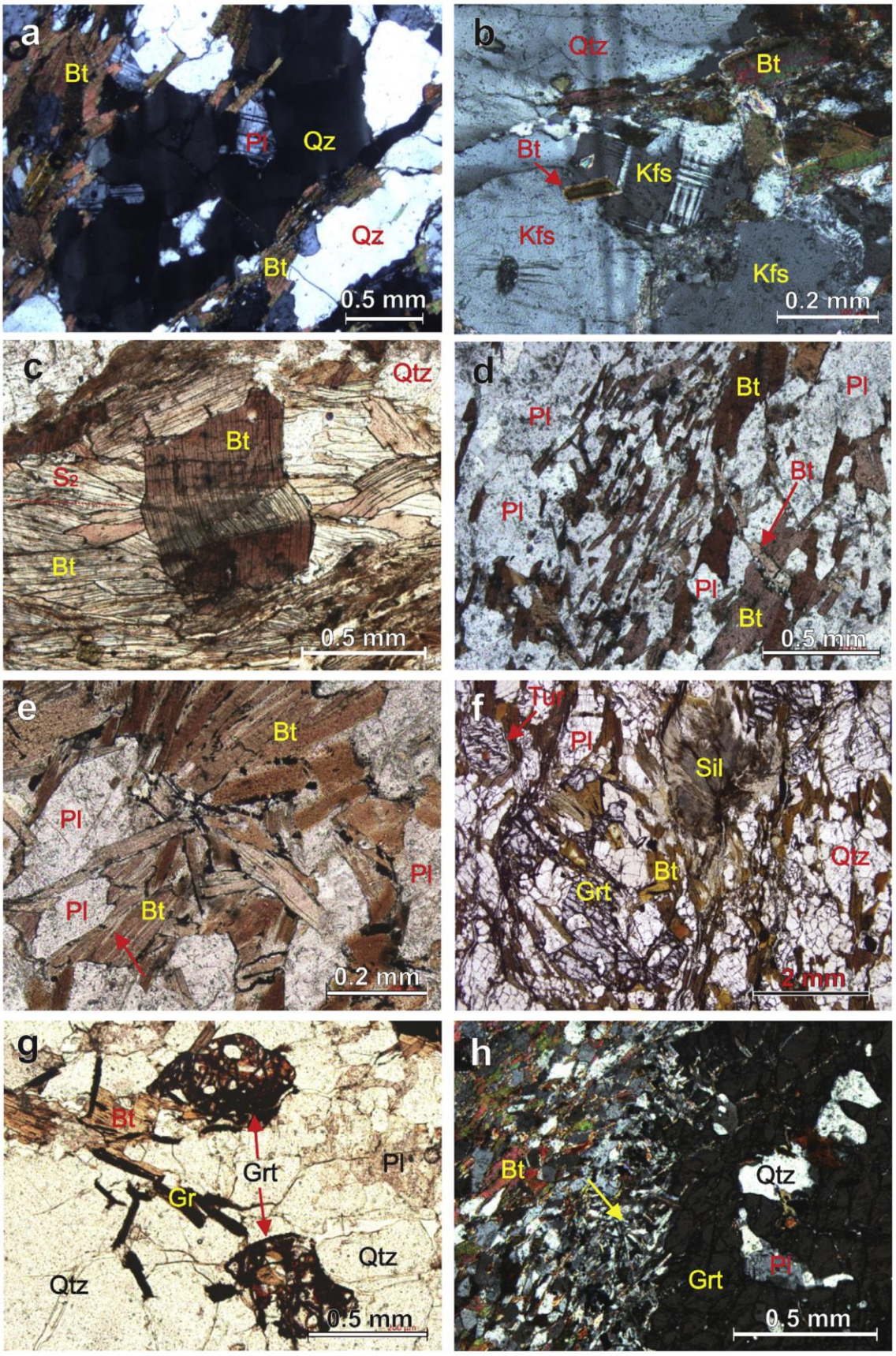

Fig. 3. Petrographic aspects of the Surubim Complex. (a) Quartz chessboard extinction (arrow). (b) Neoformed microcline grains in biotite schist. (c) Kinked biotite porphyroblast defining S_1 in a matrix

defined by the shape preferred orientation of biotite (S_2). (d) Fine biotite flakes intergrown with plagioclase (center) and new biotite lamellae (arrow) crosscutting S_2 foliation. (e) Chlorite stripes in biotite (arrow), and decussate biotite lamellae (center). (f) Skeletal garnet and fibrolite aggregate in biotite gneiss; tourmaline crystal (arrow). (g) Mimetic garnet grains and graphite lamellae in protomylonite; garnet fractures are filled with iron oxides/ hydroxides. (h) Garnet grain with corona composed of fine-grained and decussate biotite, quartz, and plagioclase (arrow). Qtz = quartz; Bt = biotite; Kfs = K-feldspar; Pl = plagioclase; Grt = garnet; Sil = sillimanite; Tur = tourmaline; Gr = graphite.

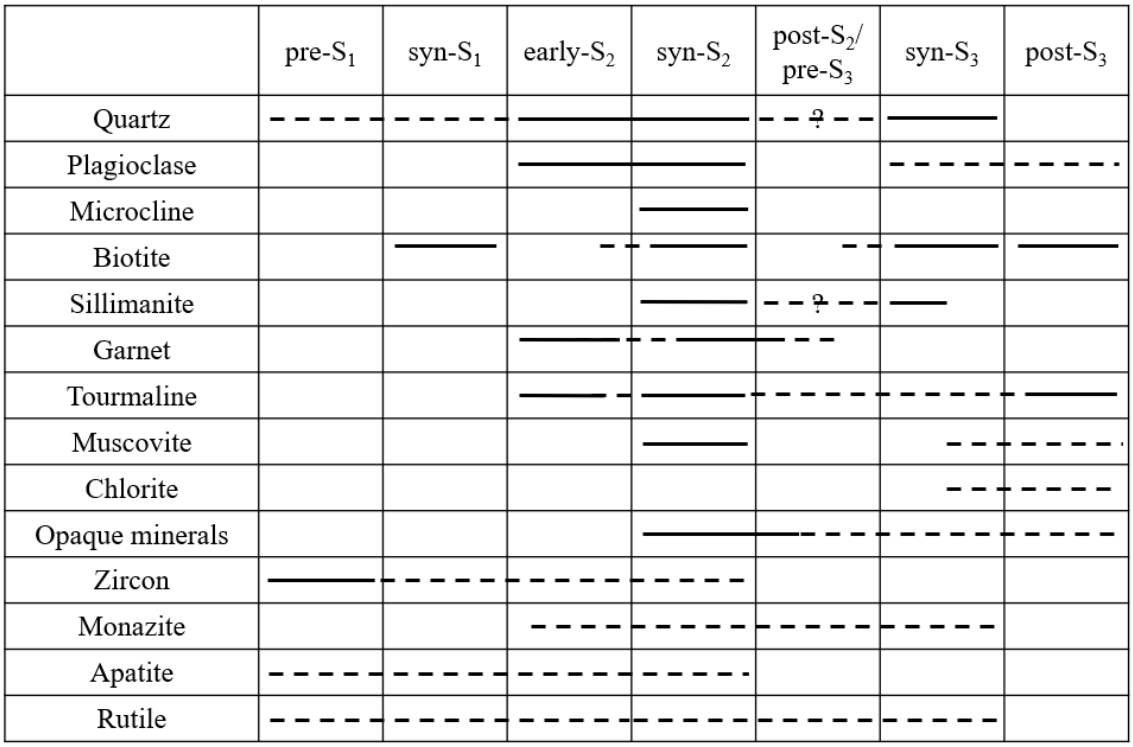

Fig. 4. Diagram showing microstructural relationships for paragneisses and schists of the Surubim Complex in the Feira Nova region.

Garnet mostly comprises early-S_2 xenoblastic to subidioblastic grains of millimetric size, equidimensional to elongated, with irregular, embayed rims, and commonly skeletal and highly fractured. Some grains are poikiloblastic, comprising random biotite, plagioclase, quartz, and opaque inclusions. Locally, early-S_2 garnet also presents a symplectitic corona composed of fine-grained and decussate biotite, feldspar, and quartz crystals along with a coarser biotite-rich matrix (Fig. 3h). In most mylonite samples, garnet also occurs as elongated, fine-to coarse-grained (< 0.6 mm) grains, locally with biotite and opaque inclusion trails defining an internal curved foliation (S_2). Some grains also present δ and σ porphyroclast shapes, suggesting

mimetic growth (Fig. 3g). In addition, fibrolite replacement by quartz, plagioclase and biotite is common in garnet grains associated with S_2 and S_3, with some decussate biotite clusters probably representing pseudomorphs. The mineral association diagram is presented in Fig. 4. The textural relationships suggest that garnet + biotite + quartz + plagioclase + sillimanite + muscovite + tourmaline, and garnet + K-feldspar + plagioclase + quartz + biotite comprise peak mineral assemblages in the studied area, and are simultaneous to S_2 development.

5. Mineral chemistry

Spot analyses of mineral chemistry and elemental X-ray maps (such as the ones presented in Fig. 6) were obtained using a JEOL JXA8230 Electron Microprobe of the Department of Petrology and Metalogeny, Universidade Estadual Paulista - UNESP. The spot analyses were made in garnet (rim-to-rim), biotite, plagioclase, and K-feldspar of four samples with operating conditions at 15 keV and ~20 nA. The samples comprise garnet- and sillimanite-bearing biotite schists (samples VAL01, VAL08 and VAL20) and a garnet-bearing biotite schist (VAL68). Ti in quartz analyses were carried out for one sample (VAL08), following Watson et al. (2006). The operating conditions were set at 15 keV and 200 nA, with synthetic rutile and quartz crystals used as calibration standards. The rutile calibration was set at 20 nA to avoid pulse-height analyzer peak shifts. The limit of detection, considering the matrix correction (ZAF) is 14 ppm (3 σ).

5.1. Spot analyses

Garnet of the analyzed samples is characterized by high almandine (XAlm = 0.68–0.77) with minor pyrope, grossular, and spessartine contents. Average variations in the main end-members almandine, pyrope and grossular are XAlm+Sps ~0.71–0.90, XPyp ~0.07–0.19, and XGrs ~0.04–0.18 (Fig. 5a). Zoning profiles show irregular patterns in most samples, but pyrope display lower contents in rims when compared with cores (Fig. 5b), and spessartine, higher contents. Most of the distribution patterns observed in the analyzed garnet grains are also detected in the X-ray map obtained for two samples. This distribution is evidence of crystal growth under decreasing pressure and temperature conditions, compatible with the other obtained mineral data. Representative mineral analyses are summarized in Tables 1–6.

5.2. Elemental X-Ray maps

X-ray maps were obtained for samples VAL20 and VAL68, with operating conditions at 15 keV and 250 nA, a focused beam, step (pixel) size of 3 μm, and a counting time of 15 ms/pixel. Diopside (Mg), wollastonite (Si), anorthite (Al), ilmenite (Fe), rodonite (Mn), wollastonite (Ca), ilmenite (Ti), zircon (Zr) and apatite (P) were used as calibration standards. The images were processed using the XMapTools software (Lanari et al., 2014).

5.2.1. Sample VAL68

The VAL68 X-ray maps (Fig. 6a–f) show a complex zoning history of garnet, suggesting three growth stages. Stage I is characterized by several cores with low contents of Fe and high Ca and Mg. It is noteworthy that the Ca contents decrease near plagioclase inclusions. Garnet grains grown during stage II envelop those of the first stage and exhibit an inverted zoning pattern with low contents of Ca and Mg and high Fe, which match the Ca rise of the matrix plagioclase. Stage III is characterized by thin rims displaying a decrease of Ca and Mg contents. Fe and Ti contents suggest two biotite growth stages: stage I, found as inclusions in garnet, displays high Fe and low Ti as compared with stage II, which is present in the matrix. Also, stage II biotite has a core with higher contents of Mg than rims, which is confirmed by the spot analyses.

5.2.2. Sample VAL20

The analyzed garnet of this sample is characterized by two growth stages registered in the garnet zoning. Stage I presents a Mg/Ca-rich and Fe-poor core, and stage II, a remarkable inversion of Mg and Fe contents toward the rims coupled with the decrease of the Ca contents. This is buffed by the presence of plagioclase, which is in accordance with the zoning pattern of the mineral. It is noteworthy a decrease of Mg contents in garnet around biotite inclusions and fractures. Three biotite growth stages can be observed in this sample. Biotite inclusions in garnet exhibit lower Ti contents in cores (stage I) when compared to rims (stage II). In the matrix, biotite displays a zoning pattern with Ti-rich cores (stage II) and Ti-poor rims (stage III), with a noteworthy decrease of Mg and an increase of Fe contents in biotite close to the garnet.

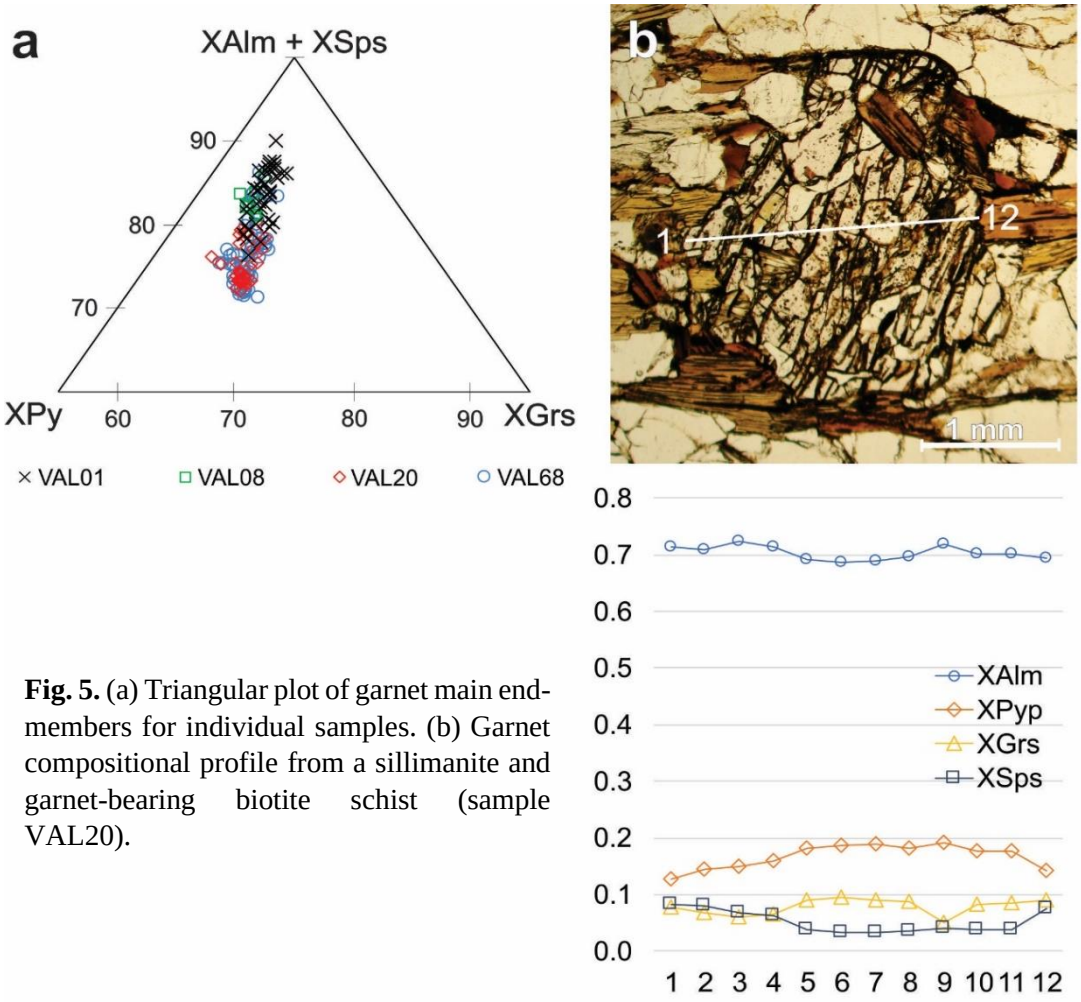

Fig. 5. (a) Triangular plot of garnet main end-members for individual samples. (b) Garnet compositional profile from a sillimanite and garnet-bearing biotite schist (sample VAL20).

6. Geothermobarometry

The temperatures estimated for the studied samples (VAL01, 08, 20, 68) were obtained from Ti in quartz (Thomas et al., 2010) and garnet-biotite conventional geothermometers. For these latter, we used the GPT Excel spreadsheet (Reche and Martinez, 1996), which allows simultaneously obtaining temperature and pressure through successive interactions. The calibration models proposed by Perchuk and Lavrent'eva (1983) (PL83), Bhattacharya et al. (1992) (BT92) and Holdaway and Lee (1977) (HL77) yielded concordant temperature values. Perchuk and Lavrent'eva models use volume changes of 0.0577 (a) and 0.0246 (b) cal.bar-1. Bhattacharya et al. (1992) use Hacker and Wood (1989) mixing parameters. Pressure values were calculated for samples VAL01, VAL20 and VAL68 using Koziol (1989) recalibration of the garnet-sillimanite-plagioclase-quartz (GASP) geobarometer. For the other samples, pressure was fixed based on these results and according to their temperature intervals. For temperatures over 570 °C, the PL83 and BT92 models were considered, which yielded variations of less than 29 °C. For this interval, the HL77 model yielded temperatures up to ~70

°C higher, probably due to the pressure limit of this model (≤0.4 GPa). The BT92 and HL77 models yielded concordant values for temperatures below 570 °C, with variations of less than 30 °C. The PL83 models were not considered for this interval due to the limit of their temperature range (575–950 °C). Core compositions of not-contacting garnet, biotite and plagioclase were combined, assumed to be the least modified from the peak conditions (e.g., Florence and Spear, 1995). Exceptionally, cores of matrix biotite in contact with garnet were combined with garnet cores. Rim compositions of contacting garnet and matrix biotite (and exceptionally, rims of not-contacting biotite) were paired with rims of not-contacting plagioclase.

The garnet crystals show retrograde zoning patterns, with some showing distinctly higher temperatures for core compositions (lowest Fe/(Fe + Mg) ratios) compared to rims (variations up to 110 °C). These higher temperatures were not always obtained from the middle of the grains. As most of them are xenoblastic, we interpreted those as core temperatures, with rims and part of the mantles probably affected by resorption. Both rim and core compositions yielded relatively uniform temperatures and pressures within individual samples, suggesting (re) equilibrium was attained at peak and retrograde conditions at least on the thin section scale. The garnet-cores yielded minimum and maximum values of ~620 °C and 650 °C for sample VAL01; ~630 °C and ~650 °C for sample VAL08; ~630 °C and ~690 °C for sample VAL20; and ~720 °C and ~760 °C for sample VAL68. Garnet-rims yielded temperatures between ~520 °C and ~560 °C for sample VAL01; ~570 °C for sample VAL08; 590 °C and 650 °C for sample VAL20; and ~630 °C and ~680 °C for sample VAL68 (Table 8). For core compositions at sample VAL01, pressure values range from ~0.58 to ~0.60 GPa (~620–650 °C), and for rim compositions, from ~0.28 to ~0.34 GPa (~520–560 °C). For sample VAL20, we obtained between ~0.74 and 0.80 GPa for core compositions (670–690 °C), and 0.4 GPa for a rim composition (~590 °C). For sample VAL68, rim compositions yielded 0.72 GPa (~660–670 °C), and a core composition, 0.91 GPa (~730 °C). Accounting for these results, we estimate pressure conditions higher than 0.9 GPa for the highest temperature obtained for this sample (~760 °C). The Ti in quartz model was applied to sample VAL 08 and yielded temperatures between ~515 and ~600 °C (Table 7). We fixed the pressure at 0.65 GPa based on the garnet core temperatures obtained for this sample (~630–650 °C) and GASP pressures obtained for sample VAL01 and VAL20 at this interval. Accounting the uncertainty of the Ti in quartz method (± 20 °C for pressures constrained to within ± 1 kbar), the highest result (~600 °C) is

in close agreement with the core temperatures estimated through the garnet-biotite geothermometers.

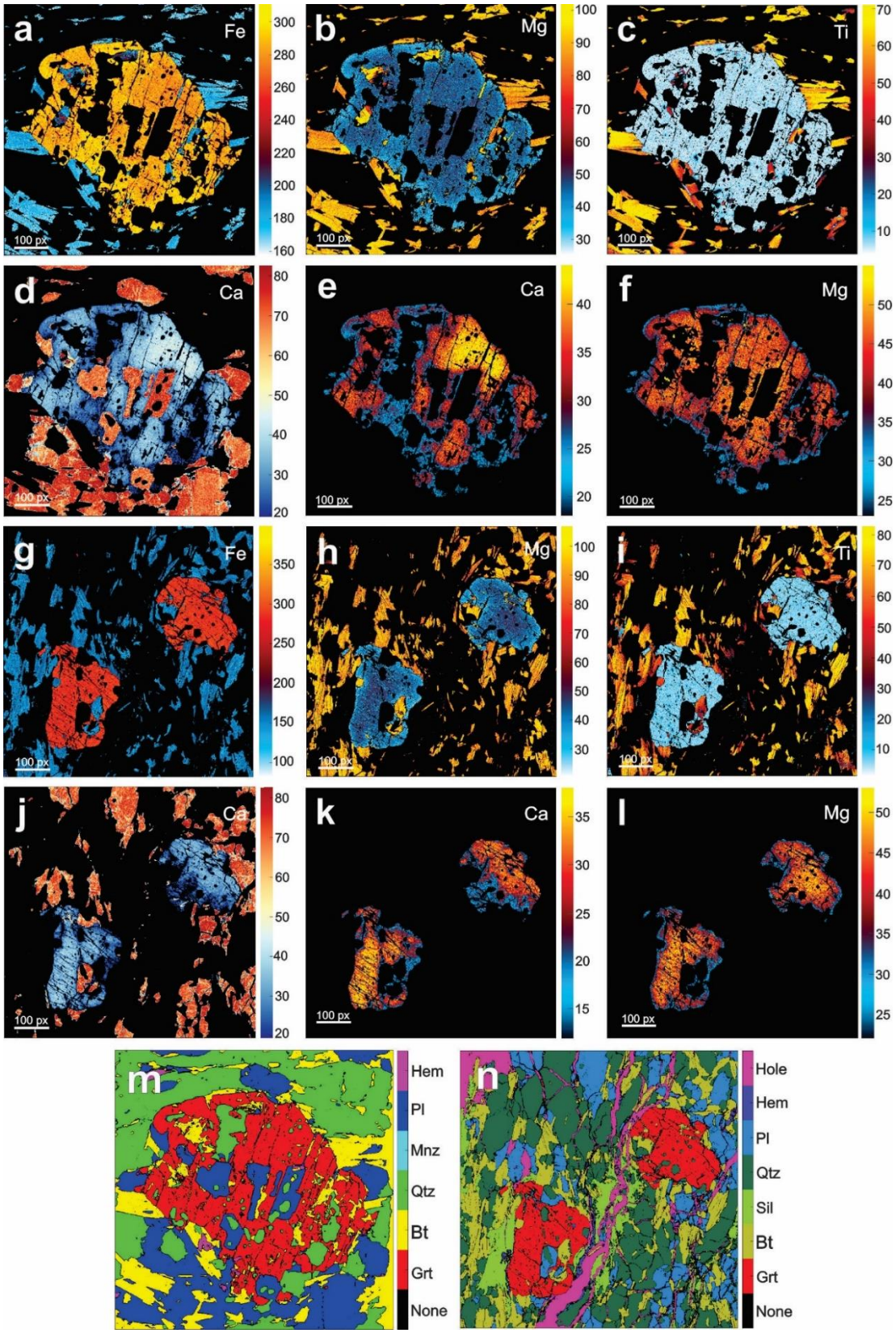

Fig. 6. X-ray element maps and phase masks of the studied samples. (a), (b), (c) Fe, Mg and Ti maps of garnet and biotite from sample VAL68. (d) Ca map of garnet and plagioclase from sample VAL68. (e), (f) Ca and Mg maps of garnet with increased contrast from sample VAL 68. (g), (h), (i) Fe, Mg and Ti maps of garnet and biotite from sample VAL20. (j) Ca map of garnet and plagioclase from sample VAL20. (k), (l) Ca and Mg maps of garnet with increased contrast from sample VAL20. (m), (n) Phase masks from samples VAL68 and VAL20, respectively. Hem = hematite; Pl = plagioclase; Mnz = monazite; Qtz = quartz; Bt = biotite; Grt = garnet; Sil = sillimanite.

7. Discussion

7.1. Metamorphic evolution

Field aspects and detailed petrographic and mineral analyses data reported in this work enable a better understanding of the metamorphic evolution of the Brasiliano Orogeny in the Feira Nova region, allowing us to place constraints on regional tectonic models. Mineral assemblages comprising (muscovite)-(rutile)-sillimanite tourmaline-garnet-biotite-plagioclase-quartz (Fig. 3f) and garnet-K-feldspar-plagioclase-quartz-biotite (Fig. 3b) along with high temperature microstructures such as chessboard quartz extinction (Fig. 3a) and local anatexis suggest peak temperatures under upper amphibolite facies conditions [e.g., Passchier and Trow (2005); Spear and Cheney (1989)].

The compositional maps patterns agree with the microstructural data, suggesting an early metamorphic evolution characterized by a prograde phase with both temperature and pressure increase. This phase is indicated by the prograde zoning of biotite inclusions in garnet, which shows low Ti contents in biotite cores and their enrichment in biotite rims (Fig. 6i). The high Ca and Mg contents in garnet cores (stage I garnet) (Fig. 6e, f, k, l) and the high Ti content in biotite (rims of biotite inclusions and cores of matrix biotite) (Fig. 6c, i) probably reflect the peak high-grade conditions. The relatively flat pattern of this garnet stage (I) suggest re-equilibrium/homogenization during peak metamorphism, which therefore erased the prograde compositions of this mineral and allowed the recording of only a partial P-T loop. The increase of Ti content in biotite may reflect the consumption of a Ti-rich phase (e.g., ilmenite or rutile) by net transfer reactions (e.g., Meinhold, 2010 and references therein). The textural relationships suggest that prograde and peak conditions are synchronous with the development of the regional flat-lying foliation (S_2), as indicated by early- and syn-S_2 mineral phases (Fig. 3b, f).

Fig. 7 shows the calculated P-T plots for garnet core and rim compositions for individual samples, which together define a partial P-T loop that reflects the peak and post-peak conditions of metamorphism. The calculated peak P-T values (630–760 °C; 0.6- > 0.9 GPa) agree with the coexistence of primary muscovite and sillimanite (i.e., above the first sillimanite isograd) in most of the studied rocks. However, the presence of neoformed microcline (syn-S_2) (Fig. 3b) spatially associated with migmatites indicates local conditions over the second sillimanite isograd. The S_2-related and probably anatetic Açudinho Orthogneiss also suggests that melting was synchronous to peak high-grade metamorphism. Migmatites crossed by the S_3 foliation along the GGSZ confirms the early nature of the melt in the studied area.

A decompression phase coupled with cooling is suggested by Ca and Mg decrease towards garnet rims (Fig. 6e, f, k, l) and by Ti decrease towards the rims of matrix biotite (bottom of Fig. 6c; left side of Fig. 6i). In sample VAL20, the relatively uniform zoning with minor Ca changes near plagioclase inclusions (Fig. 6k) may reflect diffusional relaxation at decreasing T conditions (e.g., Ague and Carlson, 2013) of the previously homogenized garnet nuclei. The garnet growth history of sample VAL68 is more complex. Here, the second stage (II) of garnet formation may be due to a coalescent growth of the garnet previous nuclei (stage I) (e.g., Spiess et al., 2001) during post-peak conditions. The reduction of Ca contents around plagioclase inclusions (Fig. 6d and e) and of Mg contents around biotite inclusions in garnet (Fig. 6b, h) suggests cation exchanges through volume diffusion between garnet-plagioclase and garnet-biotite. The reduction of Mg around fractures (Fig. 6b) in garnet probably reflects late diffusion through exchange reactions between garnet and biotite. The presence of plagioclase may have decreased the Ca availability of the system, suggesting a low mobility of this element. Syn-S_2 and syn-S_3 sillimanite and the P-T plots suggest protracted time spent in the sillimanite stability field. This inference is supported by existing geochronological data showing that regional high-grade metamorphism lasted from c. 630 to 600 Ma (Neves et al., 2006, 2012, 2020) and was followed by development of high temperature transcurrent shear zones at c. 600-570 Ma (Archanjo et al., 2008; Neves et al., 2012, 2020).

Common reactions such as minor feldspar sericitization and more local ones such as biotite chloritization (and probably, the garnet breakdown to a biotite, quartz and feldspar aggregate) (Fig. 3e) point to retrograde metamorphism under greenschist facies conditions, which is also indicated by the overprinting of high-temperature microstructures by low-temperature microstructures such as quartz bulging recrystallization. These textures are in accordance with the lowest rim P-T values (~520 °C; 0.3 GPa) (Fig. 7), which indicate conditions near the epidote-amphibolite-greenschist facies transition. The highest rim

temperature recorded for sample VAL20 (~650 °C), which is within the core temperature interval of this sample (630–690 °C), may reflect resorption of actual rims. Rimward increase of Fe in both garnet and biotite (and in biotite nearest to garnet), and of Mn in garnet may be explained by partial retrograde resorption of this mineral through net transfer reactions (e.g., Kohn and Spear, 2000), which is locally evidenced by the coronas.

The post-peak conditions are represented by the transition of compressional to transpressional regime as indicated by post S_2 (thus post-peak) and syn-S_3 mineral phases (Fig. 4). Lack of textural relationships prevent to constrain the end of the transpressional regime along with the retrograde path.

7.2. Tectonic implications

Obtained peak temperatures are consistent with the few thermobarometric estimates available for the Rio Capibaribe Domain. Accioly et al. (2003) obtained 675 °C and 0.13 GPa from metagabros of the Passira Complex using Ernst and Liu (1988) calibration of the Ti and Al in amphibole geothermobarometer, and 640–770 °C from metagabbros, metadiorites and metanorthosites using amphibole-plagioclase geothermometry (Blundy and Holland, 1990) at estimated pressures of 0.10–0.15 GPa. Barreto (2008) obtained peak temperatures between 610 and 690 °C for marbles of the Surubim Complex, calculated by multi-reaction methods provided by THERMOCALC and using simulated pressures up to 0.8 GPa. Neves et al. (2000, 2012) reported similar pressures here obtained (~0.6–0.9 GPa) to equivalent temperatures (650–730 °C) to the northwest of the study area (multi-reaction method from THERMOCALC; Powell and Holland, 1988), suggesting burial to 20–30 km depth. Kyanite occurrences in the Surubim Complex are reported by several authors [e.g., Barbosa (1990), Rocha (1990), Silva et al. (2005) and Neves et al. (2005, 2012)] and specifically research driven by Silva et al. (2005) described sillimanite after kyanite, which is probably placed somewhere between the prograde and the peak stage and allowed the inference of a clockwise P-T path (Fig. 7). Cordierite garnet-biotite and sillimanite-cordierite-garnet-biotite associations in the eastern RCD are mentioned by Barbosa (1990) and Rocha (1990), which suggest high temperature and low to medium pressure conditions, probably related to the retrograde path. The rim temperatures and pressures here obtained (520–590 °C; 0.3–0.4 GPa) (Fig. 7) are consistent with P-T conditions obtained from post-S_2 and syn-S_3 assemblages (550–605 °C; 0.5–0.6 GPa) at the northwest of the study area (Silva et al., 2005). The pressures suggest burial of the rocks to ~23–34 km depths. Considering the regional time span between peak metamorphism (630-

600 Ma) and the transcurrent regime (590- 550 Ma) (e.g. Neves et al., 2012), the temperature variation between the first stage (760-650 °C) and the end of the second one (600-500 °C) suggests that slow cooling has prevailed in the area. The lowest temperatures (~520 °C) may be placed on a large time span of slow cooling indicated by amphibole Ar-Ar ages (~590–550 Ma) from nearby orthogneisses and plutons (Neves et al., 2000, 2012). The retrograde P/T slope here obtained (Fig. 6) is in accordance with erosional unroofing (e.g. Ruppel and Hodges, 1994; Wernert et al., 2016) rather than with tectonic-related exhumation (e.g. Rey et al., 2001; Skrzypek et al., 2011; Peña-Alonso et al., 2017) since there is no evidence for late orogenic extensional deformation in the study area and in eastern Borborema Province (Neves et al., 2005, 2012).

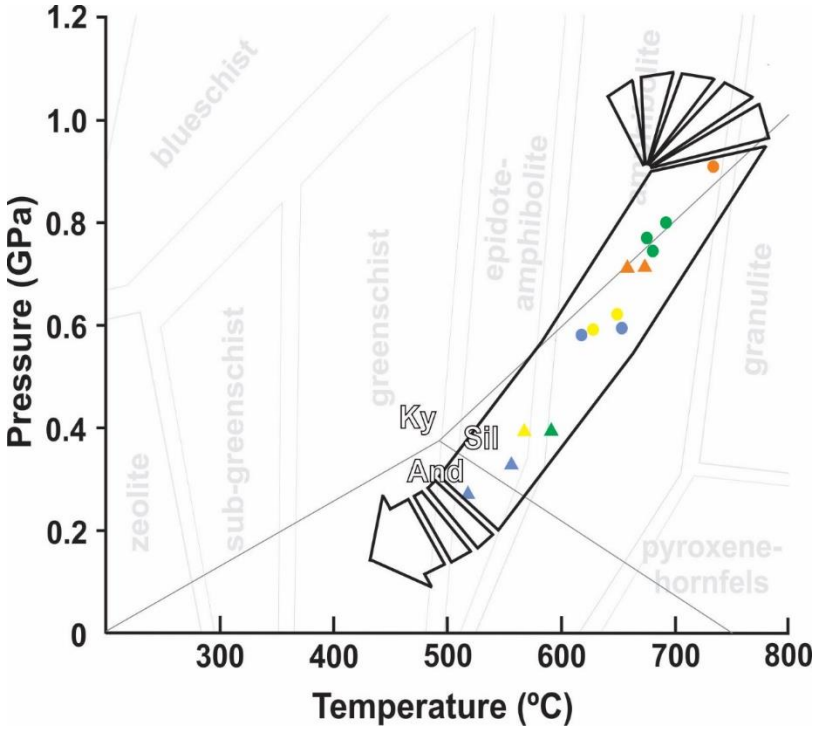

Fig. 7. P-T plot showing the estimated path of the studied rocks. Blue, green and orange markers refer to garnet-biotite temperatures along with GASP pressures from samples VAL01, VAL20 and VAL68, respectively. Yellow markers refer to obtained garnet-biotite temperatures along with inferred pressures from sample VAL08. Circles refer to core, and triangles, to rim values. The high-pressure portion of the path is based on the presence of kyanite in samples northwest of the studied area (Silva et al., 2005; Neves et al., 2012).

Previous works suggested an intracontinental setting for the tectonic evolution of the Central Subprovince during the Brasiliano Orogeny (e.g., Neves, 2003; Neves et al., 2012). Petrographic and thermobarometric data in the RCD are typical of crustal thickening

(Barrovian) metamorphism. Metamorphic evolution of compressional intracontinental orogens has been commonly associated with counterclockwise P-T-t paths due to the thermal weakening of the crust prior to thickening (e.g. Thompson, 1989; Thompson et al., 2001). Still, clockwise paths for orogens located away from plate boundaries are described in the Arunta region (Cartwright et al., 1999) and Petermann Orogeny (Raimondo et al., 2010) from Central Australia, and may occur even in the case of inherited thermal anomalies from previous rifting, as it is suggested for the Rehamna massif in Marocco (Wernert et al., 2016).

8. Conclusions

The metamorphic evolution of the Surubim Complex in the Feira Nova region is similar to the overall thermal evolution attributed to the Rio Capibaribe Domain in previous works. However, this study is the first to present thermobarometric data along with detailed petrography and to provide constraints through a retrograde P-T path. Mineral assemblages and local anatexis indicate metamorphism at upper amphibolite facies, coeval to the development of a flat-lying foliation (S_2). Peak metamorphic conditions estimated are ~630–760 °C and ~0.6–0.9 GPa (near amphibolite-granulite-facies transition), suggesting burial to middle-lower crustal levels (~23–34 km depth). Transition to lower amphibolite to greenschist facies is mostly shown as retrograde zoning in garnet and biotite crystals, and only locally as mineralogical changes. This zoning points to decompression and cooling down to ~590-520 °C and 0.4–0.3 GPa, suggesting unroofing to ~15-10 km depth, and is probably related to a transpressional regime. The inferred clockwise P-T path is attributed to thickening in a predominant intracontinental setting followed by exhumation with low erosional and cooling rates.

Declaration of competing interest

We declare that there is no conflict of interest.

Acknowledgements

We thank the Brazilian Council of Research (Conselho Nacional de Desenvolvimento Científico e Tecnológico - CNPq) and Votorantim Metais S.A. for funding this work, and Sebastián Oriolo and an anonymous reviewer for their constructive comments. VLS thanks CNPq for the scholarship.

References

Accioly, A.C.A., 2000. Geologia, Geoquímica e Significado Tectônico do Complexo Metanortosítico de Passira – Província Borborema - Nordeste Brasileiro. Ph.D. thesis, Universidade de São Paulo, 224 p.

Accioly, A.C.A., McReath, I., Santos, E.J., Guimarães, I.P., Santos, A.C., 2003. The Ages of Crystallization and Metamorphism of the Passira Anorthosite Complex Borborema Province, Northeastern Brazil. IV South American Symposium on Isotope Geology, Salvador, 487-490.

Ague, J.J., Carlson, W.D., 2013. Metamorphism as Garnet Sees It: The Kinetics of Nucleation and Growth, Equilibration, and Diffusional Relaxation. Elements, 9(6), 439-445.

Almeida, F.F.M., Hasui, Y., Brito Neves, B.B., Fuck, R. 1981. Brazilian Structural Provinces: An introduction. *Earth Science Reviews*, **17**, 1-29.

Amaral, W.S., dos Santos, T.J.S, Wernick, E., Nogueira Neto, J.A., Dantas, E.L., Matteini, M., 2012. High-pressure granulites from Carire, Borborema Province, NE Brazil: Tectonic setting, metamorphic conditions and U-Pb, Lu-Hf and Sm-Nd geochronology. Gondwana Research, 22(3-4), 892-909.

Araújo, C.E.G., Weinberg, R.F., Cordani, U.G., 2014. Extruding the Borborema Province (NE-Brazil): a two-stage Neoproterozoic collision process. Terra Nova, 26(2), 157-168.

Archanjo, C.J., Hollanda, M.H.B.M., Rodrigues, S.W.O., Brito Neves., B.B., Armstrong R., 2008. Fabrics of pre- and syn-tectonic granite plutons and chronology of shear zones in the Eastern Borborema Province, NE Brazil, Journal of Structural Geology, 30, 310-326.

Barbosa, A.G., 1990. Programa de Levantamentos Geológicos Básicos do Brasil: Geologia da Folha Limoeiro – SB.25-Y-C-V, escala 1:100.000. CPRM/DNPM, 116 p.

Barreto, M.C., 2008. Caracterização Geoquímica e Isotópica de Mármores do Terreno Rio Capibaribe na Zona Transversal da Província Borborema-Nordeste do Brasil. Ph.D. thesis, Universidade Federal de Pernambuco, 253 p.

Basto, C.F., Caxito, F.D.A., do Vale, J.A.R., Silveira, D.A., Rodrigues, J.B., Alkmin, A.R., Valeriano, C.D.M., Santos, E.J.D., 2019. An Ediacaran back-arc basin preserved in the Transversal Zone of the Borborema Province: Evidence from geochemistry, geochronology and isotope systematics of the Ipueirinha Group, NE Brazil. Precambrian Research, 320, 213-231.

Bhattacharya, A., Mohanty, L., Maji, A., Sen, S.K., Raith, M., 1992. Non-ideal mixing in the phlogopite-annite binary: constraints from experimental data on Mg-Fe partitioning and a reformulation of the biotite-garnet geothermometer. Contributions to Mineralogy and Petrology, 111, 87-93.

Blundy, J.D., Holland, T.J.B., 1990. Calcic amphibole equilibria and a new amphibole-plagioclase geothermometer. Contributions to Mineralogy and Petrology, 104(2), 208-224.

Brito Neves, B.B., Santos, E.J., Van Schmus, W.R., 2000. Tectonic history of the Borborema province. In: Cordani, U.G., Milani, E.J., Thomaz Filho, A., Campos, D.A. (Eds.), Tectonic Evolution of South America. 31st International Geological Congress, Rio de Janeiro, 151-182.

Brito Neves, B.B., Spröesser, W.M., Petronilho, L.A., Souza, S.L., 2013. Contribuição à Geologia e à Geocronologia do Terreno Rio Capibaribe (TRC, Província Borborema). Geologia USP - Série Científica, 13(2), 97-122.

Brito Neves, B.B., Santos, E.J., Fuck, R.A., Santos, L.C.M.L., 2016. A preserved early Ediacaran magmatic arc at the northernmost portion of the Transversal Zone central subprovince of the Borborema Province, Northeastern South America. Brazilian Journal of Geology, 46(4), 491-508.

Caby, R., Sial, A.N., Ferreira, V.P., 2009. High-pressure thermal aureoles around two Neoproterozoic synorogenic magmatic epidote-bearing granitoids, Northeastern Brazil. Journal of South American Earth Sciences, 27(2–3), 184-196.

Cartwright, I., Buick, I.S., Foster, D.A., Lambert, D.D., 1999. Alice Springs age shear zones from the southeastern Reynolds Range, central Australia. Australian Journal of Earth Sciences, 46(3), 355-363.

Castro, N.A., 2004. Evolução geológica proterozoica da região entre Madalena e Taperuaba, Domínio Tectônico Ceará Central (Província Borborema). Ph.D. thesis, Universidade de São Paulo, 335 p.

Corsini, M., Lambert de Figueiredo, L., Caby, R., Féraud, G., Ruffet, G., Vauchez, A., 1998. Thermal history of the Pan-African/Brasiliano Borborema Province of northeast Brazil deduced from 40Ar/39Ar analysis. Tectonophysics, 285(1-2), 103-117.

Dhuime, B., Bosch, D., Bruguier, O., Caby, R., Archanjo, C., 2003. An Early-Cambrian U-Pb apatite cooling age for the high-temperature regional metamorphism in the Piancó area, Borborema Province (NE Brazil): initial conclusions. Comptes Rendus Geoscience, 335(15), 1081-1089.

England, P.C., Richardson, S.W., 1977. The influence of erosion upon the mineral fades of rocks from different metamorphic environments. Journal of the Geological Society, 134, 201-213.

England, P.C., Thompson, A.B., 1984. Pressure-Temperature-Time Paths of Regional Metamorphism I. Heat Transfer during the Evolution of Regions of Thickened Continental Crust. Journal of Petrology, 25(4), 894-928.

Ernst, W.G., 1988. Tectonic history of subduction zones inferred from retrograde blueschist P-T paths. Geology, 16(12), 1081-1084.

Ernst, W.G., Liu, J., 1988. Experimental phase-equilibrium study of Al- and Ti-contents of calcic amphibole in MORB - A semiquantitative thermobarometer. American Mineralogist, 83(9-10), 952–969.

Florence, F.P., Spear, F.S., 1995. Intergranular diffusion kinetics of Fe and Mg during retrograde metamorphism of a pelitic gneiss from the Adirondack Mountains. Earth and Planetary Science Letters, 34(3-4), 329-340.

Guimarães, I.P., da Silva Filho, A.F., Almeida, C.N., Van Schmus, W.R., Araújo, J.M.M., Melo, S.C., Melo, E.B., 2004. Brasiliano (Pan-African) granitic magmatism in the Pajeú-Paraíba belt, Northeast Brazil: an isotopic and geochronological approach. Precambrian Research, 135, 23-53.

Guimarães, I.P., Silva Filho, A.F., Melo, S.C., Macambira, M.B., 2005. Petrogenesis of A-type Granitoids from the Alto Moxotó and Alto Pajeú Terranes of the Borborema Province, ne Brazil: Constraints from Geochemistry and Isotopic Composition. Gondwana Research, 8(3), 347-362.

Guimarães, I.P., Van Schmus, W.R., Brito Neves, B.B., Bittar, S.M., Silva Filho, A.F., Armstrong, R., 2012. U Pb zircon ages of orthogneisses and supracrustal rocks of the Cariris Velhos belt: onset of Neoproterozoic rifting in the Borborema Province, NE Brazil. *Precambrian Research,* **192-195**, 52-77.

Hacker, R.T., Wood, B.J., 1989. Experimental determination of Fe and Mg exchange between garnet and olivine and estimation of Fe-Mg mixing properties in garnet. American Mineralogist, 74, 994-999.

Halpin, J.A., Clarke, G.L., White, R.W., Kelsey, D.E., 2007. Contrasting P-T-t paths for Neoproterozoic metamorphism in MacRobertson and Kemp Lands, east Antarctica. Journal of Metamorphic Geology, 25(6), 683-701.

Hodges, K., Royden, L. 1984. Geologic thermobarometry of retrograded metamorphic rocks: an indication of the uplift trajectory of a portion of the Northern Scandinavian Caledonides. Journal of Geophysical Research, 89(B8), 7077-7090.

Hollanda, M.H.B.M., Archanjo, C.J., Souza, L.C., Armstrong, R., Vasconcelos, P.M., 2010. Cambrian mafic to felsic magmatism and its connections with transcurrent shear zones of the Borborema Province (NE Brazil): implications for the late assembly of the West Gondwana. Precambrian Research, 178,1-14.

Holdaway, M.J., Lee, S.M., 1977. Fe-Mg Cordierite Stability in High-Grade Pelitic Rocks Based on Experimental, Theoretical, and Natural Observations. Contributions Mineralogy Petrology, 63, 175-198.

Kohn, M.J., Spear, F. S., 2000. Retrograde net transfer reaction insurance for pressure-temperature estimates. Geology, 28(12), 1127-1130.

Koziol, A.M., 1989. Recalibration of the garnet-plagioclase-Al2SiOs-quartz (GASP) geobarometer and application to natural parageneses. American Geophysical Union Spring Meeting, 70, 493.

Lanari, P., Vidal, O., De Andrade, V., Dubacq, B., Lewin, E., Grosch, E.G., Schwartz, S., 2014. XMapTools: A MATLAB©-based program for electron microprobe X-ray image processing and geothermobarometry. Computers & Geosciences, 62, 227-240.

Leite, P.R.B., Bertrand, J.M., Lima, E.S., Leterrier, J., 2000. Timing of granitic magmatism in the northern Borborema Province, Brazil: A U-Pb study of granitoids from the Alto Pajeú Terrain. Journal of South American Earth Sciences, 13(6), 549-559.

Lima, H.M., Ferreira, V.P., Santos, E.J., Pimentel. M.M., Santos, L.C.M.L., 2015. Origem, significado petrogenético e idade dos ortognaisses Terra Nova: registro de magmatismo alcalino transtensional Neoproterozoico no domínio da zona transversal da Província Borborema. Geochimica Brasiliensis, 29, 70-86.

Liu, X., Wang, W.R.Z., Zhao, Y., Liu, J., Chen, H., Cui, Y., Song, B., 2016. Early Mesoproterozoic arc magmatism followed by early Neoproterozoic granulite facies metamorphism with a near-isobaric cooling path at Mount Brown, Princess Elizabeth Land, East Antarctica. Precambrian Research, 284, 30-48.

Meinhold, G., 2010. Rutile and its applications in earth sciences. Earth-Science Reviews, 102(1-2), 1-28.

Neves, S.P., Mariano, G., 2003. Heat-producing Elements-enriched Continental Mantle Lithosphere and Proterozoic Intracontinental Orogens: Insights from Brasiliano/Pan-African Belts. Gondwana Research, 7(2), 427-436.

Neves, S.P., Vauchez, A., Feraud, G., 2000. Tectono-thermal evolution, magma emplacement, and shear zone development in the Caruaru area (Borborema Province, NE Brazil). Precambrian Research, 99, 1-32.

Neves, S.P., Silva, J.M.R., Mariano, G., 2005. Oblique lineations in orthogneisses and supracrustal rocks: vertical partitioning of strain in a hot crust (eastern Borborema Province, NE Brazil). Journal of Structural Geology, 27(8), 1513-1527.

Neves, S.P., Bruguier, O., Vauchez, A., Bosch, D., Silva, J.M.R., Mariano, G., 2006. Timing of crustal formation, deposition of supracrustal sequences and Transamazonian and Brasiliano metamorphism in eastern Borborema Province (NE Brazil): Implications for western Gondwana assembly. *Precambrian Research* **149**, 197-216.

Neves, S.P., Olivier Bruguier, O., Silva, J.M.R., Bosch, D., Alcantara, V.C., Lima, C.M., 2009. The age distributions of detrital zircons in metasedimentary sequences in eastern Borborema Province (NE Brazil): Evidence for intracontinental sedimentation and orogenesis?. Precambrian Research, 175, 187–205.

Neves, S.P., Alcantara, V.C., 2010. Geochemistry of orthogneisses and metasedimentary rocks across a proposed terrane boundary in the Central Domain of Borborema Province, NE Brazil: geodynamic implications. Journal of South American Earth Sciences, 29, 498-511.

Neves, S.P., Monié, P., Bruguier, O., Silva, J.M.R., 2012. Geochronological, thermochronological and thermobarometric constraints on deformation, magmatism and thermal regimes in eastern Borborema Province (NE Brazil). Journal of South American Earth Sciences, 38, 129-146.

Neves, S.P., Lages, G.A., Brasilino, R.G., Miranda, A.W.A., 2015. Paleoproterozoic accretionary and collisional processes and the build-up of the Borborema Province (NE

Brazil): Geochronological and geochemical evidence from the Central Domain. Journal of South American Earth Sciences, 58, 165-187.

Neves, S.P., Silva, J.M.R., Bruguier, O., 2017. Geometry, kinematics and geochronology of the Sertânia Complex (central Borborema Province, NE Brazil): Assessing the role of accretionary versus intraplate processes during West Gondwana assembly. Precambrian Research, 298, 552-571.

Neves, S.P., 2018. Comment on "A preserved early Ediacaran magmatic arc at the northernmost part of the transversal zone - central domain of the Borborema Province, Northeast of South America", by B. B. de Brito Neves et al. (2016). Brazilian Journal of Geology, 48(3), 623-630.

Neves, S.P., Teixeira, C. M. L., Bruguier, O., 2020. Long-lived localized magmatism in central-eastern part of the Pernambuco-Alagoas Domain, Borborema Province (NE Brazil): Implications for tectonic setting, heat sources, and lithospheric reworking. Precambrian Research, 337, 1055592.

Passchier, C.W., Trow, R.A.J., 2005. Microtectonics. Springer Berlin Heidelberg, 371 p.

Peña-Alonso, T.A., Estrada-Carmona, J., Molina-Garza, R.S., Solari, L., Levresse, G., Latorre, C., 2017. Lateral spreading of the middle to lower crust inferred from Paleocene migmatites in the Xolapa Complex (Puerto Escondido, Mexico): Gravitational collapse of a Laramide orogen? Tectonophysics, 706-707, 143–163.

Perchuk, L.L., Lavrent'eva, I.V., 1983. Experimental investigation of exchange equilibria in the system cordierite-garnet-biotite. In: Saxena, S.K., (ed.), Kinetics and equilibrium in mineral reactions. Springer Verlag, New York, 199-239.

Powell, R., Holland, T.J.B., 1988. An internally consistent dataset with uncertainties and correlations; 3, Applications to geobarometry, worked examples and a computer program. Journal of Metamorphic Geology, 6, 173-204.

Raimondo, T., Collins, A.S., Hand, M., Walker-Hallam, A., Smithies, R.H., Evins, P.M., Howard, H.M., 2010. The anatomy of a deep intracontinental orogen. Tectonics, 29, 1-31.

Reche, J., Martinez, F.J., 1996. GPT: An excel spreadsheet for thermobarometric calculations in metapelitic rocks. Computers & Geosciences, 22(7), 775-784.

Rey, P., Vanderhaeghe, O., Teyssier, C., 2001. Gravitational collapse of the continental crust: definition, regimes and modes. Tectonophysics, 342, 435-449.

Rocha, D.E.G.A., 1990. Programa de Levantamentos Geológicos Básicos do Brasil: Geologia da Folha Vitória de Santo Antão – SC.25-V-A-II, escala 1:100.000. CPRM/DNPM, 112 p.

Ruppel, C., Hodges, K., 1994. Pressure-temperature-time paths from two-dimensional thermal models: Prograde, retrograde, and inverted metamorphism. Tectonics, 13(1), 17-44.

Santos, E.J., Nutman, A.P., Brito Neves, B.B., 2004. Idades SHRIMP U-Pb do Complexo Sertânia: implicações sobre a evolução tectônica da Zona Transversal, Província Borborema. Geologia USP - Série Científica, 4(1), 1-12.

Santos, T.J.S., Garcia, M.G.M., Amaral, V.W., Caby, R., Wernick, E., Arthaud, M.H., Dantas, E.L., Santosh, M., 2009. Relics of eclogite facies assemblages in the Ceará Central Domain, NW Borborema Province, NE Brazil: Implications for the assembly of West Gondwana. Gondwana Research, 15(3-4), 454-470.

Santos, E.J., Van Schmus, W.R., Kozuch, M., Brito Neves, B.B., 2010. The Cariris Velhos tectonic event in Northeast Brazil. Journal of South American Earth Sciences, 29, 61-76.

Santos, F.H., Amaral, W.S., Luvizotto, G.L., Martins de Sousa, D.F., 2018a. P-T evolution of metasedimentary rocks of the Santa Filomena Complex, Riacho do Pontal Orogen, Borborema Province (NE Brazil): Geothermobarometry and metamorphic modelling. Journal of South American Earth Sciences, 82, 91-107.

Santos, C.A., Fernandes, P.R., Pereira, C.S., Brito, M.F.L., Domingos, N.RR., Silva, E.P., Oliveira, R.G., 2018b. Programa Geologia do Brasil-PGB: Projeto RIO CAPIBARIBE, escala 1:250.000, CPRM, 1 mapa.

Silva Filho, A.F., Guimarães I.P, Van Schmus W.R, Armstrong R.A, Rangel, J.M.S., Osako, L.S., Cocentino, L.M., 2014. SHIIMP U-Pb geochronology and Nd signatures of supracrustal sequences and orthogneiss constrain the Neoproterozoic evolution of the Pernambuco-Alagoas domain, Southern part of Borborema Province, NE Brazil. International Journal of Earth Sciences, 103(8), 2155-2190.

Silva, J.M.R., Mariano, G., Neves, S.P., 2005. Termobarometria das rochas metapelíticas da parte Leste da Zona Transversal: Região de Surubim e Alcantil, Província Borborema, NE do Brasil. In: XXI Simpósio de Geologia do Nordeste, Sociedade Brasileira de Geologia, Recife.

Silva, V.L., Neves., S.P., Mesquita, N.M. (2019). Tectônica Transpressiva na Faixa Feira Nova, Domínio Rio Capibaribe, Província Borborema. Manuscript in preparation.

Skrzypek, E., Stipska, P., Schulmann, K., Lexa, O., Lexova, M., 2011. Prograde and retrograde metamorphic fabrics – a key for understanding burial and exhumation in orogens (Bohemian Massif). Journal Metamorphic Geology, 29, 451–472.

Sommer, H., Hauzenberger, C., Kroner, A., Muhongo, S., 2008. Isothermal decompression history in the ‘‘Western Granulite” terrain, central Tanzania: Evidence from reaction textures and trapped fluids in metapelites. Journal of African Earth Sciences, 51(3), 123-144.

Spear, F.S., Cheney, J.T., 1989. A petrogenetic grid for pelitic schists in the system SiO2-Al2O3-FeO-MgO-K2O-H2O. Contributions to Mineralogy and Petrology, 101(2), 149-164.

Spear, F.S., Selverstone, J., 1983. Quantitative P-T Paths from Zoned Minerals: Theory and Tectonic Applications. Contributions to Mineralogy and Petrology, 83(3-4), 348-357.

Spiess, R., Peruzzo, L., Prior, D.J., Wheeler, J., 2001. Development of garnet porphyroblasts by multiple nucleation, coalescence and boundary misorientation-driven rotations. Journal of Metamorphic Geology, 19, 269–290.

Teixeira, C.M.L., 2015. Evolução crustal dos domínios central e Pernambuco-Alagoas da província Borborema na folha Vitória de Santo Antão (Pernambuco – Nordeste do Brasil). Ph.D. thesis, Universidade Federal de Pernambuco, 192p.

Thomas, J.B., Watson, E.B., Spear, F.S., Shemella, P.T., Nayak, S.K., Lanzirotti, A., 2010. TitaniQ under pressure: The effect of pressure and temperature on the solubility of Ti in quartz. Contributions to Mineralogy and Petrology, 160, 743-759.

Thompson, P.H., 1989. Moderate overthickening of thinned sialic crust and the origin of granitic magmatism and regional metamorphism in low-P-high-T terranes. Geology, 17(6), 520-523.

Thompson, A.B., Schulmann, K., Jezek, J., Tolar, V., 2001. Thermally softened continental extensional zones (arcs and rifts) as precursors to thickened orogenic belts. Tectonophysics, 332, 115-141.

Van Schmus, W.R., Oliveira, E.P., Silva Filho, A.F., Toteu, S.F., Penaye, J., Guimarães, I.P. 2008. Proterozoic links between the Borborema province, NE Brazil, and the Central African Fold Belt. Geological Society of London, Special Publication, 294, 69-99.

Van Schmus, W. R.; Kozuch, M., Brito Neves, B. B., 2011. Precambrian history of the Zona Transversal of the Borborema Province, NE Brazil: Insights from Sm/Nd and U/Pb geochronology. *Journal of South American Earth Sciences*, **31**, 227-252.

Watson, E.B., Wark, D.A., Thomas, J.B., 2006. Crystallization thermometers for zircon and rutile. Contributions to Mineralogy and Petrology, 151, 413-433.

Wernert, P., Schulmann, K., Chopin, F., Stipska, P., Bosch, D., El Houicha, M., 2016. Tectonometamorphic evolution of an intracontinental orogeny inferred from P-T-t-d paths of the metapelites from the Rehamna massif (Morocco). Journal of Metamorphic Geology, 34(9), 917-940.

Table 1. Representative chemical analyses of garnet from samples VAL01 and VAL08.

	VAL01									VAL08		
	Core	Core	Core	Core	Rim	Rim	Rim	Rim	Rim	Core	Core	Rim
SiO_2	37.48	37.50	36.85	37.77	37.08	36.92	36.79	36.98	36.72	37.69	36.77	36.72
TiO_2	0.00	0.03	0.00	0.02	0.02	0.02	0.00	0.01	0.00	0.02	0.00	0.00
Al_2O_3	20.88	20.83	20.74	21.21	20.82	20.61	20.26	20.82	20.58	20.92	20.80	20.42
Cr_2O_3	0.02	0.04	0.00	0.02	0.02	0.03	0.02	0.00	0.01	0.01	0.02	0.03
FeO	32.08	32.10	31.98	32.50	31.88	31.56	30.83	31.78	31.30	32.79	31.68	31.27
MnO	3.67	2.64	4.78	2.22	6.29	6.95	7.32	5.50	6.41	1.27	5.30	6.91
MgO	3.77	3.52	3.29	4.02	2.16	2.18	2.11	2.89	2.47	3.42	3.20	2.38
CaO	2.26	2.91	1.87	2.86	1.96	1.62	1.51	1.97	1.77	4.12	1.76	1.61
Na_2O	0.00	0.00	0.02	0.00	0.00	0.02	0.00	0.00	0.01	0.00	0.01	0.00
K_2O	0.00	0.01	0.00	0.00	0.00	0.01	0.00	0.00	0.01	0.01	0.02	0.00
Total	100.16	99.58	99.53	100.62	100.21	99.92	98.84	99.95	99.28	100.24	99.55	99.33
Si	3.001	3.012	2.986	2.998	3.000	3.001	3.020	2.989	2.997	3.007	2.982	3.001
Ti	0.000	0.002	0.000	0.001	0.001	0.001	0.000	0.001	0.000	0.001	0.000	0.000
Al	1.971	1.973	1.981	1.984	1.986	1.975	1.961	1.984	1.979	1.967	1.988	1.967
Cr	0.001	0.003	0.000	0.001	0.001	0.002	0.001	0.000	0.001	0.001	0.001	0.002
Fe^{+2}	2.148	2.156	2.167	2.157	2.157	2.146	2.116	2.149	2.136	2.188	2.149	2.137
Mn	0.249	0.179	0.328	0.149	0.431	0.479	0.509	0.377	0.443	0.086	0.364	0.478
Mg	0.449	0.422	0.398	0.475	0.260	0.264	0.259	0.348	0.301	0.407	0.387	0.290
Ca	0.194	0.251	0.162	0.243	0.170	0.141	0.133	0.171	0.154	0.352	0.153	0.141
Na	0.001	0.000	0.003	0.001	0.000	0.002	0.000	0.000	0.002	0.000	0.002	0.000
K	0.000	0.001	0.000	0.000	0.000	0.001	0.000	0.000	0.001	0.001	0.002	0.000
Total	8.014	7.999	8.025	8.009	8.006	8.011	7.999	8.018	8.014	8.009	8.026	8.015
Fe/(Fe+Mg)	0.827	0.836	0.845	0.819	0.892	0.890	0.891	0.861	0.877	0.843	0.847	0.881
Prp	0.150	0.140	0.133	0.159	0.087	0.088	0.086	0.116	0.101	0.135	0.130	0.097
Grs	0.065	0.083	0.054	0.081	0.057	0.047	0.044	0.057	0.052	0.117	0.051	0.047
Alm	0.703	0.717	0.702	0.710	0.713	0.705	0.702	0.701	0.700	0.719	0.696	0.697
Sps	0.083	0.060	0.110	0.050	0.144	0.160	0.169	0.126	0.148	0.028	0.122	0.159

Table 2. Representative chemical analyses of garnet from sample VAL20.

	Core	Core	Core	Core	Rim	Rim	Rim	Rim	Rim	Rim	Rim	Rim
SiO_2	37.75	38.11	38.14	37.90	37.00	37.72	37.34	37.70	37.31	36.89	37.30	37.20
TiO_2	0.00	0.00	0.00	0.09	0.00	0.01	0.00	0.00	0.00	0.00	0.01	0.00
Al_2O_3	21.09	21.31	21.08	21.14	20.80	21.56	20.72	21.35	21.11	20.97	21.12	20.95
Cr_2O_3	0.01	0.00	0.02	0.02	0.01	0.03	0.02	0.01	0.02	0.01	0.01	0.04
FeO	31.99	32.25	32.03	32.08	32.72	32.15	32.04	32.38	32.31	31.57	32.27	32.97
MnO	1.80	1.66	1.46	1.48	3.26	3.37	3.15	3.32	3.58	3.26	2.27	3.15
MgO	4.43	4.55	4.84	4.63	3.79	3.38	3.58	3.74	3.20	3.52	3.88	4.00
CaO	3.05	3.33	3.21	3.11	2.11	2.97	2.83	2.28	2.66	3.07	3.25	1.58
Na_2O	0.00	0.02	0.00	0.01	0.02	0.00	0.01	0.00	0.01	0.01	0.01	0.00
K_2O	0.00	0.00	0.00	0.00	0.00	0.00	0.01	0.00	0.00	0.00	0.01	0.00
Total	100.11	101.22	100.77	100.46	99.71	101.19	99.68	100.78	100.20	99.30	100.12	99.88
Si	3.001	2.996	3.006	2.999	2.983	2.987	3.004	2.995	2.992	2.980	2.981	2.988
Ti	0.000	0.000	0.000	0.005	0.000	0.001	0.000	0.000	0.000	0.000	0.001	0.000
Al	1.976	1.975	1.958	1.971	1.977	2.012	1.965	1.999	1.995	1.997	1.990	1.984
Cr	0.001	0.000	0.001	0.001	0.001	0.002	0.001	0.001	0.001	0.001	0.001	0.002
Fe^{+2}	2.127	2.120	2.111	2.123	2.206	2.129	2.155	2.151	2.167	2.132	2.157	2.215
Mn	0.121	0.110	0.098	0.099	0.223	0.226	0.215	0.223	0.243	0.223	0.154	0.214
Mg	0.524	0.533	0.568	0.547	0.456	0.399	0.429	0.443	0.383	0.423	0.462	0.479
Ca	0.259	0.280	0.271	0.263	0.182	0.252	0.244	0.194	0.228	0.266	0.278	0.136
Na	0.000	0.003	0.000	0.002	0.002	0.000	0.001	0.000	0.001	0.001	0.002	0.000
K	0.000	0.000	0.000	0.000	0.000	0.000	0.001	0.000	0.000	0.000	0.001	0.000
Total	8.010	8.018	8.014	8.010	8.030	8.006	8.014	8.006	8.010	8.022	8.024	8.019
Fe/(Fe+Mg)	0.802	0.799	0.788	0.795	0.829	0.842	0.834	0.829	0.850	0.834	0.824	0.822
Prp	0.175	0.178	0.189	0.182	0.153	0.134	0.143	0.148	0.128	0.142	0.155	0.160
Grs	0.086	0.094	0.090	0.088	0.061	0.084	0.081	0.065	0.076	0.089	0.093	0.046
Alm	0.698	0.691	0.688	0.697	0.711	0.706	0.704	0.713	0.714	0.694	0.700	0.722
Sps	0.040	0.037	0.032	0.033	0.075	0.076	0.072	0.074	0.081	0.075	0.052	0.072

Table 3. Representative chemical analyses of garnet from sample VAL68.

	Core	Core	Core	Core	Rim	Rim	Rim	Rim	Rim	Rim
SiO_2	38.06	37.63	37.36	37.66	37.22	37.45	36.94	37.45	37.38	37.41

TiO_2	0.06	0.02	0.00	0.01	0.01	0.00	0.02	0.00	0.01	0.01
Al_2O_3	21.18	21.07	21.09	21.09	20.77	21.02	20.80	21.09	20.87	20.80
Cr_2O_3	0.03	0.03	0.02	0.01	0.03	0.01	0.01	0.00	0.00	0.01
FeO	31.82	32.16	32.00	31.80	32.82	32.88	32.41	31.78	32.84	32.64
MnO	1.33	1.34	1.33	1.33	1.81	1.94	2.48	2.34	2.53	2.74
MgO	4.80	4.74	4.60	4.59	3.63	3.90	3.68	3.87	3.46	3.31
CaO	3.32	3.07	2.98	3.55	2.99	3.00	3.03	2.88	2.88	3.10
Na_2O	0.00	0.01	0.00	0.00	0.02	0.00	0.02	0.00	0.02	0.01
K_2O	0.02	0.00	0.01	0.00	0.00	0.00	0.01	0.00	0.00	0.00
Total	100.63	100.05	99.38	100.03	99.29	100.21	99.40	99.41	99.99	100.03
Si	3.002	2.991	2.989	2.993	3.001	2.991	2.982	3.004	3.000	3.003
Ti	0.004	0.001	0.000	0.001	0.000	0.000	0.001	0.000	0.000	0.001
Al	1.969	1.974	1.989	1.975	1.974	1.979	1.979	1.994	1.974	1.968
Cr	0.002	0.002	0.001	0.001	0.002	0.001	0.001	0.000	0.000	0.001
Fe^{+2}	2.099	2.138	2.141	2.113	2.213	2.196	2.188	2.132	2.204	2.191
Mn	0.089	0.090	0.090	0.089	0.124	0.131	0.169	0.159	0.172	0.186
Mg	0.564	0.561	0.548	0.544	0.437	0.465	0.443	0.463	0.413	0.396
Ca	0.281	0.261	0.256	0.302	0.258	0.257	0.262	0.247	0.248	0.266
Na	0.000	0.001	0.000	0.000	0.003	0.000	0.002	0.000	0.003	0.001
K	0.002	0.000	0.001	0.000	0.000	0.000	0.001	0.000	0.000	0.000
Total	8.010	8.020	8.016	8.019	8.012	8.020	8.029	7.999	8.014	8.013
Fe/(Fe+Mg)	0.788	0.792	0.796	0.795	0.835	0.825	0.832	0.822	0.842	0.847
Prp	0.188	0.188	0.184	0.182	0.146	0.155	0.149	0.154	0.138	0.132
Grs	0.093	0.087	0.086	0.101	0.086	0.086	0.088	0.082	0.083	0.089
Alm	0.689	0.695	0.701	0.688	0.727	0.715	0.706	0.710	0.722	0.717
Sps	0.030	0.030	0.030	0.030	0.041	0.044	0.057	0.053	0.057	0.062

Table 4. Representative chemical analyses of biotite from samples VAL01 and VAL20.

	VAL01					VAL20					
	Core	Core	Rim	Rim	Rim	Core	Core	Rim	Rim	Rim	Rim
SiO_2	35.17	35.19	35.17	35.44	34.46	36.45	36.49	36.78	35.65	37.18	35.82
TiO_2	2.10	2.06	2.10	2.12	2.30	1.57	3.02	1.61	2.47	2.89	2.782

Al_2O_3	20.36	20.52	20.36	19.69	20.03	21.57	18.76	21.97	19.78	18.61	18.74
FeO	18.83	18.47	18.83	18.20	19.61	15.37	17.21	15.60	18.30	17.38	17.753
MnO	0.12	0.10	0.12	0.13	0.12	0.05	0.08	0.07	0.09	0.09	0.049
MgO	8.92	8.98	8.92	8.89	8.19	9.65	9.15	9.67	9.45	8.75	8.702
Na_2O	0.15	0.15	0.15	0.15	0.14	0.14	0.20	0.12	0.23	0.16	0.082
K_2O	8.76	8.55	8.76	8.36	8.33	8.49	8.23	8.02	7.09	8.06	8.279
BaO	0.21	0.15	0.21	0.24	0.25	0.20	0.13	0.20	0.28	0.07	0.139
Cl	0.01	0.01	0.01	0.01	0.01	0.03	0.02	0.05	0.04	0.02	0.011
Total	94.62	94.18	94.62	93.22	93.43	93.52	93.28	94.08	93.37	93.21	92.36
Si	2.933	2.925	2.922	2.973	2.911	2.989	3.035	2.989	2.965	3.086	3.022
Ti	0.129	0.129	0.131	0.134	0.146	0.097	0.189	0.099	0.155	0.180	0.177
Al	1.988	2.011	1.994	1.947	1.994	2.085	1.839	2.105	1.938	1.821	1.864
Fe^{+2}	1.282	1.285	1.308	1.277	1.386	1.054	1.197	1.060	1.272	1.206	1.253
Mn	0.010	0.007	0.008	0.276	0.009	0.003	0.006	0.005	0.006	0.006	0.004
Mg	1.116	1.113	1.104	1.111	1.032	1.180	1.134	1.171	1.171	1.083	1.094
Na	0.022	0.024	0.024	0.025	0.022	0.022	0.032	0.020	0.037	0.026	0.013
K	0.939	0.907	0.928	0.895	0.898	0.889	0.873	0.831	0.752	0.854	0.891
BaO	0.007	0.005	0.007	0.008	0.008	0.006	0.004	0.006	0.009	0.002	0.005
Cl	0.001	0.002	0.001	0.001	0.002	0.004	0.002	0.006	0.006	0.002	0.002
Total	8.426	8.407	8.427	8.647	8.407	8.330	8.312	8.292	8.312	8.266	8.324
Fe/(Fe+Mg)	0.535	0.536	0.542	0.535	0.573	0.472	0.514	0.475	0.521	0.527	0.534

	VAL08			VAL68						
	Core	Core	Rim	Core	Core	Core	Rim	Rim	Rim	Rim
SiO_2	34.74	34.96	34.97	34.68	35.20	35.09	34.90	35.26	35.38	35.03
TiO_2	2.52	2.33	2.49	2.60	2.88	2.38	2.66	2.00	2.31	2.10
Al_2O_3	19.74	20.31	20.54	18.71	19.19	19.92	19.01	19.97	20.05	19.86
FeO	19.16	18.74	18.54	19.54	19.51	20.08	20.02	19.88	19.35	19.48
MnO	0.18	0.21	0.20	0.09	0.09	0.07	0.12	0.06	0.07	0.07

MgO	8.24	8.59	8.22	8.97	8.59	8.09	8.57	8.22	8.49	8.78
Na_2O	0.11	0.10	0.10	0.12	0.12	0.10	0.15	0.11	0.13	0.13
K_2O	8.39	9.13	9.11	8.70	8.70	8.77	8.66	8.90	8.75	8.64
BaO	0.17	0.04	0.18	0.13	0.15	0.20	0.22	0.14	0.19	0.22
Cl	0.01	0.02	0.02	0.00	0.01	0.00	0.01	0.00	0.01	0.01
Total	93.27	94.43	94.36	93.54	94.43	94.70	94.31	94.53	94.73	94.31
Si	2.932	2.915	2.916	2.934	2.942	2.931	2.933	2.947	2.940	2.930
Ti	0.160	0.146	0.156	0.165	0.181	0.149	0.168	0.126	0.145	0.132
Al	1.964	1.996	2.019	1.866	1.890	1.961	1.883	1.967	1.965	1.958
Fe^{+2}	1.352	1.306	1.293	1.383	1.364	1.402	1.407	1.389	1.345	1.362
Mn	0.012	0.015	0.014	0.006	0.006	0.005	0.008	0.004	0.005	0.005
Mg	1.037	1.068	1.022	1.131	1.070	1.007	1.074	1.024	1.052	1.095
Na	0.018	0.017	0.016	0.020	0.020	0.017	0.025	0.018	0.021	0.021
K	0.904	0.971	0.969	0.938	0.928	0.935	0.929	0.948	0.928	0.921
BaO	0.003	0.001	0.006	0.004	0.005	0.006	0.007	0.005	0.006	0.007
Cl	0.002	0.003	0.002	0.000	0.001	0.000	0.001	0.000	0.001	0.001
Total	8.385	8.438	8.413	8.448	8.407	8.414	8.435	8.427	8.408	8.431
Fe/(Fe+Mg)	0.566	0.550	0.559	0.550	0.560	0.582	0.567	0.576	0.561	0.554

Table 5. Representative chemical analyses of biotite from samples VAL08 and VAL68.

Table 6. Representative chemical analyses of plagioclase from samples VAL01, VAL20 and VAL68.

	VAL01				VAL20				VAL68		
	Core	Core	Rim	Rim	Core	Core	Rim	Rim	Core	Rim	Rim
SiO_2	59.93	60.09	61.27	59.41	58.98	58.28	58.38	58.36	59.10	59.45	59.02
Al_2O_3	25.87	25.45	25.06	25.67	26.07	25.76	26.29	26.14	25.90	25.69	25.98
FeO	0.03	0.07	0.02	0.05	0.01	0.08	0.04	0.07	0.03	0.03	0.10
CaO	6.39	4.58	5.32	6.71	6.91	7.04	7.63	7.24	6.97	6.69	7.02
Na_2O	7.77	7.75	8.33	7.61	7.37	7.21	7.11	7.29	7.51	7.65	7.31
K_2O	0.08	0.87	0.26	0.06	0.12	0.11	0.09	0.13	0.12	0.11	0.12

Total	100.08	98.81	100.25	99.50	99.46	98.47	99.55	99.22	99.62	99.62	99.55
Si	2.662	2.697	2.711	2.657	2.640	2.622	2.650	2.624	2.644	2.657	2.641
Al	1.355	1.346	1.307	1.353	1.376	1.387	1.358	1.385	1.366	1.353	1.370
Fe^{+2}	0.001	0.003	0.001	0.002	0.000	0.002	0.001	0.002	0.001	0.001	0.004
Ca	0.304	0.220	0.252	0.322	0.332	0.341	0.336	0.349	0.334	0.320	0.336
Na	0.670	0.674	0.714	0.660	0.639	0.633	0.647	0.635	0.651	0.663	0.634
K	0.005	0.050	0.014	0.003	0.007	0.006	0.006	0.007	0.007	0.006	0.007
Total	4.997	4.991	5.000	4.997	4.994	4.991	4.997	5.003	5.002	5.001	4.993

Table 7. Representative chemical analysis of quartz from sample VAL08.

SiO_2	101.4815	101.6778	101.5157	100.5493	100.9903	101.2492	101.1945	100.9783	101.0628	100.7641
TiO_2	0.0048	0.0039	0.0050	0.0053	0.0022	0.0026	0.0069	0.0052	0.0056	0.0042
Total	101.4863	101.6817	101.5207	100.5546	100.9925	101.2518	101.2014	100.9835	101.0684	100.7683
Ti (ppm)	28.78	23.38	29.98	31.77	13.19	15.59	41.37	31.17	33.57	25.18

Ti in quartz Geothermometry Temperatures calculated using a pressure of 0.65 GPa										
						T(°C)				
Thomas et al. (2010)	621	603	625	630	-	568	656	629	636	609

Table 8. Calculated P-T values obtained from GPT worksheet (Reche and Martinez,1996).

	VAL01									VAL08		
	Core	Core	Core	Core	Rim	Rim	Rim	Rim	Rim	Core	Core	Rim
Garnet-Biotite Geothermometry						T(°C)						
Holdaway and Lee (1977)	666	641	623	678	518	522	555	533	561	634	661	568
Bhattacharya et al. (1992)	646	633	603	663	510	509	529	508	544	608	648	585
Perchuk and Lavrent'eva (1993)a	653	633	619	656	550	553	578	561	579	628	649	571
Perchuk and Lavrent'eva (1993)b	652	633	618	664	528	531	559	541	565	627	659	543
GASP Geobarometry						P (GPa)						
Koziol (1989)	0.59		0.58		0.28		0.34					

						VAL20					
	Core	Core	Core	Core	Rim	Rim	Rim	Rim	Rim	Rim	Rim
Garnet-Biotite Geothermometry						T(°C)					
Holdaway and Lee (1977)	634	692	714	698	613	579	587	604	635	665	668
Bhattacharya et al. (1992)	636	675	691	680	607	587	590	595	623	653	643
Perchuk and Lavrent'eva (1993)a	628	663	677	669	614	593	600	607	629	649	651
Perchuk and Lavrent'eva (1993)b	627	676	693	681	610	580	586	603	628	653	655
GASP Geobarometry						P (GPa)					
Koziol (1989)		0.77	0.8	0.74			0.4				

					VAL68					
	Core	Core	Core	Core	Rim	Rim	Rim	Rim	Rim	Rim
Garnet-Biotite Geothermometry					T(°C)					
Holdaway and Lee (1977)	765	761	803	748	668	688	690	706	651	640
Bhattacharya et al. (1992)	734	708	764	723	657	673	665	683	640	632
Perchuk and Lavrent'eva (1993)a	709	731	735	700	647	663	673	673	639	632
Perchuk and Lavrent'eva (1993)b	734	728	764	721	657	672	670	687	641	632
GASP Geobarometry					P (GPa)					
Koziol (1989)	0.91				0.72	0.72				

3 CONCLUSÕES

A Orogênese Brasiliana na região de Feira Nova imprimiu uma trama estrutural que sugere transição progressiva entre um regime contracional e um regime transpressivo. O primeiro produziu foliação de baixo ângulo (S_2) pervasiva, sob condições de pico metamórfico estimadas em ~760-650°C e ~0,6-0,9 GPa - próximo à transição anfibolito-granulito - e está associada a anatexia local. Lineação de alta obliquidade e caimento para SE e critérios cinemáticos indicam transporte tectônico para NW, associado à formação de meso- e macrodobras de mesma vergência, e de zonas de cisalhamento contracionais, incluindo a Zona de Cisalhamento Paudalho (ZCP). Uma foliação prévia que localmente desenha dobras isoclinais intrafoliais à foliação regional também pertence a esse regime e pode ser atribuída a um estágio inicial de espessamento crustal. A transpressão é representada por foliação milonítica de alto ângulo (S_3), constituindo zonas de cisalhamento transcorrentes sinistrais, incluindo Glória do Goitá (ZCGG) e componente transcorrente sinistral da ZCP. A esse regime, associam-se dobras suaves a abertas as quais redobram as dobras com vergência para NW, formando padrões de interferência do tipo 3. O redobramento, responsável pela reorientação de lineações nas rochas metassedimentares, pode ser explicado por um componente de sentido SW produzido pela movimentação da ZCGG. Bandas de cisalhamento contracionais locais com transporte para SW correlacionáveis a uma estrutura do tipo rabo de cavalo para a terminação da ZCGG corroboram essa interpretação. Zoneamento mineral sugere esfriamento e descompressão para ~590-520°C e 0,4-0,3 GPa - transição anfibolito baixo a xisto verde alto, provavelmente relacionado aos estágios finais do regime transpressivo. Os dados sugerem que as rochas da região atingiram profundidades de até ~23-34 km e foram posteriormente exumadas para ~19-11 km. Ocorrência de cianita em regiões próximas permite a inferência de uma trajetória P-T-t horária, atribuída a espessamento crustal em ambiente predominantemente intracontinental e exumação sob baixas taxas de erosão e resfriamento.

REFERÊNCIAS

ACCIOLY, A.C.A. **Geologia, Geoquímica e Significado Tectônico do Complexo Metanortosítico de Passira – Província Borborema - Nordeste Brasileiro**. 2000. 224 f. Tese. (Doutorado em Geoquímica e Geotectônica) - Universidade de São Paulo, São Paulo, 2000.

ACCIOLY, A.C.A.; MCREATH, I.; SANTOS, E.J.; GUIMARÃES, I.P.; VANNUCI, R.; BOTTAZZI, R. The Passira meta-anorthositic complex and its tectonic implication, Borborema Province, Brazil. *In*: **Proceedings of the International Geological Congress**. 31., 2000, Rio de Janeiro. International Union of Geological Sciences, 2000.

ACCIOLY, A.C.A.; MCREATH, I.; SANTOS, E.J.; GUIMARÃES, I.P.; SANTOS, A.C. The Ages of Crystallization and Metamorphism of the Passira Anorthosite Complex Borborema Province, Northeastern Brazil. *In*: **South American Symposium on Isotope Geology**. 4., 2003, Salvador. CBPM, 2003. p. 487-490.

AGUE, J.J.; CARLSON, W.D. Metamorphism as Garnet Sees It: The Kinetics of Nucleation and Growth, Equilibration, and Diffusional Relaxation. **Elements**, v. 9, n. 6, 2013, p. 439-445. Doi: 10.2113/gselements.9.6.439. Disponível em: https://pubs.geoscienceworld.org/msa/elements/article-abstract/9/6/439/137980/Metamorphism-as-Garnet-Sees-It-The-Kinetics-of?redirectedFrom=fulltext. Acesso em: 09 jan. 2021.

ALMEIDA, F.F.M.; HASUI, Y.; BRITO NEVES, B.B.; FUCK, R. Brazilian Structural Provinces: An introduction. **Earth Science Reviews**, v.**17**, p. 1-29, 1981.

AMARAL, W.S.; DOS SANTOS, T.J.S; WERNICK, E.; NOGUEIRA NETO, J.A.; DANTAS, E.L.; MATTEINI, M. High-pressure granulites from Carire, Borborema Province, NE Brazil: Tectonic setting, metamorphic conditions and U-Pb, Lu-Hf and Sm-Nd geochronology. **Gondwana Research**, v. 22, 2012, p. 892-909. Doi:10.1016/j.gr.2012.02.011. Disponível em: https://www.sciencedirect.com/science/article/abs/pii/S1342937X12000524. Acesso em: 09 jan. 2021.

ARAUJO, C.E.G.; WEINBERG, R.F.; CORDANI, U.G. Extruding the Borborema Province (NE-Brazil): a two-stage Neoproterozoic collision process. **Terra Nova**, v. 26, n. 2, 2014, p. 157-168. Doi: 10.1111/ter.12084.Disponível em: https://onlinelibrary.wiley.com/doi/abs/10.1111/ter.12084. Acesso em: 09 jan. 2021.

ARCHANJO, C.J., TRINDADE, R.I., BOUCHEZ, J.L., ERNESTO, M. Granite fabrics and regional-scale strain partitioning in the Seridó belt (Borborema Province, NE Brazil). **Tectonics**, v. 21, n. 1, 2002, p.1-14. Doi: 10.1029/2000TC001269. Disponível em: https://agupubs.onlinelibrary.wiley.com/doi/full/10.1029/2000TC001269. Acesso em: 09 jan. 2021.

ARCHANJO, C.J.; HOLLANDA, M.H.B.M.; RODRIGUES, S.W.O.; BRITO NEVES, B.B.; ARMSTRONG, R. Fabrics of pre- and syntectonic granite plutons and chronology of shear zones in the Eastern Borborema Province, NE Brazil. **Journal of Structural Geology**, v. 30,

2008, p. 310-326. Doi:10.1016/j.jsg.2007.11.011. Disponível em: https://www.sciencedirect.com/science/article/abs/pii/S0191814107002192. Acesso em: 09 jan. 2021.

ARCHANJO, C.J.; VIEGAS, L.G.F.; HOLLANDA, M.H.B.M.; SOUZA, L.C.; LIU, D. Timing of the HT/LP transpression in the Neoproterozoic Seridó Belt (Borborema Province, Brazil): Constraints from U-Pb (SHRIMP) geochronology and implications for the connections between NE Brazil and West Africa. **Gondwana Research**, v. 23, n. 2, 2013, p. 701-714. Doi:10.1016/j.gr.2012.05.005. Disponível em: https://www.sciencedirect.com/science/article/abs/pii/S1342937X12001815. Acesso em: 09 jan. 2021.

BAIRD, G.B.; SHRADY, C.H. Timing and kinematics of deformation in the northwest Adirondack Lowlands, New York State: Implications for terrane relationships in the southern Grenville Province. **Geosphere**, v. 7, n. 6, 2011, p. 1303-1323. doi:10.1130/GES00689.1. Disponível em: https://pubs.geoscienceworld.org/gsa/geosphere/article/7/6/1303/132492/Timing-and-kinematics-of-deformation-in-the. Acesso em: 09 jan. 2021.

BARANOV, V.; NAUDY, H. Numerical Calculation of the Formula of Reduction to the Magnetic Pole. **Geophysics**, v. 29, n. 1, 1964, p. 67-79. Doi: 10.1130/GES00689. Disponível em: https://pubs.geoscienceworld.org/geophysics/article-abstract/29/1/67/70611/Numerical-calculation-of-the-formula-of-reduction?redirectedFrom=fulltext. Acesso em: 09 jan. 2021.

BARBOSA, A. G. **Programa de Levantamentos Geológicos Básicos do Brasil: Geologia da Folha Limoeiro - SB.25-Y-C-V, escala 1:100.000.** Brasília, 1990. CPRM/DNPM. 116 f.

BARRETO, M. C. **Caracterização Geoquímica e Isotópica de Mármores do Terreno Rio Capibaribe na Zona Transversal da Província Borborema-Nordeste do Brasil**. 2008. 253 f. Tese. (Doutorado em Geociências) - Universidade Federal de Pernambuco, Recife, 2008.

BASTO, C. F.; CAXITO, F. D. A.; DO VALE, J. A. R.; SILVEIRA, D. A.; RODRIGUES, J. B.; ALKMIN, A. R.; VALERIANO, C. D. M.; SANTOS, E. J. D. An Ediacaran back-arc basin preserved in the Transversal Zone of the Borborema Province: Evidence from geochemistry, geochronology and isotope systematics of the Ipueirinha Group, NE Brazil. **Precambrian Research**, v. 320, 2019, p 213-231. Doi: 10.1016/j.precamres.2018.11.002. Disponível em: https://www.sciencedirect.com/science/article/abs/pii/S0301926818302250. Acesso em: 09 jan. 2021.

BHATTACHARYA, A.; MOHANTY, L.; MAJI, A.; SEN, S. K.; RAITH, M. Non-ideal mixing in the phlogopite-annite binary: constraints from experimental data on Mg-Fe partitioning and a reformulation of the biotite-garnet geothermometer. **Contributions to Mineralogy and Petrology**, v. 111, 1992, p. 87-93. Doi: 10.1007/BF00296580. Disponível em: https://link.springer.com/article/10.1007/BF00296580. Acesso em: 09 jan. 2021.

BHATTACHARYA, A.; REKHA, S.; SEQUEIRA, N.; CHATTERJEE, A. Transition from shallow to steep foliation in the Early Neoproterozoic Gangpur accretionary orogen (Eastern India): Mechanics, significance of mid-crustal deformation, and case for subduction polarity reversal? **Lithos**, v. 348-349, 105196, 2019. Doi: 10.1016/ j.lithos.2019.105196. Disponível

em: https://www.sciencedirect.com/science/article/abs/pii/S002449371930355X. Acesso em: 09 jan. 2021.

BLUNDY, J. D.; HOLLAND, T. J. B. Calcic amphibole equilibria and a new amphibole-plagioclase geothermometer. **Contributions to Mineralogy and Petrology**, v. 104, n. 2, 1990, p. 208-224. Doi: 10.1007/BF00306444. Disponível em: https://link.springer.com/article/10.1007/BF00306444. Acesso em: 09 jan. 2021.

BRITO NEVES, B. B.; SANTOS, E. J.; VAN SCHMUS, W. R. Tectonic history of the Borborema province. *In*: PROCEEDINGS OF THE INTERNATIONAL GEOLOGICAL CONGRESS. 31., 2000, Rio de Janeiro. International Union of Geological Sciences, 2000. p. 151-182.

BRITO NEVES, B. B.; SPRÖESSER, W. M.; PETRONILHO, L. A.; SOUZA, S. L. Contribuição à Geologia e à Geocronologia do Terreno Rio Capibaribe (TRC, Província Borborema). **Geologia USP - Série Científica**, v. 13, n. 2, 2013, p. 97-122. Doi: http://dx.doi.org/10.5327/Z1519-874X2013000200006. Disponível em: http://www.ppegeo.igc.usp.br/index.php/GUSPSC/article/view/1210. Acesso em: 09 jan. 2021.

BRITO NEVES, B. B.; SANTOS, E. J.; FUCK, R. A.; SANTOS, L. C. M. L. A preserved early Ediacaran magmatic arc at the northernmost portion of the Transversal Zone central subprovince of the Borborema Province, Northeastern South America. **Brazilian Journal of Geology**, v. 46, n. 4, 2016, p. 491-508. Doi: 10.1590/2317-4889201620160004. Disponível em: https://www.scielo.br/scielo.php?pid=S2317-48892016000400491&script=sci_abstract. Acesso em: 09 jan. 2021.

CABY, R.; SIAL, A. N.; FERREIRA, V. P. High-pressure thermal aureoles around two Neoproterozoic synorogenic magmatic epidote-bearing granitoids, Northeastern Brazil. **Journal of South American Earth Sciences**, v. 27, n. 2–3, 2009, p. 184-196. Doi: 10.1016/j.jsames.2008.09.005. Disponível em: https://www.sciencedirect.com/science/article/abs/pii/S089598110800093X. Acesso em: 09 jan. 2021.

CARTWRIGHT, I.; BUICK, I. S.; FOSTER, D. A.; LAMBERT, D. D. Alice Springs age shear zones from the southeastern Reynolds Range, central Australia. **Australian Journal of Earth Sciences**, v. 46, n. 3, 2009, p. 355-363. Doi: https://doi.org/10.1046/j.1440-0952.1999.00710.x. Disponível em: https://onlinelibrary.wiley.com/doi/abs/10.1046/j.1440-0952.1999.00710.x. Acesso em: 09 jan. 2021.

CARRERAS, J.; DRUGUET, E.; GRIERA, A. Shear zone-related folds. **Journal of Structural Geology**, v. 27, 2005, p. 1229-1251. Doi: 10.1016/j.jsg.2004.08.004. Disponível em: https://www.sciencedirect.com/science/article/abs/pii/S0191814104001403. Acesso em: 09 jan. 2021.

CARRERAS, J.; DRUGUET, E. Complex fold patterns developed by progressive deformation. **Journal of Structural Geology**, v. 125, 2019, p. 195-201. Doi: 10.1016/j.jsg.2018.07.015. Disponível em: https://www.sciencedirect.com/science/article/abs/pii/S0191814118303857. Acesso em: 09 jan. 2021.

CASTRO, N.A. **Evolução geológica proterozoica da região entre Madalena e Taperuaba, Domínio Tectônico Ceará Central (Província Borborema)**. 2004. 335 f. Tese. (Doutorado em Geoquímica e Geotectônica) - Universidade de São Paulo, São Paulo, 2004. Acesso em: 09 jan. 2021.

CONNORS, K.C.; LISTER, G. S. Polyphase deformation in the western Mount Isa Inlier, Australia: episodic or continuous deformation? **Journal of Structural Geology**, v. 17, n. 3, 1995, p. 305-328. Doi: https://doi.org/10.1016/0191-8141(94)00057-7. Disponível em: https://www.sciencedirect.com/science/article/abs/pii/0191814194000577. Acesso em: 09 jan. 2021.

CORSINI, M.; LAMBERT DE FIGUEIREDO; L., CABY, R.; FÉRAUD, G.; RUFFET, G.; VAUCHEZ, A. Thermal history of the Pan-African/Brasiliano Borborema Province of northeast Brazil deduced from 40Ar/39Ar analysis. **Tectonophysics**, v. 285, n. 1-2, 1998, p. 103-117. Doi: https://doi.org/10.1016/S0040-1951(97)00192-3. Disponível em: https://www.sciencedirect.com/science/article/abs/pii/S0040195197001923. Acesso em: 09 jan. 2021.

DANTAS, E. L.; SILVA, A. M.; ALMEIDA, T.; MORAES, R. A. V. Old geophysical data applied to modern geological mapping problems: a case-study in the Seridó Belt, NE Brazil. **Revista Brasileira de Geociências**, v. 33, n. 2, 2003, p. 65-72. Disponível em: http://www.ppegeo.igc.usp.br/index.php/rbg/article/view/9843. Acesso em: 09 jan. 2021.

DHUIME, B.; BOSCH, D.; BRUGUIER, O.; CABY, R.; ARCHANJO, C. An Early-Cambrian U-Pb apatite cooling age for the high-temperature regional metamorphism in the Piancó area, Borborema Province (NE Brazil): initial conclusions. **Comptes Rendus Geoscience**, v. 335, n. 15, 2003, p. 1081-1089. Doi: 10.1016/j.crte.2003.09.012. Disponível em: https://www.sciencedirect.com/science/article/pii/S1631071303001895. Acesso em: 09 jan. 2021.

DUEBENDORFER, E. M. The interpretation of stretching lineations in multiply deformed terranes: an example from the Hualapai Mountains, Arizona, USA. **Journal of Structural Geology**, v. 25, n. 9, 2003, p. 1393-1400. Doi: 10.1016/S0191-8141(02)00203-1. Disponível em: https://www.sciencedirect.com/science/article/abs/pii/S0191814102002031. Acesso em: 09 jan. 2021.

ENGLAND; P. C., RICHARDSON, S.W. The influence of erosion upon the mineral fades of rocks from different metamorphic environments. **Journal of the Geological Society**, v. 134, 1977, p. 201-213. Doi: 10.1144/gsjgs.134.2.0201. Disponível em: https://jgs.lyellcollection.org/content/134/2/201. Acesso em: 10 jan. 2021.

ENGLAND, P. C.; THOMPSON, A. B. Pressure-Temperature-Time Paths of Regional Metamorphism I. Heat Transfer during the Evolution of Regions of Thickened Continental Crust. **Journal of Petrology**, v. 25, n. 4, 1984, p. 894-928. Doi: 10.1093/petrology/25.4.894. Disponível em: https://academic.oup.com/petrology/article-abstract/25/4/894/1386927. Acesso em: 10 jan. 2021.

ERNST, W. G. Tectonic history of subduction zones inferred from retrograde blueschist P-T paths. **Geology**, v. 16, n. 12, 1988, p. 1081-1084. Doi: 10.1130/0091-

7613(1988)016<1081:THOSZI>2.3.CO;2**.** Disponível em: https://pubs.geoscienceworld.org/gsa/geology/article-abstract/16/12/1081/204628/Tectonic-history-of-subduction-zones-inferred-from. Acesso em: 10 jan. 2021.

ERNST, W. G.; LIU, J. Experimental phase-equilibrium study of Al- and Ti-contents of calcic amphibole in MORB - A semiquantitative thermobarometer. **American Mineralogist**, v. 83, n. 9-10, 1988, p. 952–969. Doi: 10.2138/am-1998-9-1004. Disponível em: https://pubs.geoscienceworld.org/msa/ammin/article-abstract/83/9-10/952/43578/Experimental-phase-equilibrium-study-of-Al-and-Ti?redirectedFrom=fulltext. Acesso em: 10 jan. 2021.

ESCHER, A.; WATERSON, J. Stretching fabrics, folds and crustal shortening. **Tectonophysics**, v. 22, 1974, p. 223-231. Doi: 10.1016/0040-1951(74)90083-3. Disponível em: https://www.sciencedirect.com/science/article/abs/pii/0040195174900833. Acesso em: 10 jan. 2021.

FLORENCE, F. P.; SPEAR, F. S. Intergranular diffusion kinetics of Fe and Mg during retrograde metamorphism of a pelitic gneiss from the Adirondack Mountains. **Earth and Planetary Science Letters**, v. 34, n. 3-4, 1995, p. 329-340. Doi: 10.1016/0012-821X(95)00129-Z. Disponível em: https://www.sciencedirect.com/science/article/abs/pii/0012821X9500129Z. Acesso em: 10 jan. 2021.

FORBES, C. J.; BETTS, P. G.; LISTER, G. S. Synchronous development of Type 2 and Type 3-fold interference patterns: evidence for recumbent sheath folds in the Allendale Area, Broken Hill, NSW, Australia. **Journal of Structural Geology**, v. 26, n. 1, 2004, p. 113-126. Doi: 10.1016/S0191-8141(03)00074-9. Disponível em: https://openresearch-repository.anu.edu.au/handle/1885/80734?mode=full. Acesso em: 10 jan. 2021.

FOSSEN, H.; TEYSSIER, C.; WHITNEY, D. L. Transtensional folding. **Journal of Structural Geology**, v. 56, 2013, p. 89-112. Doi: 10.1016/j.jsg.2013.09.004. Disponível em: https://www.sciencedirect.com/science/article/abs/pii/S0191814113001570. Acesso em: 10 jan. 2021.

FOSSEN, H. Writing papers with an emphasis on structural geology and tectonics: advices and warnings. **Brazilian Journal of Geology**, v. 49, n. 4, 2019, p. 1-6. Doi: 10.1590/2317-4889201920190109. Disponível em: https://www.scielo.br/scielo.php?script=sci_arttext&pid=S2317-48892019000400200. Acesso em: 10 jan. 2021.

FOSSEN, H.; CAVALCANTE, G.C.; PINHEIRO, R.V.L.; ARCHANJO, C.J. Deformation – progressive or multiphase? **Journal of Structural Geology**, v. 125, 2019, p. 82-99. Doi: 10.1016/j.jsg.2018.05.006 Disponível em: https://www.sciencedirect.com/science/article/abs/pii/S0191814118300142. Acesso em: 10 jan. 2021.

FORSTER, M. A.; LISTER, G. S. Tectonic sequence diagrams and the structural evolution of schists and gneisses in multiply deformed terranes. **Journal of Geological Society**, v. 165, 2008, p. 923-939. Doi: 10.1144/0016-76492007-016 Disponível em: https://jgs.lyellcollection.org/content/165/5/923. Acesso em: 10 jan. 2021.

GOSCOMBE, B. D.; GRAY, D. R. Structure and strain variation at mid-crustal levels in a transpressional orogen: A review of Kaoko Belt structure and the character of West Gondwana amalgamation and dispersal. **Gondwana Research**, v. 13, n. 1, 2008, p. 45-85. Doi: 10.1016/j.gr.2007.07.002. Disponível em: https://www.sciencedirect.com/science/article/abs/pii/S1342937X07001578. Acesso em: 10 jan. 2021.

GRAY, M. B.; MITRA, G. Ramifications of four-dimensional progressive deformation in contractional mountain belts. **Journal of Structural Geology**, v. 21, n. 8, 1999, p. 1151–1160. Doi: 10.1016/S0191-8141(99)00059-0. Disponível em: https://www.sciencedirect.com/science/article/abs/pii/S0191814199000590. Acesso em: 10 jan. 2021.

GUIMARÃES, I. P. **The petrological evolution and tectonic associations of the Bom Jardim Complex, Pernambuco State, NE Brazil**. 1989. 423 f. Tese. (Doutorado em Geologia) - University of London, Londres, 1989.

GUIMARÃES, I. P.; SILVA FILHO, A. F. Evolução petrológica e geoquímica do complexo Bom Jardim, Pernambuco. **Revista Brasileira**, v. 2, n. 22, 1992, p. 29-42. Disponível em: http://www.ppegeo.igc.usp.br/index.php/rbg/article/view/11728. Acesso em: 10 jan. 2021.

GUIMARÃES, I. P.; DA SILVA FILHO; A. F., ALMEIDA; C. N.; VAN SCHMUS; W. R.; ARAÚJO, J. M. M.; MELO, S. C.; MELO, E. B. Brasiliano (Pan-African) granitic magmatism in the Pajeú-Paraíba belt, Northeast Brazil: an isotopic and geochronological approach. **Precambrian Research**, v. 135, 2004, p. 23-53. Doi: 10.1016/j.precamres.2004.07.004 Disponível em: https://www.sciencedirect.com/science/article/abs/pii/S0301926804001846. Acesso em: 10 jan. 2021.

GUIMARÃES, I. P.; SILVA FILHO, A. F.; MELO, S. C.; MACAMBIRA, M. B. Petrogenesis of A-type Granitoids from the Alto Moxotó and Alto Pajeú Terranes of the Borborema Province, NE Brazil: Constraints from Geochemistry and Isotopic Composition. **Gondwana Research**, v. 8, n. 3, 2005, p. 347-362. Doi: 10.1016/S1342-937X(05)71140-0. Disponível em: https://www.sciencedirect.com/science/article/abs/pii/S1342937X05711400. Acesso em: 10 jan. 2021.

GUIMARÃES, I. P.; VAN SCHMUS, W. R.; BRITO NEVES, B. B.; BITTAR, S. M.; SILVA FILHO, A. F.; ARMSTRONG, R. U-Pb zircon ages of orthogneisses and supracrustal rocks of the Cariris Velhos belt: onset of Neoproterozoic rifting in the Borborema Province, NE Brazil. **Precambrian Research**, v. 192-195, 2012, p. 52-77. Doi: 10.1016/j.precamres.2011.10.008. Disponível em: https://www.sciencedirect.com/science/article/abs/pii/S0301926811002166. Acesso em: 10 jan. 2021.

HACKER, R. T.; WOOD, B. J. Experimental determination of Fe and Mg exchange between garnet and olivine and estimation of Fe-Mg mixing properties in garnet. **American Mineralogist**, v. 74, 1989, p. 994-999. Disponível em: https://pubs.geoscienceworld.org/msa/ammin/article-abstract/74/9-

10/994/42342/Experimental-determination-of-Fe-and-Mg-exchange?redirectedFrom=fulltext. Acesso em: 10 jan. 2021.

HALPIN, J. A.; CLARKE, G. L.; WHITE, R. W.; KELSEY, D. E. Contrasting P-T-t paths for Neoproterozoic metamorphism in MacRobertson and Kemp Lands, east Antarctica. **Journal of Metamorphic Geology**, v. 25, n. 6, 2007, p. 683-701. Doi: 10.1111/j.1525-1314.2007.00723.x. Disponível em: https://onlinelibrary.wiley.com/doi/abs/10.1111/j.1525-1314.2007.00723.x. Acesso em: 10 jan. 2021.

HODGES, K.; ROYDEN, L. Geologic thermobarometry of retrograded metamorphic rocks: an indication of the uplift trajectory of a portion of the Northern Scandinavian Caledonides. **Journal of Geophysical Research**, v. 89, n. B8, 1984, p 7077-7090. Doi: 10.1029/JB089iB08p07077. Disponível em: https://agupubs.onlinelibrary.wiley.com/doi/abs/10.1029/JB089iB08p07077. Acesso em: 10 jan. 2021.

HOLDSWORTH, R. E. Progressive deformation structures associated with ductile thrusts in the Moine Nappe, Sutherland, N. Scotland. **Journal of Structural Geology**, v. 12(4), 1990, p. 443-452. Doi: 10.1016/0191-8141(90)90033-U. Disponível em: https://www.sciencedirect.com/science/article/abs/pii/019181419090033U. Acesso em: 10 jan. 2021.

HOLDAWAY, M. J.; LEE, S. M. Fe-Mg Cordierite Stability in High-Grade Pelitic Rocks Based on Experimental, Theoretical, and Natural Observations. **Contributions Mineralogy Petrology**, v. 63, 1977, p. 175-198. Doi: 10.1007/BF00398778. Disponível em: https://link.springer.com/article/10.1007/BF00398778. Acesso em: 10 jan. 2021.

HOLLANDA, M. H. B. M.; ARCHANJO, C. J.; SOUZA, L. C.; ARMSTRONG, R.; VASCONCELOS, P. M. Cambrian mafic to felsic magmatism and its connections with transcurrent shear zones of the Borborema Province (NE Brazil): implications for the late assembly of the West Gondwana. **Precambrian Research**, v. 178, 2010, p. 1-14. Doi: 10.1016/j.precamres.2009.12.004. Disponível em: https://www.sciencedirect.com/science/article/abs/pii/S0301926809002514. Acesso em: 10 jan. 2021.

KOHN, M. J.; SPEAR, F. S. Retrograde net transfer reaction insurance for pressure-temperature estimates. **Geology**, v. 28, n. 12, 2000, p. 1127-1130. Doi: 10.1130/0091-7613(2000)28<1127:RNTRIF>2.0.CO;2. Disponível em: https://pubs.geoscienceworld.org/gsa/geology/article-abstract/28/12/1127/207188/Retrograde-net-transfer-reaction-insurance-for?redirectedFrom=fulltext. Acesso em: 10 jan. 2021.

KOZIOL, A. M. Recalibration of the garnet-plagioclase-Al_2SiO_5-quartz (GASP) geobarometer and application to natural parageneses. *In*: AMERICAN GEOPHYSICAL UNION SPRING MEETING, v. 70, 1989, Baltimore. American Geophysical Union, 1989.

LANARI, P.; VIDAL, O.; DE ANDRADE, V.; DUBACQ, B.; LEWIN, E.; GROSCH, E.G.; SCHWARTZ, S. XMapTools: A MATLAB©-based program for electron microprobe X-ray image processing and geothermobarometry. **Computers & Geosciences**, v. 62, 2014, p. 227-240. Doi: 10.1016/j.cageo.2013.08.010. Disponível em:

https://www.sciencedirect.com/science/article/pii/S0098300413002379. Acesso em: 10 jan. 2021.

LEITE, P. R. B.; BERTRAND, J. M.; LIMA, E. S.; LETERRIER, J. Timing of granitic magmatism in the northern Borborema Province, Brazil: A U-Pb study of granitoids from the Alto Pajeú Terrain. **Journal of South American Earth Sciences**, v. 13, n. 6, 2000, p. 549-559. Doi: 10.1016/S0895-9811(00)00041-9. Disponível em: https://www.sciencedirect.com/science/article/abs/pii/S0895981100000419. Acesso em: 10 jan. 2021.

LIMA, H. M.; SANTOS, E. J.; SANTOS, L. C. M. L. Compartimentação estrutural da faixa Feira Nova e blocos adjacentes: Implicações para a evolução do terreno Rio Capibaribe da Província Borborema, NE do Brasil. **Revista Brasileira de Mineração e Meio Ambiente**, v. 5, n. 2, 2015a, p. 32-38. Disponível em: https://www.researchgate.net/publication/307594181_Compartimentacao_estrutural_da_faixa_Feira_Nova_e_blocos_adjacentes_Implicacoes_para_a_evolucao_do_terreno_Rio_Capibaribe_da_Provincia_Borborema_NE_do_Brasil. Acesso em: 10 jan. 2021.

LIMA, H. M.; FERREIRA, V. P.; SANTOS, E. J.; PIMENTEL. M. M.; SANTOS, L. C. M. L. Origem, significado petrogenético e idade dos ortognaisses Terra Nova: registro de magmatismo alcalino transtensional Neoproterozoico no domínio da zona transversal da Província Borborema. **Geochimica Brasiliensis**, v. 29, 2015b, p. 70-86. Doi: 10.21715/GB2358-2812.2015292070. Disponível em: http://www.ppegeo.igc.usp.br/index.php/geobras/article/view/10048. Acesso em: 10 jan. 2021.

LIMA, H. M.; PIMENTEL, M. M.; SANTOS, L. C. M. L.; MENDES, V. A. Análise tectônica da porção Nordeste da Faixa Sergipana, Província Borborema: Dupla vergência em resposta a colisão oblíqua entre o cráton do São Francisco e o Terreno Pernambuco-Alagoas. **Geonomos**, v. 25, n. 2, 2017, p. 20-30. Doi: 10.18285/ geonomos. v25i2.1078. Disponível em: https://periodicos.ufmg.br/index.php/revistageonomos/article/view/11449. Acesso em: 10 jan. 2021.

LIU, X.; WANG, W. R. Z.; ZHAO, Y.; LIU, J.; CHEN, H.; CUI, Y.; SONG, B. Early Mesoproterozoic arc magmatism followed by early Neoproterozoic granulite facies metamorphism with a near-isobaric cooling path at Mount Brown, Princess Elizabeth Land, East Antarctica. **Precambrian Research**, v. 284, 2016, p. 30-48. Doi: 10.1016/j.precamres.2016.08.003. Disponível em: https://www.sciencedirect.com/science/article/abs/pii/S0301926816301437. Acesso em: 10 jan. 2021.

MEINHOLD, G. Rutile and its applications in earth sciences. **Earth-Science Reviews**, v. 102, n. 1-2, 2010, p. 1-28. Doi: 10.1016/j.earscirev.2010.06.001. Disponível em: https://www.sciencedirect.com/science/article/abs/pii/S0012825210000656#:~:text=Rutile%20has%20a%20wide%20range,the%20Earth's%20crust%20and%20mantle. Acesso em: 10 jan. 2021.

MELO, A. A.; SIQUEIRA, L. P. Novas considerações sobre a geologia do pré-cambriano de Pernambuco Oriental. **Revista da Associação dos Geólogo de Pernambuco**, v. 1, n. 2, p. 32-41, 1971.

MILLIGAN, P. R.; GUNN P. J. Enhancement and presentation of airborne geophysical data. **AGSO Journal of Australian Geology and Geophysics**, v. 17, n. 2, 1997, p. 62-75. Disponível em: https://inis.iaea.org/search/search.aspx?orig_q=RN:28049084. Acesso em: 10 jan. 2021.

NEVES, S. P.; MARIANO, G. Assessing the tectonic significance of a large-scale transcurrent shear zone system: the Pernambuco lineament, northeastern Brazil. **Journal of Structural Geology**, v. 21, n. 10, 1999, p. 1369-1383. Doi: 10.1016/S0191-8141(99)00097-8. Disponível em: https://www.sciencedirect.com/science/article/abs/pii/S0191814199000978. Acesso em: 10 jan. 2021.

NEVES, S. P.; MARIANO, G. Heat-producing Elements-enriched Continental Mantle Lithosphere and Proterozoic Intracontinental Orogens: Insights from Brasiliano/Pan-African Belts. **Gondwana Research**, v. 7, n. 2, 2003, p. 427-436. Doi: 10.1016/S1342-937X(05)70794-2. Disponível em: https://www.sciencedirect.com/science/article/abs/pii/S1342937X05707942. Acesso em: 10 jan. 2021.

NEVES, S. P.; VAUCHEZ, A.; FERAUD, G. Tectono-thermal evolution, magma emplacement, and shear zone development in the Caruaru area (Borborema Province, NE Brazil). **Precambrian Research**, v. 99, 2000, p. 1-32. Doi: 10.1016/S0301-9268(99)00026-1. Disponível em: https://www.sciencedirect.com/science/article/abs/pii/S0301926899000261. Acesso em: 10 jan. 2021.

NEVES, S. P.; SILVA, J. M. R./ MARIANO, G. Oblique lineations in orthogneisses and supracrustal rocks: vertical partitioning of strain in a hot crust (eastern Borborema Province, NE Brazil). **Journal of Structural Geology**, v. 27, n. 8, 2005, p. 1513-1527. Doi: 10.1016/j.jsg.2005.02.002. Disponível em: https://www.sciencedirect.com/science/article/abs/pii/S0191814105000635. Acesso em: 10 jan. 2021.

NEVES S. P.; MARIANO G.; CORREIA P. B.; SILVA J. M. R. 70 m.y. of synorogenic plutonism in eastern Borborema Province (NE Brazil): temporal and kinematic constraints on the Brasiliano Orogeny. **Geodinamica Acta**, v. 19, 2006a, p. 213-236. Doi: 10.3166/ga.19.213-236. Disponível em: https://www.tandfonline.com/doi/abs/10.3166/ga.19.213-236. Acesso em: 10 jan. 2021.

NEVES, S. P.; BRUGUIER, O.; VAUCHEZ, A.; BOSCH, D.; SILVA, J. M. R.; MARIANO, G. Timing of crustal formation, deposition of supracrustal sequences and Transamazonian and Brasiliano metamorphism in eastern Borborema Province (NE Brazil): Implications for western Gondwana assembly. **Precambrian Research**, v. 149, 2006b, p. 197-216. Doi: 10.1016/j.precamres.2006.06.005 Disponível em: https://www.sciencedirect.com/science/article/abs/pii/S030192680600146X. Acesso em: 10 jan. 2021.

NEVES, S. P.; BRUGUIER, O.; BOSCH, D.; SILVA, J. M. R.; MARIANO, G. U–Pb ages of plutonic and metaplutonic rocks in southern Borborema Province (NE Brazil): Timing of Brasiliano deformation and magmatism. **Journal of South American Earth Science**, v. 25, n. 3, 2008, p. 285-297. Doi: 10.1016/j.jsames.2007.06.003. Disponível em:

https://www.sciencedirect.com/science/article/abs/pii/S0895981107000831. Acesso em: 10 jan. 2021.

NEVES, S. P.; OLIVIER BRUGUIER, O.; SILVA, J. M. R.; BOSCH, D.; ALCANTARA, V. C.; LIMA, C. M. The age distributions of detrital zircons in metasedimentary sequences in eastern Borborema Province (NE Brazil): Evidence for intracontinental sedimentation and orogenesis? **Precambrian Research**, v. 175, 2009, p. 187–205. Doi: 10.1016/j.precamres.2009.09.009. Disponível em: https://www.sciencedirect.com/science/article/abs/pii/S0301926809001995. Acesso em: 10 jan. 2021.

NEVES, S. P.; ALCANTARA, V. C. Geochemistry of orthogneisses and metasedimentary rocks across a proposed terrane boundary in the Central Domain of Borborema Province, NE Brazil: geodynamic implications. **Journal of South American Earth Sciences**, v. 29, 2010, p. 498-511. Doi: 10.1016/j.jsames.2009.08.002. Disponível em: https://www.sciencedirect.com/science/article/abs/pii/S0895981109001096. Acesso em: 10 jan. 2021.

NEVES, S. P.; MONIÉ, P.; BRUGUIER, O.; SILVA, J. M. R. Geochronological, thermochronological and thermobarometric constraints on deformation, magmatism and thermal regimes in eastern Borborema Province (NE Brazil). **Journal of South American Earth Sciences**, v. 38, 2012, p. 129-146. Doi: 10.1016/j.jsames.2012.06.003. Disponível em: https://www.sciencedirect.com/science/article/abs/pii/S0895981112000697. Acesso em: 10 jan. 2021.

NEVES, S. P.; LAGES, G. A.; BRASILINO, R. G.; MIRANDA, A.W.A. Paleoproterozoic accretionary and collisional processes and the build-up of the Borborema Province (NE Brazil): geochronological and geochemical evidence from the Central Domain. **Journal of South American Earth Science**, v. 58, 2015, p. 165-187. Doi: 10.1016/j.jsames.2014.06.009. Disponível em: https://www.sciencedirect.com/science/article/abs/pii/S0895981114000856. Acesso em: 10 jan. 2021.

NEVES, S. P.; SILVA, J. M. R.; BRUGUIER, O. Geometry, kinematics and geochronology of the Sertânia Complex (central Borborema Province, NE Brazil): Assessing the role of accretionary versus intraplate processes during West Gondwana assembly. **Precambrian Research**, v. 298, 2017, p. 552-571. Doi: 10.1016/j.precamres.2017.07.006. Disponível em: https://www.sciencedirect.com/science/article/abs/pii/S0301926816305903. Acesso em: 10 jan. 2021.

NEVES, S. P. Comment on "A preserved early Ediacaran magmatic arc at the northernmost part of the transversal zone - central domain of the Borborema Province, Northeast of South America", by B. B. de Brito Neves et al. (2016). **Brazilian Journal of Geology**, v. 48, n. 3, 2018, p. 623-630. Doi: 10.1590/2317-4889201820180049. Disponível em: https://www.scielo.br/scielo.php?script=sci_abstract&pid=S2317-48892018000300623&lng=en&nrm=iso. Acesso em: 10 jan. 2021.

NEVES, S. P.; SANTOS, T. A. S.; MEDEIROS, P. C.; AMORIM, L. Q.; CASIMIRO, D. C. G. Interference fold patterns in regional unidirectional stress fields; a result of local kinematic interactions. **Journal of Structural Geology**, v. 115, 2018, p. 304-310. Doi: 10.1016/j.jsg.2018.04.012. Disponível em:

https://www.sciencedirect.com/science/article/abs/pii/S0191814117303176. Acesso em: 10 jan. 2021.

NEVES, S. P.; TEIXEIRA, C. M. L.; BRUGUIER, O. Long-lived localized magmatism in central-eastern part of the Pernambuco-Alagoas Domain, Borborema Province (NE Brazil): Implications for tectonic setting, heat sources, and lithospheric reworking. **Precambrian Research**, v. 337, n. 1055592, 2020. Doi: 10.1016/j.precamres. 2019.105559 Disponível em: https://www.sciencedirect.com/science/article/abs/pii/S0301926819302554. Acesso em: 10 jan. 2021.

PASSCHIER, C. W.; TROW, R. A. J. **Microtectonics**. Nova York: Springer Berlin Heidelberg, 2005.

PEÑA-ALONSO, T. A.; ESTRADA-CARMONA, J.; MOLINA-GARZA, R. S.; SOLARI, L.; LEVRESSE, G.; LATORRE, C. Lateral spreading of the middle to lower crust inferred from Paleocene migmatites in the Xolapa Complex (Puerto Escondido, Mexico): Gravitational collapse of a Laramide orogen? **Tectonophysics**, v. 706-707, 2017, p. 143–163. Doi: 10.1016/j.tecto.2017.04.010. Disponível em: https://www.sciencedirect.com/science/article/abs/pii/S0040195117301440. Acesso em: 10 jan. 2021.

PERCHUK, L. L.; LAVRENT'EVA, I. V. Experimental investigation of exchange equilibria in the system cordierite-garnet-biotite. *In*: Saxena, S.K., (ed.), **Kinetics and equilibrium in mineral reactions**. New York: Springer Verlag, 1983. p. 199-239.

POWELL, R.; HOLLAND, T. J. B. An internally consistent dataset with uncertainties and correlations; 3, Applications to geobarometry, worked examples and a computer program. **Journal of Metamorphic Geology**, v. 6, 1988, p. 173-204. Doi: 10.1111/j.1525-1314.1988.tb00415.x. Disponível em: https://onlinelibrary.wiley.com/doi/10.1111/j.1525-1314.1988.tb00415.x. Acesso em: 10 jan. 2021.

RAIMONDO, T.; COLLINS, A. S.; HAND, M.; WALKER-HALLAM, A.; SMITHIES, R. H.; EVINS, P. M.; HOWARD, H. M. The anatomy of a deep intracontinental orogen. **Tectonics**, v. 29, 2010, p. 1-31. Doi: 10.1029/2009TC002504. Disponível em: https://agupubs.onlinelibrary.wiley.com/doi/full/10.1029/2009TC002504. Acesso em: 10 jan. 2021.

RAMSAY, J. G. Folding and Fracturing of Rocks. New York: McGraw-Hill, 1967.

RECHE, J.; MARTINEZ, F. J. GPT: An excel spreadsheet for thermobarometric calculations in metapelitic rocks. **Computers & Geosciences**, v. 22, n. 7, 1996, p. 775-784. Doi: 10.1016/0098-3004(96)00007-6. Disponível em: https://www.sciencedirect.com/science/article/pii/0098300496000076. Acesso em: 10 jan. 2021.

REY, P.; VANDERHAEGHE, O.; TEYSSIER, C. Gravitational collapse of the continental crust: definition, regimes and modes. **Tectonophysics**, v. 342, 2001, p. 435-449. Doi: 10.1016/S0040-1951(01)00174-3. Disponível em: https://www.sciencedirect.com/science/article/abs/pii/S0040195101001743. Acesso em: 10 jan. 2021.

ROCHA, D. E. G. A. **Programa de Levantamentos Geológicos Básicos do Brasil: Geologia da Folha Vitória de Santo Antão – SC.25-V-A-II, escala 1:100.000.** Brasília, 1990. CPRM/DNPM. 112 f.

RUPPEL, C.; HODGES, K. Pressure-temperature-time paths from two-dimensional thermal models: Prograde, retrograde, and inverted metamorphism. **Tectonics**, v. 13, n. 1, 1994, p. 17-44. Doi: 10.1029/93TC01824. Disponível em: https://agupubs.onlinelibrary.wiley.com/doi/abs/10.1029/93TC01824. Acesso em: 10 jan. 2021.

SÁ, J. M.; BERTRAND, J. M.; LETERRIER, J.; MACEDO, M. H. F. Geochemistry and geochronology of pre-Brasiliano rocks from the Transversal Zone, Borborema Province, Northeast Brazil. **Journal of South American Earth Sciences**, v. 14, 2002, p. 851–866. Doi: 10.1016/S0895-9811(01)00081-5. Disponível em: https://www.sciencedirect.com/science/article/abs/pii/S0895981101000815. Acesso em: 10 jan. 2021.

SANTOS, E. J.; MEDEIROS, V.C. Constraints from granitic plutonism on proterozoic crustal growth of the Transverse Zone, Borborema Province, NE-Brazil. **Revista Brasileira de Geociências**, v. 29, 1999, p. 73-84. Disponível em: http://rigeo.cprm.gov.br/xmlui/handle/doc/548. Acesso em: 10 jan. 2021.

SANTOS, E. J.; NUTMAN, A. P.; BRITO NEVES, B. B. Idades SHRIMP U-Pb do Complexo Sertânia: implicações sobre a evolução tectônica da Zona Transversal, Província Borborema. **Geologia USP - Série Científica**, v. 4, n. 1, 2004, p. 1-12. Doi: 10.5327/s1519-874x2004000100001. Disponível em: http://ppegeo.igc.usp.br/index.php/GUSPSC/article/view/1090. Acesso em: 10 jan. 2021.

SANTOS, T. J. S.; GARCIA, M. G. M.; AMARAL, V. W.; CABY, R.; WERNICK, E.; ARTHAUD, M. H.; DANTAS, E. L.; SANTOS, H. M. Relics of eclogite facies assemblages in the Ceará Central Domain, NW Borborema Province, NE Brazil: Implications for the assembly of West Gondwana. **Gondwana Research**, v. 15, n; 3-4, 2009, p. 454-470. Doi: 10.1016/j.gr.2009.01.003. Disponível em: https://www.sciencedirect.com/science/article/abs/pii/S1342937X09000045. Acesso em: 10 jan. 2021.

SANTOS, E. J.; VAN SCHMUS, W. R.; KOZUCH, M.; BRITO NEVES, B. B. The Cariris Velhos tectonic event in Northeast Brazil. **Journal of South American Earth Sciences**, v. 29, 2010, p. 61-76. Doi: 10.1016/j.jsames.2009.07.003. Disponível em: https://www.sciencedirect.com/science/article/abs/pii/S0895981109000996. Acesso em: 10 jan. 2021.

SANTOS, F. H.; AMARAL, W. S.; LUVIZOTTO, G. L.; MARTINS DE SOUSA, D. F. P-T evolution of metasedimentary rocks of the Santa Filomena Complex, Riacho do Pontal Orogen, Borborema Province (NE Brazil): Geothermobarometry and metamorphic modelling. **Journal of South American Earth Sciences**, v. 82, 2018a, p. 91-107. Doi: 10.1016/j.jsames.2017.12.013. Disponível em: https://www.sciencedirect.com/science/article/abs/pii/S0895981116302991. Acesso em: 10 jan. 2021.

SANTOS, C. A.; FERNANDES, P. R.; PEREIRA, C. S.; BRITO, M. F. L.; DOMINGOS, N. R. R.; SILVA, E. P.; OLIVEIRA, R. G. **Programa Geologia do Brasil-PGB: Projeto RIO CAPIBARIBE, escala 1:250.000**, CPRM, 2018.

SILVA FILHO, A. F.; GUIMARÃES I. P; VAN SCHMUS W. R.; ARMSTRONG R. A; RANGEL, J .M. S.; OSAKO, L. S.; COCENTINO, L. M. SHIIMP U-Pb geochronology and Nd signatures of supracrustal sequences and orthogneiss constrain the Neoproterozoic evolution of the Pernambuco-Alagoas domain, Southern part of Borborema Province, NE Brazil. **International Journal of Earth Sciences**, v. 103, n. 8, 2014, p. 2155-2190. Disponível em: Acesso em: 10 jan. 2021.

SILVA, J. M. R.; MARIANO, G.; NEVES S. P. Termobarometria das rochas metapelíticas da parte Leste da Zona Transversal: Região de Surubim e Alcantil, Província Borborema, NE do Brasil. *In*: SIMPÓSIO DE GEOLOGIA DO NORDESTE. 21., 2004, Recife. **Anais**. Recife: Sociedade Brasileira de Geologia, 2005.

SILVA, V. L.; NEVES., S. P. Tectônica Transpressiva na Faixa Feira Nova, Domínio Rio Capibaribe, Província Borborema. 2019. Manuscrito em preparação.

SILVA, V. L; PEREIRA, S.; BUSTAMANTE, A.; NEVES, S. P. Metamorphic evolution of metasedimentary rocks of the Feira Nova region: Tectonic implications for the Brasiliano orogeny in eastern Borborema Province Northeast Brazil. **Journal of South American Earth Sciences**, v. 100, n. 102590, 2020. Doi: 10.1016/j.jsames. 2020.102590. Disponível em: https://www.sciencedirect.com/science/article/abs/pii/S0895981120301036. Acesso em: 10 jan. 2021.

SKRZYPEK, E.; STIPSKA, P.; SCHULMANN, K.; LEXA, O.; LEXOVA, M. Prograde and retrograde metamorphic fabrics – a key for understanding burial and exhumation in orogens (Bohemian Massif). **Journal Metamorphic Geology**, v. 29, 2011, p. 451–472. Doi: 10.1111/j.1525-1314.2010.00924.x. Disponível em: https://onlinelibrary.wiley.com/doi/abs/10.1111/j.1525-1314.2010.00924.x. Acesso em: 10 jan. 2021.

SOMMER, H.; HAUZENBERGER, C.; KRONER, A.; MUHONGO, S. Isothermal decompression history in the ‘‘Western Granulite” terrain, central Tanzania: Evidence from reaction textures and trapped fluids in metapelites. **Journal of African Earth Sciences**, v. 51, n. 3, 2008, p. 123-144. Doi: 10.1016/j.jafrearsci.2008.01.003. Disponível em: https://www.sciencedirect.com/science/article/abs/pii/S1464343X08000022. Acesso em: 10 jan. 2021.

SPEAR, F. S.; CHENEY, J. T. A petrogenetic grid for pelitic schists in the system SiO_2-Al_2O_3-FeO-MgO-K_2O-H_2O. **Contributions to Mineralogy and Petrology**, v. 101, n. 2, 1989, p. 149-164. Doi: 10.1007/BF00375302. Disponível em: https://link.springer.com/article/10.1007/BF00375302. Acesso em: 10 jan. 2021.

SPEAR, F. S.; SELVERSTONE, J. Quantitative P-T Paths from Zoned Minerals: Theory and Tectonic Applications. **Contributions to Mineralogy and Petrology**, v. 83, n. 3-4, 1983, p. 348-357. Doi: 10.1007/BF00371203. Disponível em: https://link.springer.com/article/10.1007/BF00371203. Acesso em: 10 jan. 2021.

SPIESS, R.; PERUZZO, L.; PRIOR, D.J.; WHEELER, J. Development of garnet porphyroblasts by multiple nucleation, coalescence, and boundary misorientation-driven rotations. **Journal of Metamorphic Geology**, v. 19, n. 2, 2001, p. 69–290. Doi: 10.1046/j.1525-1314.2001.00311.x. Disponível em: https://onlinelibrary.wiley.com/doi/full/10.1046/j.1525-1314.2001.00311.x. Acesso em: 10 jan. 2021.

TEIXEIRA, C. M. L. **Evolução crustal dos domínios central e Pernambuco-Alagoas da província Borborema na folha Vitória de Santo Antão (Pernambuco – Nordeste do Brasil)**. 2015. 192 f. Tese. (Doutorado em Geociências) - Universidade Federal de Pernambuco, Recife, 2015.

THOMAS, J. B.; WATSON, E. B.; SPEAR, F. S.; SHEMELLA, P. T.; NAYAK, S. K.; LANZIROTTI, A. TitaniQ under pressure: The effect of pressure and temperature on the solubility of Ti in quartz. **Contributions to Mineralogy and Petrology**, v. 160, 2010, p. 743-759. Doi: 10.1007/s00410-010-0505-3. Disponível em: https://link.springer.com/article/10.1007/s00410-010-0505-3. Acesso em: 10 jan. 2021.

THOMPSON, P. H. Moderate overthickening of thinned sialic crust and the origin of granitic magmatism and regional metamorphism in low-P-high-T terranes. **Geology**, v. 17, n. 6, 1989, p. 520-523. Doi: 10.1130/0091-7613(1989)017<0520:MOOTSC>2.3.CO;2. Disponível em: https://pubs.geoscienceworld.org/gsa/geology/article-abstract/17/6/520/204890/Moderate-overthickening-of-thinned-sialic-crust?redirectedFrom=fulltext. Acesso em: 10 jan. 2021.

THOMPSON, A. B.; SCHULMANN, K.; JEZEK, J.; TOLAR, V. Thermally softened continental extensional zones (arcs and rifts) as precursors to thickened orogenic belts. **Tectonophysics**, v. 332, 2001, p. 115-141. Doi: 10.1016/S0040-1951(00)00252-3. Disponível em: https://www.sciencedirect.com/science/article/abs/pii/S0040195100002523. Acesso em: 10 jan. 2021.

TIKOFF, B.; GREENE, D. Stretching lineations in transpressional shear zones: an example from the Sierra Nevada Batholith, California. **Journal of Structural Geology**, v. 19, 1997, p. 29–39. Doi: 10.1016/S0191-8141(96)00056-9. Disponível em: https://www.sciencedirect.com/science/article/abs/pii/S0191814196000569. Acesso em: 10 jan. 2021.

VAN SCHMUS, W. R.; OLIVEIRA, E. P.; SILVA FILHO, A. F.; TOTEU, S. F.; PENAYE, J.; GUIMARÃES, I. P. Proterozoic links between the Borborema province, NE Brazil, and the Central African Fold Belt. **Geological Society of London**, **Special Publication**, v. 294, 2008, p. 69-99. Doi: 10.1144/SP294.5. Disponível em: https://sp.lyellcollection.org/content/294/1/69. Acesso em: 10 jan. 2021.

VAN SCHMUS, W. R.; KOZUCH, M.; BRITO NEVES, B. B. Precambrian history of the Zona Transversal of the Borborema Province, NE Brazil: Insights from Sm/Nd and U/Pb geochronology. **Journal of South American Earth Sciences**, v. 31, 2011, p. 227-252. Doi: 10.1016/j.jsames.2011.02.010. Disponível em: https://www.sciencedirect.com/science/article/abs/pii/S0895981111000186. Acesso em: 10 jan. 2021.

VAUCHEZ A.; NEVES S. P.; CABY R.; CORSINI M.; EGYDIO-SILVA M.; ARTHAUD M. H.; AMARO V. The Borborema shear zone system, NE Brazil. **Journal of South American Earth Sciences**, v. 8, 1995, p. 247-266. Doi: 10.1016/0895-9811(95)00012-5. Disponível em: https://www.sciencedirect.com/science/article/abs/pii/0895981195000125. Acesso em: 10 jan. 2021.

VIEGAS L. G. F.; ARCHANJO C. J.; HOLLANDA M. H. B. M.; VAUCHEZ A. Microfabrics and zircon U-Pb (SHRIMP) chronology of mylonites from the Patos shear zone (Borborema Province, NE Brazil). **Precambrian Research**, v. 243, 2014, p. 1-17. Doi: 10.1016/j.precamres.2013.12.020. Disponível em: https://www.sciencedirect.com/science/article/abs/pii/S0301926814000023. Acesso em: 10 jan. 2021.

WATSON, E. B.; WARK, D. A.; THOMAS, J. B. Crystallization thermometers for zircon and rutile. **Contributions to Mineralogy and Petrology,** v. 151, 2006, p. 413-433. Doi: 10.1007/s00410-006-0068-5. Disponível em: https://link.springer.com/article/10.1007/s00410-006-0068-5. Acesso em: 10 jan. 2021.

WERNERT, P.; SCHULMANN, K.; CHOPIN, F.; STIPSKA, P.; BOSCH, D.; EL HOUICHA, M. Tectonometamorphic evolution of an intracontinental orogeny inferred from P-T-t-d paths of the metapelites from the Rehamna massif (Morocco). **Journal of Metamorphic Geology**, v. 34, n. 9, 2016, p. 917-940. Doi: 10.1111/jmg.12214. Disponível em: https://hal.archives-ouvertes.fr/hal-01468009. Acesso em: 10 jan. 2021.